

McGill University

THERMAL MATURATION PATTERNS
IN CAMBRO-ORDOVICIAN FLYSCH
SEDIMENTS OF THE TACONIC
BELT, GASPE PENINSULA

by

C

Shafiul Islam

M.Sc. (Dhanbad, India)

A thesis submitted to the Faculty of Graduate Studies and
Research in partial fulfillment of the requirements
for the degree of Master of Science in
the Department of Geological Sciences

C

Montreal, Québec
Canada

May 1981

ABSTRACT

Systematic variations in illite crystallinity (IC, 350 samples) and mean random reflectance of asphaltic pyrobitumen (\bar{R}_O , 95 samples) in Cambro-Ordovician deep-water shales of the Taconic Belt of Gaspé Peninsula are closely correlated and show nearly identical patterns. A thermal dome of epimetamorphic and higher grade conditions ($IC < 1.9mm$; $\bar{R}_O \geq 5.0\%$) forms a halo around the Devonian McGerrigle Mountains pluton in the centre of the study area. West, north, and east of the dome the epimetamorphic zone passes into the anchizone ($1.9 < IC < 3.3mm$; $2.7 < \bar{R}_O \leq 5.0\%$) which eastward and westward grades further into the late diagenetic zone ($IC > 3.3mm$; $\bar{R}_O \leq 2.7\%$).

The unusually large width (16-20km) of the epizone around the McGerrigle Mountains pluton (8km) is easiest to explain by the extension of the pluton beneath the epizone at shallow sub-surface levels. The bulging (30km) of the epizone toward north-east may reflect a subsurface trend of the intrusive body in that direction.

West of the thermal dome maturation level decreases northward with decreasing age. Here pre-orogenic diagenetic grade reached during sedimentary burial at the original site of deposition may have been preserved.

East of the thermal dome, the diagenetic grade increases northward to anchizone conditions in progressively younger sediments, it is unlikely to have been induced by stratigraphic burial and is possibly syn- to postorogenic in nature.

A depth of burial of 6km for the Lower Ordovician Tourelle Formation has been estimated assuming a geothermal gradient of 30°C/km. This implies that a thickness of 5 km of the Tourelle Formation or younger units has been denuded. A depth of burial of 6km for the Cap-des-Rosiers Group appears reasonable from the field observation.

Isotopic composition of ferroan dolomite concretions varies from +7.57 to +0.88‰ $\delta^{13}\text{C}$ and -1.74 to -6.61‰ $\delta^{18}\text{O}$ (PDB) between core and rim. Porosity also decreases from 85 (core) to 65% (rim) of the concretions. These values suggest that decomposition of organic matter by methane producing bacteria may be responsible for the carbonate concretions. Probably they began to develop just below the sediment-water interface and continued to grow at greater depth with sedimentation.

RESUME

Une très bonne corrélation existe entre les variations systématiques dans la cristallinité de l'illite (IC, 350 spécimens) et de la réflectance moyenne du pyrobitumine asphaltique (Ro, 95 spécimens) dans les argiles Cambro-Ordoviciens déposés en eaux profondes de la ceinture Taconique de la péninsule de la Gaspésie, et les deux variables indiquent une zonation presque identique. Un dôme thermique de grade épimetamorphique et plus (IC \leq 1.9mm; Ro \geq 5.0%) forme une auréole autour du pluton de la montagne McGerrigle (Dévonien) au centre du lieu de l'étude. A l'ouest, au nord et à l'est du dôme la zone épimetamorphique passe dans l'anchizoné (1.9 \leq IC \geq 3.3mm; 2.7 \leq Ro \leq 5.0%) lequel continue, à l'est et à l'ouest, de passer dans la zone diagenétique (IC \geq 3.3mm; Ro \leq 2.7%).

La largeur inhabituelle (16-20 km) de l'épizone autour du pluton de la montagne McGerrigle (8 km) est facilement expliquée par l'extension du pluton sous la surface à des niveaux peu profonds. La structure, gonflée (30 km) de l'épizone au Nord-Est reflète une extension de l'intrusion dans cette direction.

A l'ouest du dôme thermique le niveau de maturation décroît au nord en même temps que l'âge des roches diminue. Ici, un grade diagenétique pré-orogénique atteint durant un enfouissement sédimentaire au site original de déposition aurait peut-être été préservé.

A l'est du dôme thermique, le grade diagenétique augmente au nord jusqu'à l'anchizoné mais les sédiments deviennent plus jeunes, il est peu probable que ceci soit dû à un simple enfouissement. Au contraire, l'augmentation de grade avec une diminution de l'âge est peut-être syn-à post-orogénique.

Supposant une variation géothermique de 30°C/km, la profondeur d'enfouissement de la formation Tourelle de l'Ordovicien inférieur serait 6 km. Ceci implique qu'une épaisseur de 5 km de la formation Tourelle ou des unités cadètes a été dénudée. Une profondeur d'enfouissement de 6 km pour le Groupe Cap-des-Rosiers paraît raisonnable d'après les observations sur le terrain.

La composition isotopique des concrétions de dolomite ferrique varie de +7.57 à +0.88 ‰ $\delta^{13}\text{C}$ de -1.74 à -6.61 ‰ $\delta^{18}\text{O}$ (PDB) du centre aux marges. La porosité diminue aussi de 85% (centre) à 65% (marges). Ces chiffres suggèrent que la décomposition des matières organiques par des bactéries produisant du méthane peut être responsable pour la genèse des concrétions de carbonate. Probablement, ceux-ci ont commencés à croître immédiatement sous l'interface sédiment-eau et ont continués à croître à des profondeurs plus grandes.

ACKNOWLEDGEMENTS

The author is sincerely grateful to Dr. R. Hesse for supervising this study. His critical review of my work has been a source of encouragement for completion of this thesis.

I deeply appreciate the efforts of Drs. C.W. Stearn, A. Hynes, E.W. Mountjoy, A.E. Williams-Jones, S. Ruppel and Mr. B. Murphy for their thoughtful comments on different sections of the thesis.

My friends and colleagues at McGill University, in particular C. Polan, D. Hudson, G.P. Smith, D. Smith, H. Sawh, C. Fong and Dr. O. Ogunyomi assisted me in numerous ways with their interest and discussion. Thanks to T. Shahzada for assisting me both in the field and in the laboratory.

Mr. S. Biron of Dept. Nat. Resources, Quebec City kindly showed me some areas of interest in the Taconic Belt of Gaspé peninsula. His knowledge and experience in the area has been of great help to me.

Acknowledgements are also due to the Director (Dr. M. Desjardins) and staff of INRS, Pétrole, Québec City, for their technical assistance and hospitality. Thanks to Mr. A. Chagnon, Drs. Y. Heroux, and A. Achab of the INRS-Pétrole, Québec City for their time and suggestions.

Especial thanks to R.A. Yates who drafted some of the diagrams for this thesis and Ingrid Lashley-Hudson who did the typing.

Financial assistance through grants to Dr. R. Hesse by the National Science and Engineering Research Council (NSERC); Dept. of Energy, Mines and Resources, Ottawa (DEMR); Imperial Oil and Ministère de l'Éducation du Québec through its formation des chercheurs et action concerté program (FCAC) are gratefully acknowledged.

TABLE OF CONTENTS

	Page
ABSTRACT	1
RESUME	111
ACKNOWLEDGEMENTS	v
LIST OF FIGURES	viii
LIST OF TABLES	x
LIST OF PLATES	xi
LIST OF APPENDICES	xii
 <u>CHAPTER 1</u> - INTRODUCTION	 1
 <u>CHAPTER 2</u> - REGIONAL GEOLOGY	 5
LOCAL GEOLOGY	13
SAMPLING PROCEDURE	22
 <u>CHAPTER 3</u> - CLAY MINERALOGY AND ILLITE CRYSTALLINITY	 24
ORGANIC MATTER MATURATION	29
INDICATORS FOR THE LEVEL OF DIAGENESIS AND LOW # GRADE METAMORPHISM	 36
 <u>CHAPTER 4</u> - RESULTS - General	 48
ILLITE CRYSTALLINITY	50
PYROBITUMEN REFLECTANCE	67
 <u>CHAPTER 5</u> - INTERPRETATION - General	 76
BURIAL DEPTH	80
EFFECT OF FOLDING ON ILLITE CRYSTALLINITY	94
CORRELATION BETWEEN ILLITE CRYSTALLINITY AND REFLECTANCE	 101

	Page
<u>CHAPTER 6</u> - DIAGENESIS OF CARBONATE CONCRETIONS	111
FIELD DESCRIPTIONS	115
SAMPLING	115
RESULTS	115
CARBON AND OXYGEN ISOTOPES	120
<u>CHAPTER 7</u> - SUMMARY AND CONCLUSIONS	135
REFERENCES	138
APPENDICES	160

LIST OF FIGURES

	Page
1. Tectonic Units of the Québec Appalachians	9
2. Tectonic Units of the Study Area	19
3. Four-fold Subdivision of Kerogen	32
4. Scales of Thermal Maturation of Organic Matter	39
5. Correlation of % Ro (mean) with Zones of Diagenesis, Anchimetamorphism and epimetamorphism	43
6. Correlation of Illite Crystallinity with Zones of Diagenesis, Anchimetamorphism and Epimetamorphism	45
7. Boundary Between Diagenetic Zone, Anchizone and Epimetamorphic Zone by Illite Crystallinity	47
8. Isopleth Map of Illite Crystallinity, Taconic Belt, Gaspé Peninsula	52
9. Sections in the Study Area	54
10. Illite Crystallinity Values Plotted Along North-South Cross Sections in the Study Area	56
11. Illite Crystallinity vs. Illite 002/001 Intensity Ratio West of the Thermal Dome	60
12. Illite Crystallinity vs. Illite 002/001 Intensity Ratio East of the Thermal Dome	62
13. Illite Crystallinity and Illite 002/001 Intensity Ratio in the Tourelle Formation	64
14. Illite Crystallinity and Illite 002/001 Intensity Ratio in the Cap Chat Melange	66
15. Isopleth Map of Pyrobitumen Reflectance of the Taconic Belt, Gaspé Peninsula	71
16. North-South Cross-sections Showing Plotted Values of Pyrobitumen Reflectance in the Study Area	73
17. Stratigraphic Table of Various Cambrian and Ordovician Stratigraphic Units in the Taconic Belt of Gaspé Peninsula ..	85
18. Tectonic Model of the Taconic Belt of Gaspé Peninsula	87

	Page
19. Estimates of Temperatures and Burial Depths for the Tourelle Formation and the Cap-des-Rosiers Group	89
20. Relationship Between Reflectance, Time and Temperature from Karweil (1956)	91
21. Relationship Between Reflectance, Time and Temperature from Hood et al. (1975)	93
22. Effect of Folding on Illite Crystallinity, Cloridorme Formation (γ - members)	97
23. Effect of Folding on IC and Reflectance, Cloridorme Formation (β - members)	100
24. Correlation Coefficient of IC vs. Reflectance for Different Formation and Zones	106
25. Correlation of IC and Reflectance in Different Formations ...	108
26. Correlation of IC vs. Reflectance in Different Maturation Zones	110
27. Locations of Carbonate Concretion Samples, Cloridorme Formation	117
28. The Sampling Pattern of Concretions for Laboratory Studies ..	119
29. Variations of Carbon and Oxygen Isotopes, and Carbonate and Organic Carbon Content of the Concretions	124
30. Schematic Diagram Showing Depth Related Reaction Zones Involving Breakdown of Organic Matter in an Area of Fairly Rapid Sedimentation	129
31. Flow Chart for Organic Matter and Clay Mineral Analyses	164
32. Types of Relationship Between Illite Crystallinity and Illite Intensity Ratio ($I(002) / I(001)$)	176
33. X-Ray Diffractograms of Natural and Glycolated Samples - Finer Fraction ($<2 \mu m$), and Natural Samples - Coarser Fraction ($2 - 16 \mu m$)	178
34. X-Ray Diffractograms of Natural and Glycolated Samples	180
35. X-Ray Diffractograms of Four Samples Immediately East of the McGerrigle Mountains Pluton	182

LIST OF TABLES

	Page
Table 1. Lithology and Structure of the Various Stratigraphic Units of the Cambro-Ordovician Rocks, Gaspé Peninsula	12
Table 2. Lithology of the Different Members of the Middle Ordovician Cloridorme Formation	16
Table 3. Percentage of Carbon and Oxygen Isotopes, and Carbonate and organic carbon content of the concretions	122
Table 4. Organic Carbon Content of Black, Green and Red Shales, Taconic Belt, Gaspé Peninsula	169
Table 5. Illite Crystallinity of Natural (<2 μ m and 2-16 μ m) and Glycolated (<2 μ m) Sample	185

LIST OF PLATES

	Page
1. Structure and Rock Types, Taconic Belt, Gaspé Peninsula	157
2. Carbonate Concretions from the Cloridorme Formation, Gaspé Peninsula	158
3. Organic Matter in Transmitted and Reflected Light from Cambro-Ordovician Shales of Gaspé Peninsula	159

LIST OF APPENDICES

<u>Appendix</u>		<u>Page</u>
1	Sample preparation and analytical techniques for clay mineralogy	160
2	Sample preparation and procedure for reflectance measurements	162
3	Determination of total organic carbon...	167
4	Analytical techniques for isotopic analysis	170
5	Identification of clay minerals	171
6	Clay mineralogy	174
7	Differences in crystallinity between various size fractions	183
8	Reflectance data and calculated statistical parameters	186

CHAPTER ONE

INTRODUCTION

During the last decade progress has been made in establishing stages of diagenesis and low-grade metamorphism in sedimentary sequences. Progressive thermal maturation of clastic rocks with increasing time and depth of burial results in the transformation of organic and inorganic compounds. During the sixties, sedimentologists were mainly looking at the inorganic components, especially in sandstones, to establish diagenetic changes. This was due to lack of communication between sedimentologists and coal petrologists, who had long back established coal ranks as a scale for thermal maturation of coal seams and associated sedimentary deposits. Also, the usefulness of clay minerals as indicator of diagenetic grade in the 60's had been recognised but was not yet widely known. This has changed profoundly in the 1970's.

Recognition of the progressive transformation of smectite through mixed layer clay minerals to illite and finally to dioctahedral mica has provided the impetus for diagenetic studies of pelitic rocks. Since these diagenetic changes are influenced by a number of factors not necessarily related to burial depth, interpretation of regional maturation patterns as well as correlation of results between different regions is difficult. Maturation of the dispersed organic matter in shales is mainly temperature dependent,

i.e., reactions are less controlled by pressure.

Despite various limitations that have been recognised recently, application of diagenetic studies to orogenic belts has provided significant results. Organic matter reflectance, illite crystallinity and fluid inclusion data are presently used as tools for mapping regional variations in maturation and establishing a zonation in diagenetic and low-grade metamorphic terranes. This zonation is similar to the mapping of isograds in higher-grade metamorphic belts. In several orogenic belts the study of the thermal maturation of shales has lead to interesting and surprising findings. For instance in the Taconic Belt of the Québec Appalachians the occurrence of preorogenic inverted diagenesis has been recognised (Ogunyomi et al., 1980). Inverted diagenesis has also been reported from the external parts of the Alps in Switzerland and France (Frey et al., 1980; Kübler et al., 1979) and from the Northern Apennines in Italy (Reutter et al., 1978).

The first objective of this study was to obtain estimates for the stratigraphic thickness of the parautochthonous Cloridorme Formation on eastern Gaspé Peninsula. Enos (1969) estimated it to be about 7km thick, but admitted that this could be in error by as much as 100%. If preorogenic diagenesis is preserved, the thermal maturation of organic matter will provide evidence on burial depth, i.e. maximum thickness. Ogunyomi et al., (1980) estimated maximum burial temperatures and corresponding

depths from the reflectance values in Cambro-Ordovician flysch deposits in the Québec City area by assuming paleo-geothermal gradients equal to present day average gradients. The maturation parameters used in Ogumyomi's study (reflectance of organic matter and illite crystallinity) were not at that time calibrated in terms of paleotemperatures and paleopressures. Calibration is now possible, however, by using methane-bearing fluid inclusions as an independent geothermometer and geobarometer (Mullis, 1979). The burial depths of sedimentary rocks provides information useful not only for hydrocarbon exploration but also for an understanding of the regional patterns of subsidence of ancient continental margins such as the lower Paleozoic continental margin of North America.

Sampling was started in the most external part of the Taconic Belt of Gaspé Peninsula along the shorelines of the Gulf of St. Lawrence. Initial results showed that within the parautochthonous Cloridorme Formation the youngest γ -members - those lying north of the Devonian granitic McGerrigle Mountains pluton - are in general much more mature than the older β -members. Also, in the γ -members there is a belt of highly matured rocks not showing any obvious relationship to burial depth. To explain these abnormally high maturation levels it was necessary to extend the study over the entire Taconic belt of eastern Gaspé Peninsula in order to obtain a broader picture of the regional maturation patterns.

In this study information on the earlier stages of diagenesis at the time of formation of carbonate concretions was also obtained. Close association of certain black shales and carbonate concretions suggests that the decomposition of organic matter plays a significant role in the concretion-forming process by providing the carbonate alkalinity necessary for the inorganic precipitation of carbonates. Isotopic composition of the concretions records some of the changes in interstitial water composition of the sediments as the concretions grew. This information on water composition may help in obtaining a more complete insight into the various stages of alteration which initially are strongly affected by the oxidation and break-down of organic matter and ultimately (at higher levels of maturation) are recorded by the reflectance of organic matter and illite crystallinity.

CHAPTER TWO

GENERAL GEOLOGY

The synthesis of stratigraphic and structural data for the Northern Appalachians has resulted in a number of tectono-stratigraphic schemes (e.g. Zen, 1967, 1972; Rodgers 1968). Since 1970 these schemes have been based on plate tectonic concepts (Bird and Dewey 1970; Cady 1972; Dewey and Kidd 1974; St. Julien and Hubert 1975; Poole 1976; Rust et al. 1976; Ruitenberg et al. 1977; Schenk 1978; Williams 1979). For the Quebec Appalachians the tectonic classification of St. Julien and Hubert (1975) is most elaborate and is adopted here as it encompasses the study area of this thesis.

St. Julien and Hubert (1975) have suggested a three-fold tectonic subdivision of the Northern Appalachians in Quebec: 1. the Autochthonous Domain; 2. the External Domain of the Allochthon comprising an outer belt of thrust-imbricated structures and an inner belt of nappes; and 3. the Internal Domain. These domains correspond to fundamental subdivisions recognised in many orogenic belts; that is, relatively undeformed sediments in the more external parts (Autochthonous Domain) and more highly deformed and metamorphosed rocks in the internal axial zones.

The Taconic structural domains of St. Julien and Hubert (1975) comprise Cambro-Ordovician sediments derived from different portions of a former continental

margin. The Autochthonous Domain consists of sediments deposited on the continental shelf bordering and overlying the crystalline basement that was formed by the Grenville orogeny. The stratigraphic succession of the Autochthonous Domain is made up of Cambro-Ordovician continental and shallow marine siliciclastic rocks (Potsdam Sandstone), of Lower to Middle Ordovician shallow marine carbonates (Beekmantown, Chazy, Black River, and Trenton Groups) overlain by marine black shales (Utica Shale) and a regressive sequence (Queenston equivalents). The External Domain is dominantly made up of deep water flysch sediments. The rocks of this domain were deposited partly on the outer continental shelf, and partly in adjacent deep-water areas interpreted as continental slope and rise environments. The deep water flysch of the External Domain appears to be quite thick. This implies a rapid subsidence of the Early Paleozoic passive continental margin. In the Internal Domain sediments were deposited partly on oceanic crust represented by the Eastern Townships ophiolite complex. In addition to the ultramafic bodies of Mt. Albert and Thetford Mines, the Internal Domain is characterized by the occurrence of shale melange, tuff, and calcalkaline volcanic sequences. The principal difference between the Internal and External Domains is the involvement of basement in the deformation of the Internal Domain. In the External Domain the tectonism is confined to cover rocks.

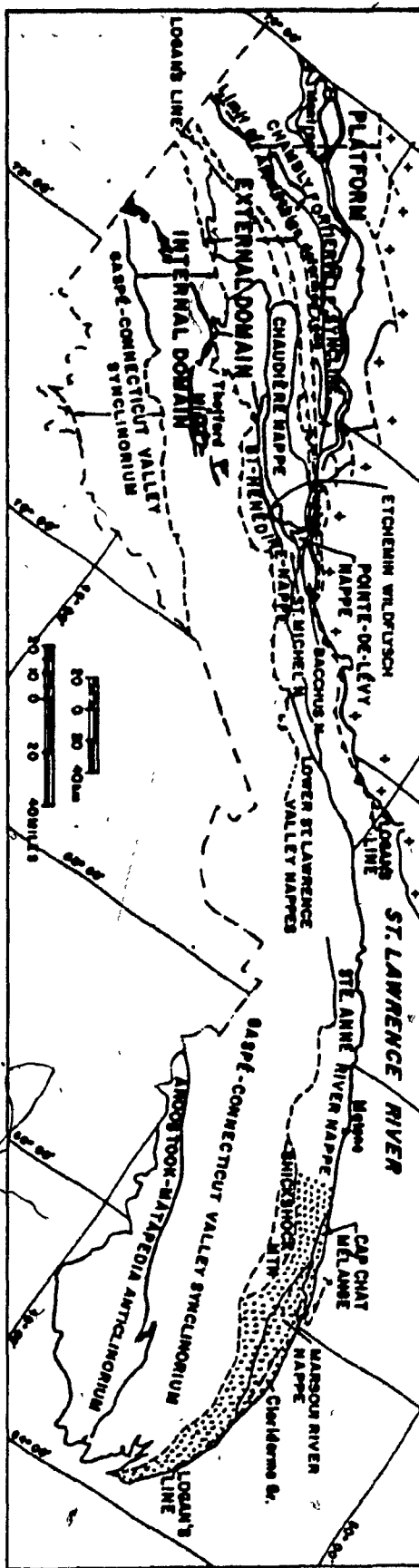
The study area extends from the St. Lawrence River southward for 10 to 40 km to include the Québec Group (Logan, 1863). This group comprises the Middle Ordovician Cloridorme and Deslandes Formations (Normanskill) and the Lower Ordovician to Upper Cambrian Tourelle Formation and Cap-des-Rosiers Group (Deekill) rocks (McGerrigle, 1959). It extends from Les Mechins in the west to Cap-des-Rosiers at the eastern tip of Gaspé Peninsula. This region includes the eastern part of the Taconic Belt. The age of the Taconic Orogeny, based on K/Ar determinations on hornblende from the amphiboles of Mount Albert and Mount Serpentine, is 443 ± 18 Ma and 437 ± 20 Ma, respectively (Wanless et al., 1973, 1972, quoted in St. Julien and Hubert, 1975).

Structurally these rocks occupy the External Domain of St. Julien and Hubert (1975) and in part Logan's zone of Bird and Dewey (1970). Schenk (1978) adopted Williams' (1976) terminology for the tectono-stratigraphic zones of the Canadian Appalachians, for the purpose of comparing Québec and western Newfoundland. The Lomond Zone is equivalent to the parautochthonous Cloridorme Formation and the Fleur de Lys Zone is equivalent of the Marsoui River Nappe and Ste-Anne River Nappe of the study area.

The most important thrust in the study area is Logan's Line which separates the parautochthonous Middle Ordovician Cloridorme Formation (zone of thrust imbricated structures, St. Julien and Hubert, 1975) from the nappes in the south. The nappes with older rock assemblages rest on the younger

FIGURE 1

Tectonic units of the Quebec Appalachians. Stippled area represents study area. (From Ogunyomi: 1980, modified after St. Julien and Hubert, 1975).



parautochthonous unit.

Another important tectonic feature of the study area is the McGerrigle Mountains pluton. According to K/Ar dates the pluton has post-kinematically intruded the Cambro-Ordovician rocks around 350 Ma (Late Devonian) (de Rômer, 1977). One sample has provided an exceptionally young age of 319 ± 10 Ma (early Mississippian).

The southern half of Gaspé Peninsula consists of the Acadian orogen comprising the Gaspé-Metapédia-Aroostook Anticlinorium and Gaspé-Connecticut Valley Synclinorium. The main phase of deformation during the Acadian Orogeny here occurred during Early Devonian time (Rast et al, 1976 b).

In the next section the stratigraphic subdivisions of each of the major units in the study area, i.e. the

Middle Ordovician	Cloridorme Formation,
Middle Ordovician	Deslandes Formation,
Lower Ordovician	Tourelle Formation,
Lower Ordovician	Cap-Chat Melange,
Lower Ordovician to	
Upper Cambrian	Cap-des-Rosiers Group

are described in detail.

There are continuous and spectacular exposures, especially of the Cloridorme and Tourelle Formations along the coast. Inland, however, outcrops of Cambro-Ordovician rocks in eastern Gaspé Peninsula are scarce and widely scattered. Table 1 shows the stratigraphic

Table 1. Lithology and Structure of the Various
Stratigraphic Units of the Cambro-Ordovician Rocks, Gaspé
Peninsula, modified from McGerrigle (1959); Riva (1968);
Biron (1974); St. Julien and Hubert (1975); Hiscott (1978);
Pers. Com. Biron (1980).

PERIOD		ORDOVICIAN										GROUP/FORMATION	GRAPTOLITE ZONE	LITHOLOGY	TYPE OF DEPOSITS	STRUCTURE		
Ma																		
450	St. Julien & Osborne (1973)											Thrust Imbricated Structures	CLONIDORME FORMATION	CENTRAL WESTERN BLOCK	CLINACOGAPTUS SPINIFERUS MINIMUS CORVNAIDES CALICULARIS VAR. AMERICANA.	Black shales often dolomitic, graywacke, calcisiltite, dolastone.	Turbiditic facies with predominance of graywacke.	Faulted, tightly folded and overturned, one set of cleavages and two generations of folding.
460	McGerrigle (1959)															CLONIDORME FORMATION	CENTRAL WESTERN BLOCK	
470	St. Julien & Hubert (1975)											Thrust Imbricated Structures	CLONIDORME FORMATION	CENTRAL WESTERN BLOCK	CLINACOGAPTUS SPINIFERUS MINIMUS CORVNAIDES CALICULARIS VAR. AMERICANA.	Black calcareous shales and sandstones with dark gray calcisiltite and dolomitic limestone.	Monotonous rhythmic turbiditic association of silty and argillaceous bed. Highly fissile.	Repeatedly folded shales, siltstones and slates. One set of cleavage and two generations of folding.
480																CLONIDORME FORMATION	CENTRAL WESTERN BLOCK	
490												Thrust Imbricated Structures	CLONIDORME FORMATION	CENTRAL WESTERN BLOCK	CLINACOGAPTUS SPINIFERUS MINIMUS CORVNAIDES CALICULARIS VAR. AMERICANA.	Black calcareous shales and sandstones with dark gray calcisiltite and dolomitic limestone.	Monotonous rhythmic turbiditic association of silty and argillaceous bed. Highly fissile.	Repeatedly folded shales, siltstones and slates. One set of cleavage and two generations of folding.
500																CLONIDORME FORMATION	CENTRAL WESTERN BLOCK	
510												Thrust Imbricated Structures	CLONIDORME FORMATION	CENTRAL WESTERN BLOCK	CLINACOGAPTUS SPINIFERUS MINIMUS CORVNAIDES CALICULARIS VAR. AMERICANA.	Black calcareous shales and sandstones with dark gray calcisiltite and dolomitic limestone.	Monotonous rhythmic turbiditic association of silty and argillaceous bed. Highly fissile.	Repeatedly folded shales, siltstones and slates. One set of cleavage and two generations of folding.
520																CLONIDORME FORMATION	CENTRAL WESTERN BLOCK	

relationship between the various formations.

LOCAL GEOLOGY

Cloridorme Formation:

The Cloridorme Formation is exposed along the southern shore of the St. Lawrence River in the eastern part of Gaspé Peninsula. It has been divided into three structural blocks, i.e. the eastern, central, and western blocks, respectively, by Enos (1965). The Cloridorme Formation is assigned to the 'Orthograptus truncatus intermedius zone' of Late Wilderness and Trenton age from the graptolites collected by Enos (1965) and identified by Berry. Later studies of graptolites by Riva (1968) from samples collected by himself, McGerrigle (1954), and Stevens (1968) show two distinct and in part coeval sequences in the Cloridorme Formation. The first sequence consists of Enos' β - and γ -members along the coast east of Marsoui to Pointe Jaune. It contains Canajoharie and Lower Utica graptolites, such as Climacograptus spiniferus and others. These are characteristic for the γ -members west of Gros-Morne. Upper Canajoharie Orthograptus ruedemanni (Gurley) is most common in the γ -members near Gros-Morne. Orthograptus calcaratus, c.f. var. basilicus Lapw. of Early Canajoharie age is dominant in the β -members. The second sequence comprises Enos' α -members and yields Normanskill, post-Normanskill and Lower Utica graptolites (e.g. Nema-

graptus gracilis). The fault west of Grand Vallée marks the boundary between the δ -members in the western block against the β -members in the central block. This fault and the one west of Cloridorme (affecting the β -members) are the major faults reported for the area by Enos (1969). In the field, the effect of the latter is clearly visible.

The Cloridorme Formation consists of 60% dark slaty argillite. Interbedded are coarse greywackes (15%), calcareous wackes (3%), and calcisiltite (20%), dolomite, limestone, volcanic ash and silty dolomitic argillite (Enos, 1969). The rocks are often faulted, tightly folded, and overturned, but have not suffered extensive metamorphism. Enos (1965) referred to them as lower green-schist facies.

The Cloridorme Formation is best described as typical flysch, both from a sedimentological and a tectonic point of view, i.e., it consists of a thick succession of marine turbidites deposited in an elongate trough just prior (i.e. pretectonically) to the main (Taconic) orogeny. Paleocurrent directions indicate predominantly axial transport by turbidity currents, i.e. parallel to the axis of the present structural belt which probably corresponds to an elongated foredeep trough (Enos 1965).

Table 2 shows the lithology of the different members in the Cloridorme Formation.

Table 2. Lithology of the different members of the
Middle Ordovician Cloridorme Formation, modified from Enos' (1969),
Riva (1968), Biron (1971).

	AGE	BLOCK	MEMBERS	ESTIMATED THICKNESS IN METRES	LITHOLOGY
MIDDLE ORDOVICIAN	LOWER UTICA	WESTERN	γ_4	510	Predominantly graywacke, interbedded with shale and calcisiltite.
	UPPER		γ_3	475	Black shales, dolomitic shales, calcisiltite, calcareous wackes, minor dolostone.
	CANA-JOHARIE		γ_2	800	Graywacke, black shales, little calcisiltite.
			γ_1	550	Dolomitic silty shale, black shale with less abundant graywacke.
	LOWER CANA-JOHARIE	CENTRAL	β_7	835	Predominantly graywacke, interbedded with black shales.
			β_6	255	Black shales, thin bedded calcisiltite, dolostone.
			β_5	80	Graywacke, calcisiltite, shale.
			β_4	78.5	Black shale, calcisiltite, calcareous wacke nearly absent.
			β_3	43	Shale, calcisiltite, graywacke, base defined by first occurrence of graywacke.
			β_2	490	Shale, calcisiltite, calcareous wackes less abundant near the base.
			β_1	1175	Shale, graywacke, calcareous wacke, calcisiltite, dolostones.

Deslandes Formation:

The eastern block comprising the ~~ac~~ -members of Cloridorme Formation of Enos (1969) has been renamed Deslandes Formation by Biron (1974). It is characterized in larger part by a monotonous rhythmic turbiditic association of sandy, silty and argillaceous beds. Regionally the Deslandes Formation extends for tens of kilometers across strike with a maximum width of 15km. It also occurs in small outliers west of Marsoui (Fig. 2).

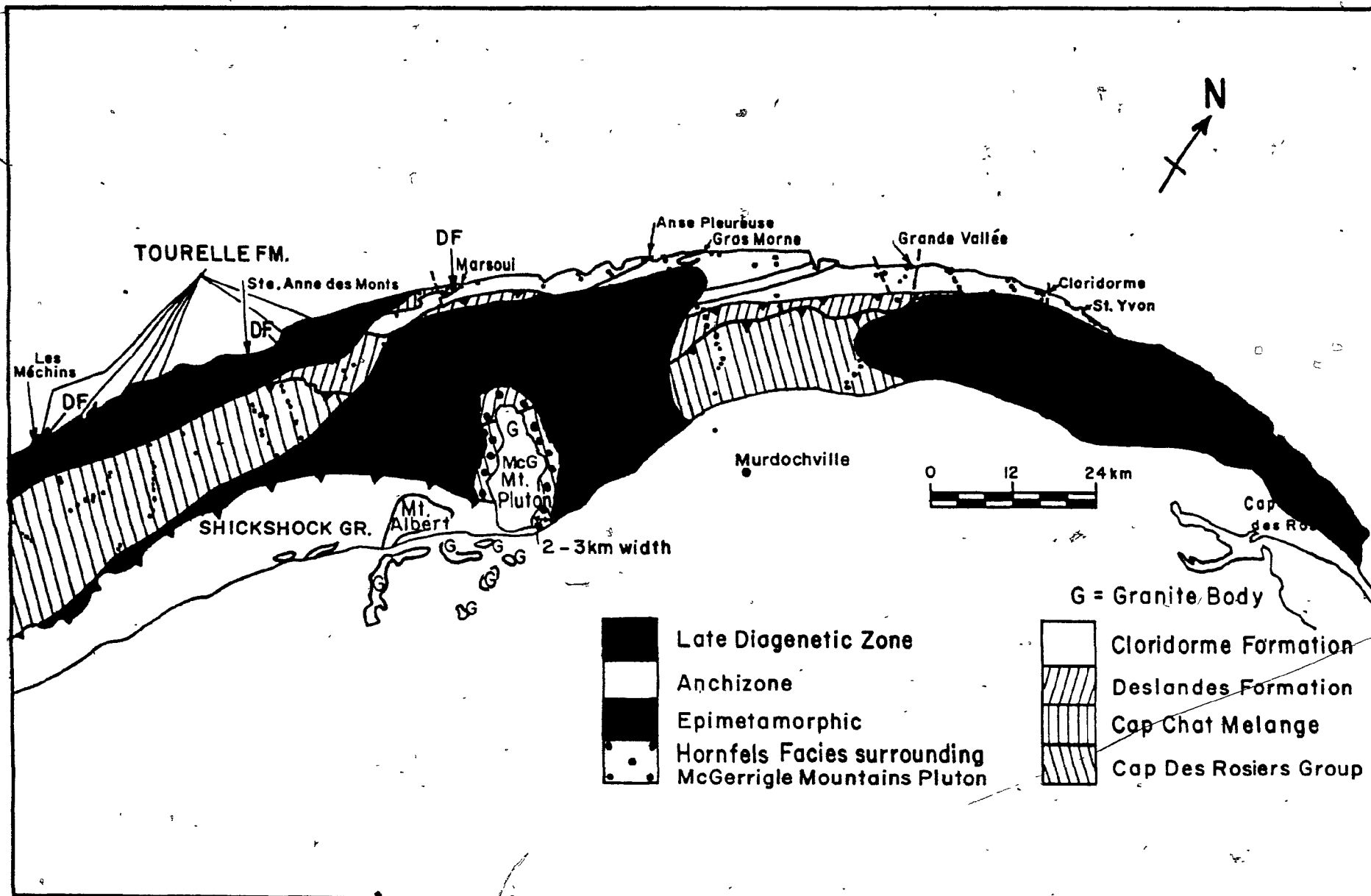
Tourelle Formation

The Tourelle Formation is of Late Arenigian to Early Llanvirnian age as determined from the occurrence of Glyptograptus dentatus (Riva, 1968). This is equivalent to zone D of the Levis Formation at Quebec City (Raymond, 1914 quoted in Hiscott, 1977). The formation outcrops between Les Mechins in the west and Ruisseau Castor in the east (Biron, 1974), although correlative units extend as far west as Riviere-du-Loup in Quebec. According to Hiscott (1977) predominantly thick, coarse graded sandstone layers of the Tourelle Formation represent deposits on a series of small coalescing submarine fans which formed in front of moving allochthons, during the early phase of the Taconic orogeny. The formation is believed to be 500 to 1000m thick; the top is not exposed, being truncated tectonically or by erosion (Hiscott, 1977).

FIGURE 2

Tectonic units of the study area (DF = Outliers of Deslandes Formation).

Y



Cap-Chat Melange:

The Cap-Chat Melange extends from Marsoui in the east to Cap des Mechins in the west and is moderately to intensely deformed. Liard (1972) described a similar zone of mélange beneath the Métis Formation south of Matane. In the Cap-Chat Melange blocks of various sizes are embedded in an argillaceous matrix in a chaotic manner. The Cap-Chat Melange is believed to represent the disintegrated debris of the upper part of the Ste-Anne River Nappe (Cap-des-Rosiers Group). According to St. Julien and Hubert (1975) this melange is a gravity induced accumulation of debris at the front of the thrust sheets. These chaotic masses consist predominantly of green and black shales. The Cap-Chat Melange is unconformably overlain by the Tourelle Formation and the former tectonically overlies the Cloridorme Formation near Marsoui (Biron, 1973).

Cap-des-Rosiers Group:

The Cap-des-Rosiers Group of Upper Cambrian to Lower Ordovician age, is exposed both along the coast and inland in the Ste-Anne River Nappe (Biron, 1974). This group consists of black and green shales or slates, limestones and some quartzites. According to St. Julien and Hubert (1975) it is a slope type deposit, characterized by coarse lenses of quartz arenite and limestone conglomerates and occurs throughout the Québec Appalachians (Lévis Fm., Pointe-de-la-Martinière Fm., St. Hénédine Fm., Stanbridge Fm.,

Kamouraska Fm., Ladrière Fm.). Similar bank-foot limestone breccias occur throughout most of the Appalachian fold belt, and give a rough estimate of the location of the former continental margin in Late Cambrian-Early Ordovician time (Rodgers, 1968). The Cap-des-Rosiers Group has been folded repeatedly and is at places overturned (Biron, 1974).

Shickshock Group:

The Shickshock Group forms part of the Internal Domain of St. Julien and Hubert (1975). It is a 6 to 16km wide zone of basic volcanic and pyroclastic rocks, interstratified with metasedimentary rocks. Here the ultramafic rocks of Mount Albert and Mount Serpentine are interpreted as obducted slices of oceanic crust (Laurent 1975, 1978). The Shickshock Group occupies the highest structural unit. Its relation with the Cap-des-Rosiers Group is not clear. There is evidence of a faulted contact between the two groups (de Römer, 1977).

McGerrigle Mountains Pluton:

The McGerrigle Mountains pluton is a northerly elongate discordant body of leucocratic rocks of approximately 130km² areal extent. It represents a multiple intrusion and consists of hybrid granitic rocks complexly invading an earlier basic phase (de Römer, 1977). Radiometric dating (K/Ar) of porphyritic granite, biotite granodiorite, and a coarse

red granite indicates that the pluton has post-kinematically intruded the Cambro-Ordovician rocks around 350m.y. (Late Devonian). However, the dating from a hornblende-biotite metasediment shows a younger 319 ± 10 m.y., i.e. Early Mississippian age (de Römer, 1977). Isolated outcrops of nearby plutonic bodies of Mount Hog's Back and Mount Valliers-de-Saint-Réal in the Acadian belt also show an early Devonian age of emplacement. The McGerrigle Mountains pluton has produced a 1.5 to 3km wide high-grade metamorphic aureole in which metamorphic grade reaches the potash-cordierite hornfels facies.

SAMPLING PROCEDURE

Sampling was done in successive stages during 1979. In the early summer of 1979 the most external part of the Taconic Belt of Gaspé Peninsula along the south shore of the Gulf of St. Lawrence was sampled. This region is readily accessible and has remarkably well exposed outcrops. In late summer and fall 1979 samples were collected from different north-south sections across strike of various formations in order to establish a broader picture of regional maturation patterns. Continuous sampling from the northernmost parts of the External Domain to the Internal Domain of the Taconic Belt in the south was difficult due to scarcity of outcrops and limited accessibility of the area. In the final stage, sampling was concentrated on areas of

special interest. The sampling interval depended to a large extent on the availability of outcrops. Sample interval ranges from 10 to 20 m where shales are thick and abundant (e.g. in the Cloridorme Formation). Sampling distance is reduced to around 10m where the shales are thin and less abundant (e.g. in the Cap-des-Rosiers Group). In the vicinity of local fold structures, faults, and across thrust boundaries detailed sampling was carried out. A total of 350 samples were collected for thermal maturation studies from 20 north-south sections and one east-west section along the coast (Fig. 9). The number of samples taken from individual sections ranges from 5 to 20. Most of the samples are black shales with a few green (11) and red (3) shales. All samples were processed for clay mineralogy and of these 145 black shales were also processed for reflectance studies.

CHAPTER THREE

CLAY MINERALOGY AND ILLITE CRYSTALLINITY

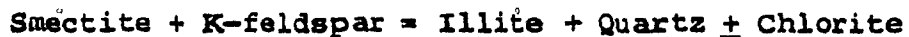
Quantitative and semi-quantitative determinations of the clay mineralogy and crystal chemistry provide the fastest and most easily useable tool for assessing diagenetic grade. In this study the following parameters were measured: illite crystallinity, intensity ratio of illite peaks 002/001 and 004/003 peak intensities (Brindley, 1961) and the illite 002/ chlorite 004 ratio.

Two important changes occur in clay minerals during diagenesis. The first is the transformation of smectite to illite or chlorite through a sequence of mixed layer clay minerals that begins with random interstratification, then proceeds to short-range ordering and later long-range ordering of the illite (or chlorite) and smectite layers (Weaver, 1958; Dunoyer de Segonzac, 1970; Perry and Hower, 1970). Secondly, at higher grades illite is transformed into well crystallized dioctahedral mica (Maxwell and Hower, 1967; Frey et al., 1980, Kisch, 1980).

Transformation of poorly crystallized illite into well developed dioctahedral mica results in increased sharpness of the illite (001) diffraction peak at 10 Å. The sharpness of this peak was first used as a parameter of maturation by Weaver (1960, 1961). The width of the

illite (001) peak at half height is taken as a measure of illite crystallinity (Kübler, 1967, 1968) and is now widely used as a method of establishing the degree of clay mineral diagenesis. The higher the thermal diagenesis the better is the crystallinity, the narrower the peak and the lower is the index of crystallinity. A second method used for inferring diagenetic grade is the percent of smectite in mixed-layer clays. The expandibility of the mixed-layer illite/smectite can be determined from the shift of the characteristic illite 10Å reflection upon glycol saturation (Reynolds and Hower, 1970). Zero percent expandibility corresponds to 100 weight percent illite and 100 percent expandibility corresponds to 100 weight percent smectite.

In general, the mineralogical changes during burial diagenesis in shales under alkaline conditions can be represented by the reaction:



(Hower et al, 1976).

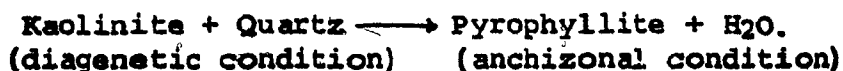
Hower et al. (1976) emphasized that shales at different stages of clay diagenesis behave essentially as chemically closed systems with respect to iron, magnesium, silica and aluminium. However, these authors do not discuss the significance of the cements that may be transferred in pore water into the interbedded sandstone units during compaction of shales when interparticle pore water as well as interlayer water from montmorillonitic clays migrates

from the shales to the sands. The conversion of smectite to illite involves an increase in net negative layer charge of the expandable layers either due to tetrahedral substitution of Al^{3+} for Si^{4+} or by substitution of Fe, Mg for Al^{3+} in the octahedral layer. The balancing of the negative layer charge can be achieved by incorporation of K^+ in interlayer positions. The aluminium and potassium for this conversion may be provided by the breakdown of K-feldspar or mica. During this transformation of smectite to illite, there is a release of silica. The excess of silica may form quartz overgrowths in intercalated sandstones. Iron and magnesium released during illitization of smectite probably forms chlorite (Hower et al, 1976). The question still remains whether or not decomposition of K-feldspar necessary for illitization is also an adequate source for the formation of chlorite. Boles and Franks (1979) stated that aluminous smectite layers are preferentially converted to illite, leaving behind the more iron- and magnesium-rich smectite layers. These smectite layers, when transformed to illite, release iron and magnesium which would lead to the formation of late diagenetic chlorite and carbonates. Another possible source of Fe and Mg for chlorite formation is the decomposition of detrital biotite, and other mafic minerals as well as possibly dolomite.

Other factors besides thermal maturation may influence illite crystallinity, i.e., (i) previous weathering



history, (ii) lithology of the shale, particularly the amount of organic matter, (iii) the chemical composition of pore fluids, and (iv) tectonics. During continental weathering potassium is leached from micas and illites and mixed-layer clays are formed. 'Blocking' of the open sheets of either illite or swelling minerals by either organic matter or metallic elements may inhibit the process of illitization. Also, the oxidation of organic matter in black shales creates an acidic environment which appears to be unfavourable to illitization. An insufficient supply of potassium in calcareous shales, low porosity and permeability may also hinder the process of illitization. During syndeformational recrystallization, on the other hand, illite crystallinity increases from the flanks of anticlines to hinges (Kalkreuth, 1979). Due to these factors, the reactions involving the disappearance of certain clay minerals (e.g. kaolinite, alleverdite, etc.) or the appearance of new ones (e.g. illite, pyrophyllite, paragonite, chlorite, margarite, etc.) during progressive diagenesis does not always take place under the same physical conditions. The reactions involved in these processes have recently been discussed by Frey (1978) in a study of the progressive diagenesis and metamorphism of Liassic black shales in Switzerland (in a cross-section from the Jura Mountains to the Swiss Central Alps). One of his reactions is listed below:



The circulation of dilute acidic solutions favours the diagenetic formation of kaolinite, especially in sandstones (Dunoyer de Segonzac, 1970). Reactions of pyrophyllite with calcite leads to the formation of margarite in the epimetamorphic zone. Finally, at higher metamorphic grades margarite is consumed by a continuous reaction producing plagioclase (Frey, 1978).

In x-ray diffraction instrumental factors affect the analysis of illite crystallinity. Therefore, results of different laboratories can be compared only to a limited extent. Some of the differences due to the goniometer (scanning) and chart speeds can to some extent be 'normalized' by expressing the peak widths at half heights in degrees $\Delta 2\theta$, rather than in mm. For identical slit settings, time constant, radiation, and scale factors, the peaks (in 2θ) tend to be broadened for a faster scanning rate. Weber (1972) used a quartz standard to determine relative illite crystallinity:

$$\frac{H_p(001) \text{ illite (mm)}}{H_p(001) \text{ quartz (mm)}} \times 100$$

H_p = peak width at half height.

This method reduces instrument effect and would render measurements comparable between different laboratories. Also, the crystallinity of the quartz standard has to be the same for every laboratory.

The main advantages of using illite crystallinity as a diagenetic indicator are speed of determination and

relatively low expense. If the disturbances caused by other factors mentioned above are kept in mind, illite crystallinity can be applied to discern differences in the degree of diagenesis and lowest-grade metamorphism as a consequence of thermal alteration (Frey et al, 1980; Kisch, 1980).

ORGANIC MATTER MATURATION

Modern sediments rich in organic matter include sapropel and gyttja. The terms refer to sediments formed under reducing and oxidizing conditions in the bottom waters, respectively. Red shales indicate oxidizing conditions within the sediment and have a low content of organic matter. Absence of molecular oxygen from bottom waters favours the accumulation of organic matter rich (sapropelic) black muds. In the Quebec Appalachians, quantitative analyses have shown that the black shales have an organic carbon content (0.90 - 1.45%) an order of magnitude higher than that of green shales (0.10 - 0.28%), whose organic carbon, in turn, is an order of magnitude higher than that of red shales (0.02 - 0.05%) (Ogunyomi, 1980). Studies of 800 samples of black shales from different localities of North America, however, show an average of 3% organic carbon content (Vine and Tourtelot, 1970). According to Dow (1977) 0.4% organic carbon is a minimum value required for potential source rocks to generate any significant amounts of petroleum.

The stages before, during, and after the generation of commercially significant hydrocarbons correspond to 3 facies of organic matter maturation: (1) the immature, (2) mature, and (3) supermature zones, respectively. However, the appearance and disappearance of liquid and gaseous hydrocarbons is not sharply defined in terms of subsurface temperature depending on type of organic matter, the age of the sedimentary basin, and to some extent on analytical techniques. During the initial stages of diagenesis, the most important chemical progenitors of petroleum which include humic acids, fulvic acids, amino acids, fatty acids etc. derived from lower organisms (i.e. algae, animal plankton, bacteria etc.) are incorporated into kerogen. Kerogen is a higher molecular weight, insoluble, complex polymeric material. From the beginning of the mature facies the proportion of kerogen in sediments progressively decreases during burial as liquid and/or gaseous products, especially hydrocarbons and an insoluble carbon rich residue are formed. Natural kerogens are usually classified into four groups which vary greatly in composition. Fig. 3 shows kerogen types and principal products of kerogen evolution. Humic kerogen will yield mostly dry gas and CO_2 at high maturity levels although very small quantities of liquid petroleum may also be formed but not expelled (Teichmüller, 1974). Liptinite kerogen will yield a full suite of hydrocarbon products, while algal kerogen will generate predominantly oil and very little CO_2 and H_2O

FIGURE 3

Four-fold subdivision of kerogen or coal.

Modified from Bostic (1979) and Tissot et al. (1980).

Pennsylvanian coal (Hardwood, 1978).

Arrows show directions of change with increasing thermal maturation (Tissot et al., 1977).

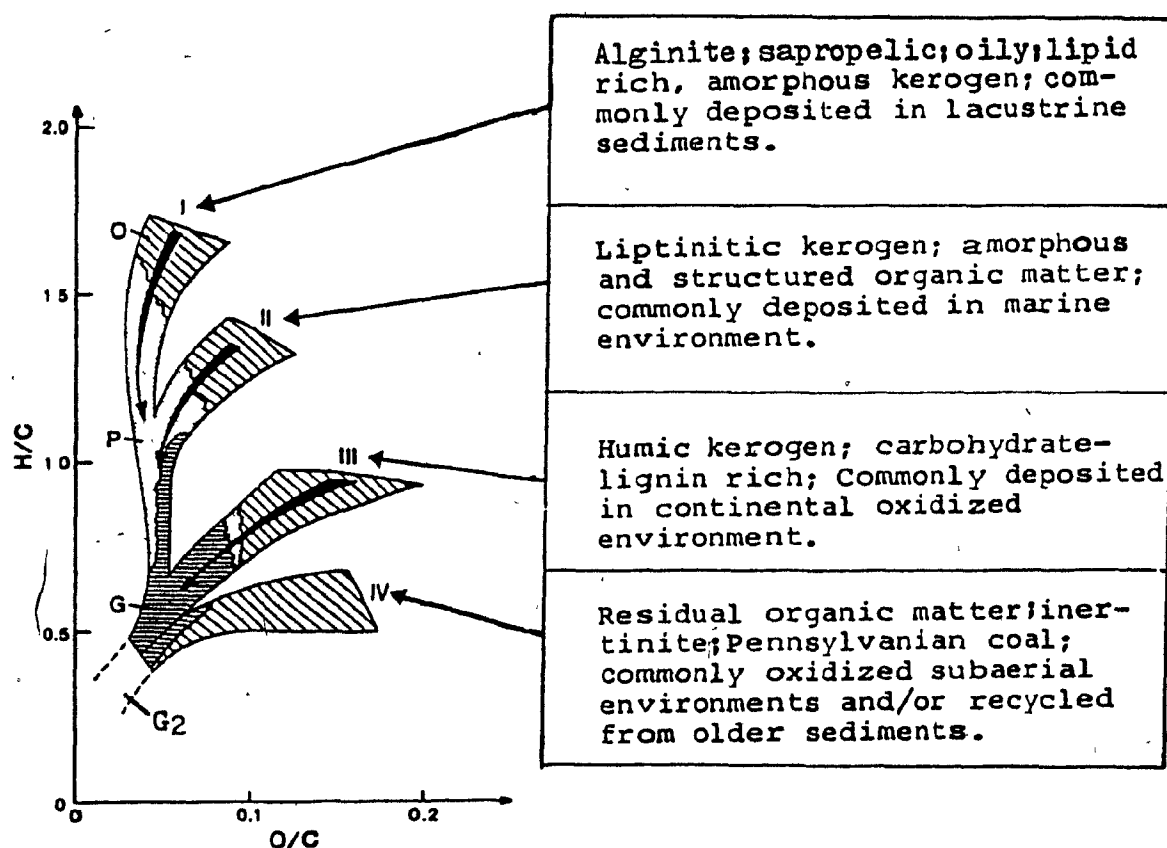
O, Formation of oxygenated products (CO_2 , H_2O , heavy heteroatomic molecules) plus N_2 .

P, Formation of petroleum.

G, Formation of wet gas C_2H_6 to C_6H_{14} .

G₂, Formation of dry gas.

In advanced stages of thermal maturation, the characterization of the original type of kerogen becomes difficult, because the chemical compositions of the different kerogen types converge.



because of its low initial oxygen content (Tissot et al, 1974).

Coal petrologists long ago established coal ranks as a scale for the thermal maturation of coal seams. This scale has been used over the entire range from lignite to anthracite. The beginning phases of maturation as well as concluding phases in kerogen closely parallel those of coal. The wealth of data that exists on coal maturation can be applied to kerogen maturation (Stach et al, 1975). Recently (Frey et al, 1980; Kisch, 1980) the concept of thermal maturation of kerogen has been applied in the realm of low-grade metamorphism.

The techniques used to define kerogen types and levels of thermal maturation are based on optical and chemical characteristics of extractables (e.g. hydrocarbons) and nonextractables (kerogen). Scales established by optical means from the study of organic matter reflectance and spore and pollen coloration have been applied in this study of nonextractables.

Changes in the kerogen with burial (mainly dependant on temperature and heating time) are expressed in its chemical and physical appearance. The simplest indicator of thermal maturation is the color of kerogen in transmitted light. The opacity of kerogen varies directly with the degree of thermal alteration. A related technique involves color changes in conodonts. Epstein et al. (1977) have shown that conodonts taken from rocks which have undergone only

shallow burial are generally light yellow in color. With increasing depth of burial conodonts progressively darken through golden yellow to brown (mature) and finally to black (post-mature). According to Correia (1967) amorphous kerogen is the most suitable material for determination of levels of thermal maturation of organic matter. Other materials that can be used, in order of preference, are miospores, acritarchs, chitinozoans, and woody tissue fragments. The maximum level of organic maturity of the authigenic kerogen can be obtained from the lightest colored kerogen in prepared samples. Elemental analysis is a useful method of identifying and comparing kerogen types and coal macerals. Tissot et al. (1974) have defined pathways for different types of kerogen applying Van Krevelen's diagram (1961), in which the atomic H/C ratio is plotted against the atomic O/C ratio of coal macerals, to kerogens. To date, this serves as the most effective tool of predicting maturation level, oil and gas potential, type of organic matter, and facies variations in sediments.

Microscopic study of organic matter in reflected light, has shown that the progressive carbonization of organic matter with depth of burial may be viewed as analogous to the gradual increase of the optical reflectance of vitrinite. Vitrinite owes its origin to the carbohydrate-rich woody tissue of higher plants, all of which contain considerable quantities of oxygen. The 'reflectance' (R_o) of vitrinite is used to assess the thermal maturation of or-

ganic matter because (i) of its predictable behavior and and because (ii) vitrinite has a relatively uniform composition. The term ' R_o ' stands for 'percent reflectance in oil'. The limitations of this technique have been discussed by Jones and Edison (1978) and Heroux et al. (1979). In pre-Devonian sediments reflectance is measured on asphaltic pyrobitumen owing to lack of vitrinite in these deposits. The lack of higher plants in pre-Devonian sediments means that the fossiliferous sediments of this age do not contain any quantities of lignin and its derivatives. Bituminous substances which decompose before melting are called pyrobitumens (Bell and Hunt, 1963). Low-oxygen (<5%) pyrobitumens are called asphaltic pyrobitumens. For a more detailed genetic classification of organic matter see Rogers et al. (1974).

Robert (1973) and Ammosov et al. (1975) have tried to establish an R_o scale for asphaltic pyrobitumen. They assumed that reflectance values for pyrobitumen and vitrinite are the same with increasing temperature in the range of 1.0 to 2.0 R_o (mean), although reflectance values from pyrobitumen show a greater scatter than those from vitrinite of equal rank. The influence of each type of asphaltic pyrobitumen (elaterite, wurtzilite, albertite, impsonite, and anthracolite) or 'asphaltic pyrobitumen-like' fragments (acritarchs, chitinozoans, graptolites, etc.) on reflectance is not yet fully understood. Sikander and Pitton (1978) have found that organic matter from Cambro-Ordovician

platform rocks of Quebec Appalachians closely resemble vitrinite. In the light of Abraham's (1960) work these authors describe this vitrinite-like organic matter as dispersed asphaltic pyrobitumen. The organic matter from the study area is mainly in the form of dispersed asphaltic pyrobitumen. Organoclasts like black fragments, dispersed amorphous particles, chitinozoans, and graptolites are also present. Achab (pers. comm., 1980), reported similar types of organic matter from different localities in the Quebec Appalachians.

Organic matter reflectance is more reliable than illite crystallinity for determining the thermal maturation that defines low-grade boundary of the anchizone (and lower grades), however, it is less reliable for the higher-grade boundary of the anchizone. It is less sensitive to lithology or pore fluid chemistry than illite crystallinity. Reflectance values can also be calibrated with temperature provided that the duration of heating is known (Karweil, 1956).

INDICATORS FOR THE LEVEL OF DIAGENESIS AND LOW GRADE

METAMORPHISM

Tissot et al. (1974) used 'diagenesis' for rocks containing immature kerogen, i.e., those having reflectance values $R_o < 0.5\%$. This stage is characterized by the production of CO_2 , H_2O and CH_4 owing to the oxidation of organic matter and the break down of the $C=O$ bond. This zone is equivalent to the early diagenetic zone of Foscolos et al. (1976) and extends from the surface down

to 1000-1500m (50°C) depth. In the mature stage hydrocarbons are formed, the H/C ratio drops, and there is a decrease in aliphatic bonds. The 'oil window', wet gas, and gas condensate zones constitute the so-called mature stage. This stage constitutes the 'middle diagenetic zone' of Foscolos et al (1976); reflectance ranges from 0.5 to 1.5%. This middle diagenetic zone where most hydrocarbons are generated is also called catagenesis zone. The latter is defined by Tissot and Welte (1978) with reflectance values ranging from 0.5 to 2.0. For catagenesis Tissot and Welte (1978) have suggested a temperature range of 50°C and 150°C. Hunt (1977) extends catagenesis to 200°C, near the end of the dry gas zone. According to Winkler (1975), a temperature of approximately 200°C also marks the boundary between 'diagenesis' and 'very low-grade metamorphism' (Laumontite-prehnite-quartz facies; pumpellyite-prehnite-quartz facies etc.). A temperature of about 300°C (biotite isograde, 300°C) defines the boundary between 'very low-grade metamorphism' and 'true regional metamorphism' (green schist facies).

Shales subjected to conditions less intense than true regional metamorphism react sluggishly and are sensitive to the chemical environment. Seemingly, no sharp boundary exists between the realms of diagenesis and metamorphism. The transitional zone between diagenesis and metamorphism (epimetamorphic zone) is called the anchizone. This zone generally marks the end of dry gas generation (Kisch, 1975; Frey et al., 1980; Kübler et al., 1979; Heroux et al., 1979). The term

FIGURE 4

Scales of thermal maturation of organic matter based on different parameters.

anchimetamorphism was first used by Harrassowitz (1927, 1928) and later popularized by Kübler (1967). Various other terms have also been suggested to define this stage, e.g.: incipient metamorphism (Wilson 1926); metagenesis (Kossovskaia and Shutov 1958); burial or very low stage metamorphism (Winkler 1975); eometamorphism (Landis 1967) etc.

Kisch (1980) noted that in normal circumstances the development of anchizone illite crystallinity corresponds with coal ranks near the semi-anthracite/anthracite boundary (2.6 to 2.7%, $\bar{R}_{O,max}$). This result is in agreement with that obtained by Foscolos and Kodama (1974) and Foscolos et al. (1976) in the Lower Cretaceous sediment of north-east British Columbia. There the anchizone illite crystallinity is associated with reflectance of 2.5 to 2.7% $\bar{R}_{O,max}$. On the other hand Wolf (1975) observed a much higher reflectance value, 5% $\bar{R}_{O,max}$ (high-rank anthracite) in rocks with anchizone illite crystallinity values in areas that underwent heating by deep seated plutons.

In this study the maturation zones are denoted by the terms diagenetic zone, anchizone, and epimetamorphic zone. The boundary between the diagenetic zone and anchizone is defined by a reflectance value of 2.7% and an illite crystallinity value of 3.3mm. The boundary between the anchizone and epimetamorphic zone is defined by a reflectance value of 5.0% and illite crystallinity value of 1.9mm. Illite crystallinity is a better parameter to define

the boundary between anchi- and epimetamorphic zones because of its consistent and predictable behavior at this level of maturation. On the other hand, organic matter reflectance better defines the boundaries between various stages of diagenesis and anchimetamorphism. Beyond the diagenetic zone, organic matter reflectance values show high anisotropy. Figures 5 and 6 show correlation of % \bar{R}_o (mean) and illite crystallinity with zones of diagenesis, anchimetamorphism and epimetamorphism.

FIGURE 5

Correlation of % R_o (mean) with zones of diagenesis, anchi-metamorphism and epimetamorphism.

X-ray	Foscolos et al. (1976)	Tissot & Welte (1978)	Teichmüller et al. (1979)	Heroux et al. (1979)	Kubler et al. (1979)	Kisch (1980)	This study
	Early Diagenesis 0.5 Middle diagenesis 1.5 Late diagenesis ?	Diagenesis 0.5 0.9 Cata- genesis 2.0 Meta- genesis 4.0 META - MORPHISM	Diagenesis 4% Max Anchi- zone 5% Max to 10 %Max Epizone	DIAGENE- SIS 2.5 ANCHI- ZONE 4.2 EPIZONE	Diagenesis 2.6 Anchi- zone 4.2 Epizone	2.6 2.9 Max 4% Max	Diagenesis 2.7 Anchi- zone 5.0 Epi- zone

FIGURE 6

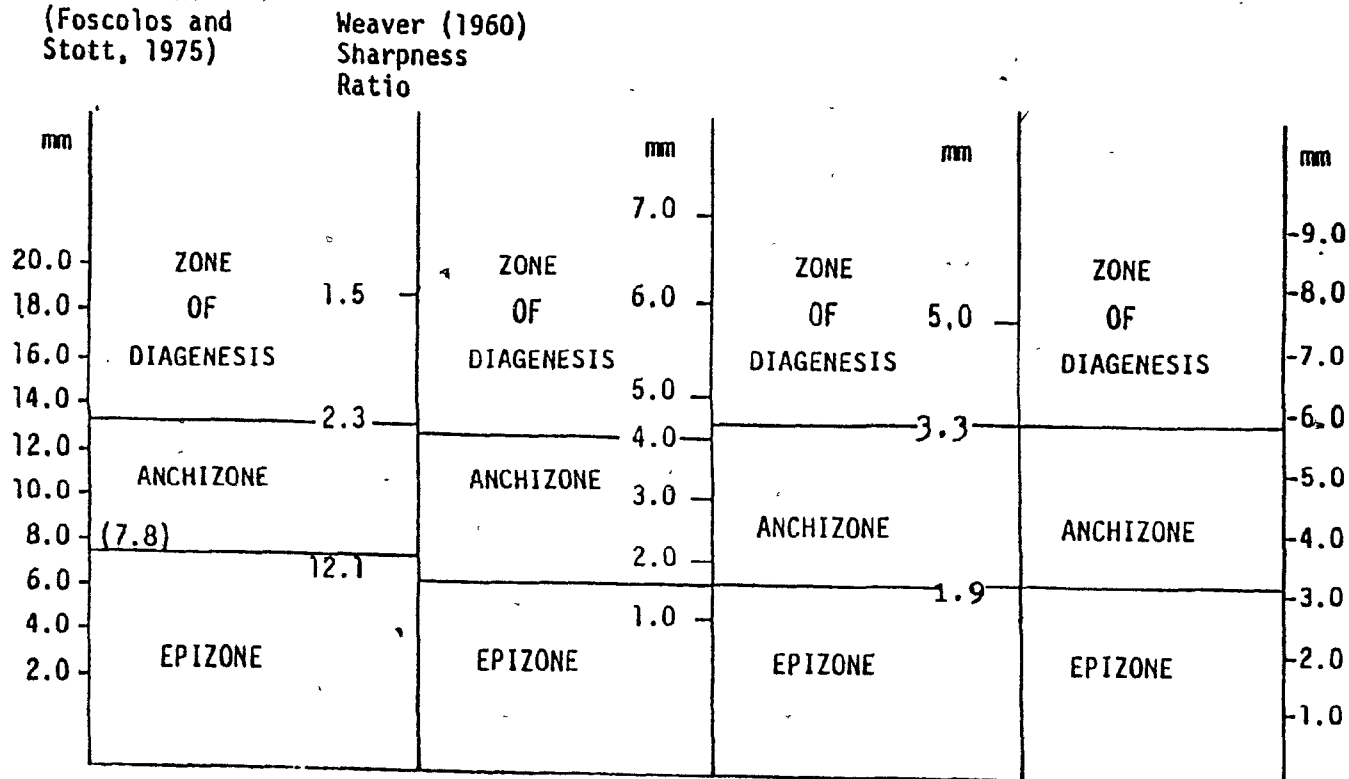
Correlation of illite crystallinity with zones of diagenesis, anchimetamorphism and epimetamorphism (modified after Foscolos and Stott, 1975).

Institute of
Sedimentary
and Petroleum
Geology, G.S.C.
Philips 1200mm/h
1°/2cm/min
CoK α radiation
k satur. samples
at 50% R.H.
(Foscolos and
Stott, 1975)

Pau
(S.N.P.A.) X'Y
8°/2cm/min
(Kubler,
1968)

I.N.R.S.
(PETROLE)
X'Y
2.4°/2cm/min
CuK α
radiation
(this
study)

Strasbourg
X'Y
241 mm pour
28°
2°/2cm/min
(Dunoyer
de Segonzac,
1970)



Correlation of illite crystallinity with zones of diagenesis,
anchimetamorphism and epimetamorphism
(Modified after Foscolos and Stott, 1975).

FIGURE 7

Boundary between diagenetic zone, anchizone and epimeta-
morphic zone by illite crystallinity.

7



CHAPTER FOUR

RESULTS

The study area has been subdivided into three diagenetic to low-grade metamorphic zones on the basis of asphaltic pyrobitumen reflectance (95 samples) and illite crystallinity (350 samples). These zones are: (i) the epimetamorphic zone (mean reflectance $> 5.0\%$; illite crystallinity $< 1.9\text{mm}$); (ii) the anchizone ($2.7 \leq \bar{R}_0 < 5.0\%$; $1.9\text{mm} < \text{IC} \leq 3.3\text{mm}$); (iii) the late diagenetic zone ($\bar{R}_0 < 2.7\%$; $\text{IC} > 3.3\text{mm}$) (Fig. 8, 15).

Assuming the reflectance values are controlled primarily by temperature the maturation pattern based on reflectance values consists of a broad central thermal dome, east of which a trough with a thermal low at the centre extends to the eastern tip of the peninsula, and west of which a thermal slope with progressively lower isotherms from south to north occupies the western part of the study area (Fig. 15). Similar general patterns of maturation are observed using illite crystallinity, however, with some modifications in detail (Fig. 8).

The central thermal dome displays a concentric array of zones around the McGerrigle Mountains pluton. These zones comprise the anchizone, epimetamorphic zone, and higher grade metamorphic zones in the immediate contact aureole around the pluton. The epizone forms a broad thermal halo which averages 16 to 20km in width. Toward the north-

east the zone is even wider extending as far as 30km from the pluton. The westward extension of the epizone west of the halo, i.e. north of the Shickshock Group, is only about 1km wide. The epizone comprises mainly the Cap-des-Rosiers Group and Deslandes Formation, as well as a small part of the Cloridorme (X-members) Formation to the northeast. The anchizone in this area to the north of the epizone, has an exposed width of 3 to 5km along the shoreline of the St. Lawrence River. It is mostly developed in the Cloridorme Formation, a small part of the Cap-Chat Melange in the west and a part of the Deslandes Formation to the south.

East of the thermal dome the late diagenetic zone attains a width of 8 to 14km. Here both the anchizone and diagenetic zones are developed in part of the Cap-des-Rosiers Group, Deslandes and Cloridorme Formations.

In the area west of the thermal dome, the late diagenetic zone extends to the western boundary of the study area at Les Mechins. It includes the late Ordovician Tourelle Formation, Cap-Chat Melange and outliers of the Deslandes Formation. In this region, the anchizone encompasses the Cap-des-Rosiers Group and a part of the melange.

The results of illite crystallinity determinations and pyrobitumen reflectance values are discussed separately under the following headings: (i) central thermal dome around the McGerrigle Mountains pluton; anchi- and late diagenetic zones (ii) east, and (iii) west of the central

thermal dome.

ILLITE CRYSTALLINITY

Illite crystallinity values were determined for 350 samples. From these data, an isopleth map of the area was constructed (Fig. 8). The contour intervals range from 0.2 to 0.5 mm. In detail, the shape of the isopleths is affected by local variations in illite crystallinity and availability or accessibility of outcrops, which is the reason for using different contour intervals in different parts of the map.

In the central thermal dome illite crystallinity improves radially inward towards the McGerrigle Mountains pluton from anchizonal to epizonal conditions. Immediately east of the north-south trend of the McGerrigle Mountains pluton an anomaly has been noted with few samples showing relatively poor crystallinity (1.4 to 2.6mm) in the Rivière Claude section (Fig. 10, Section 12). However, best crystallinity (1.0mm) has been noted in this section just north of this anomaly.

In the late diagenetic and anchizone, west of the thermal halo the isopleths are regular and approximately northeast trending as contrasted with the concentric patterns in the thermal dome. The thermal slope (systematic improvement in crystallinity perpendicular to strike) becomes less steep from the eastern Ste-Anne-des-Monts I

FIGURE 8

Isopleth map of illite crystallinity (mm), Taconic Belt, Gaspé Peninsula. The value of IC in mm can be converted to 2θ notation by multiplication by 0.13.

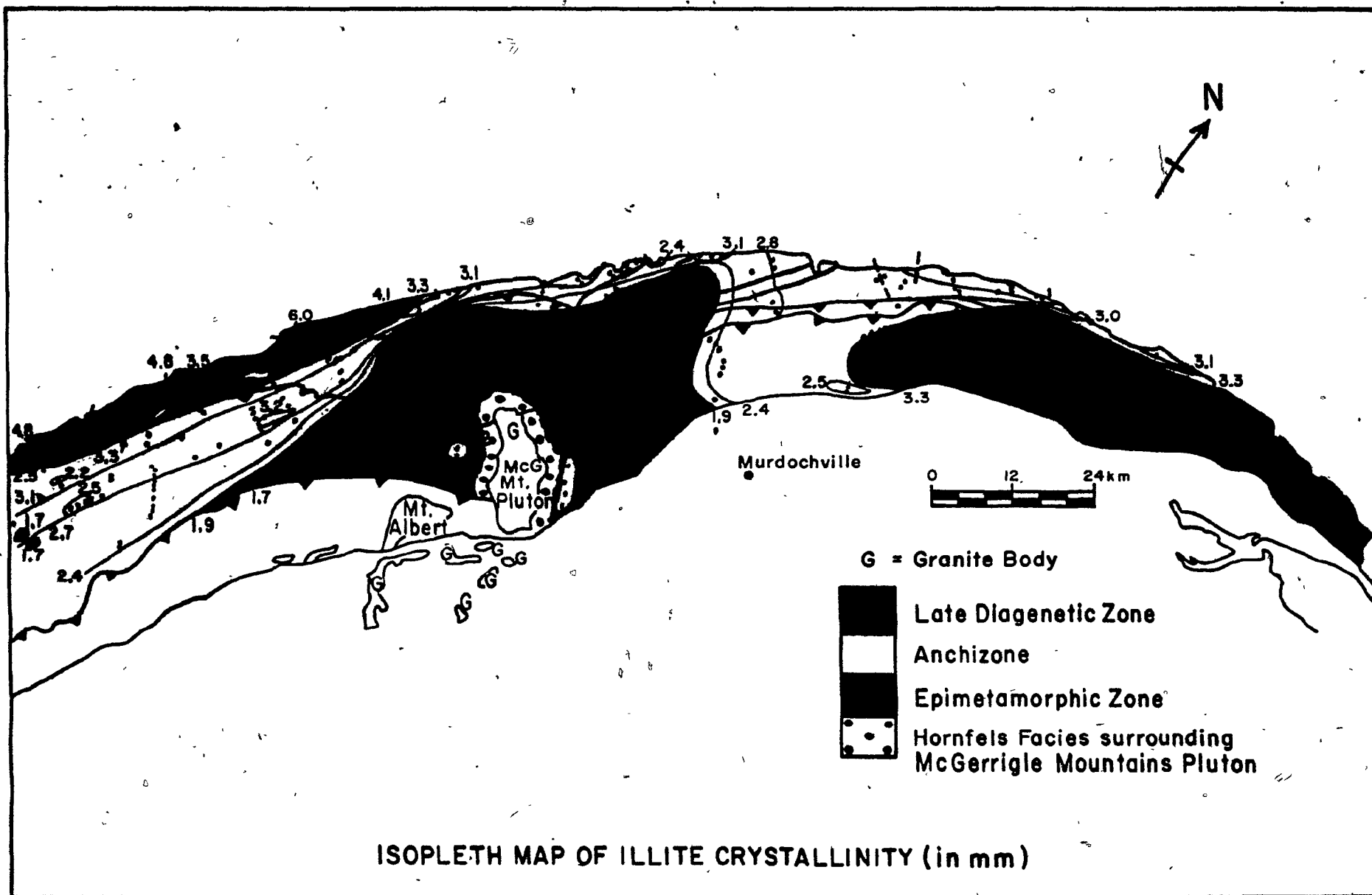


FIGURE 9

Selected sections in the study area.

- | | |
|---------------------------|--------------------------|
| 1. Anse-au-Griffon | 2. Rivière-au-Renard |
| 3. Petit Cap | 4. Fame point |
| 5. Cloridorme | 6. Pointe-a-la-Fregate |
| 7. Grande Vallée | 8. Manche-d'-Epee |
| 9. Anse Pleureuse | 10. Mont-Louis |
| 11. Mont-St-Pierre | 12. Rivière-à-Claude |
| 13. Marsoui | 14. Ste-Marthe |
| 15. Tourelle | 16. Ste-Anne-des-Monts I |
| 17. Ste-Anne-des-Monts II | 18. Cap-Chat I |
| 19. Cap-Chat II | 20. Les Mechins. |

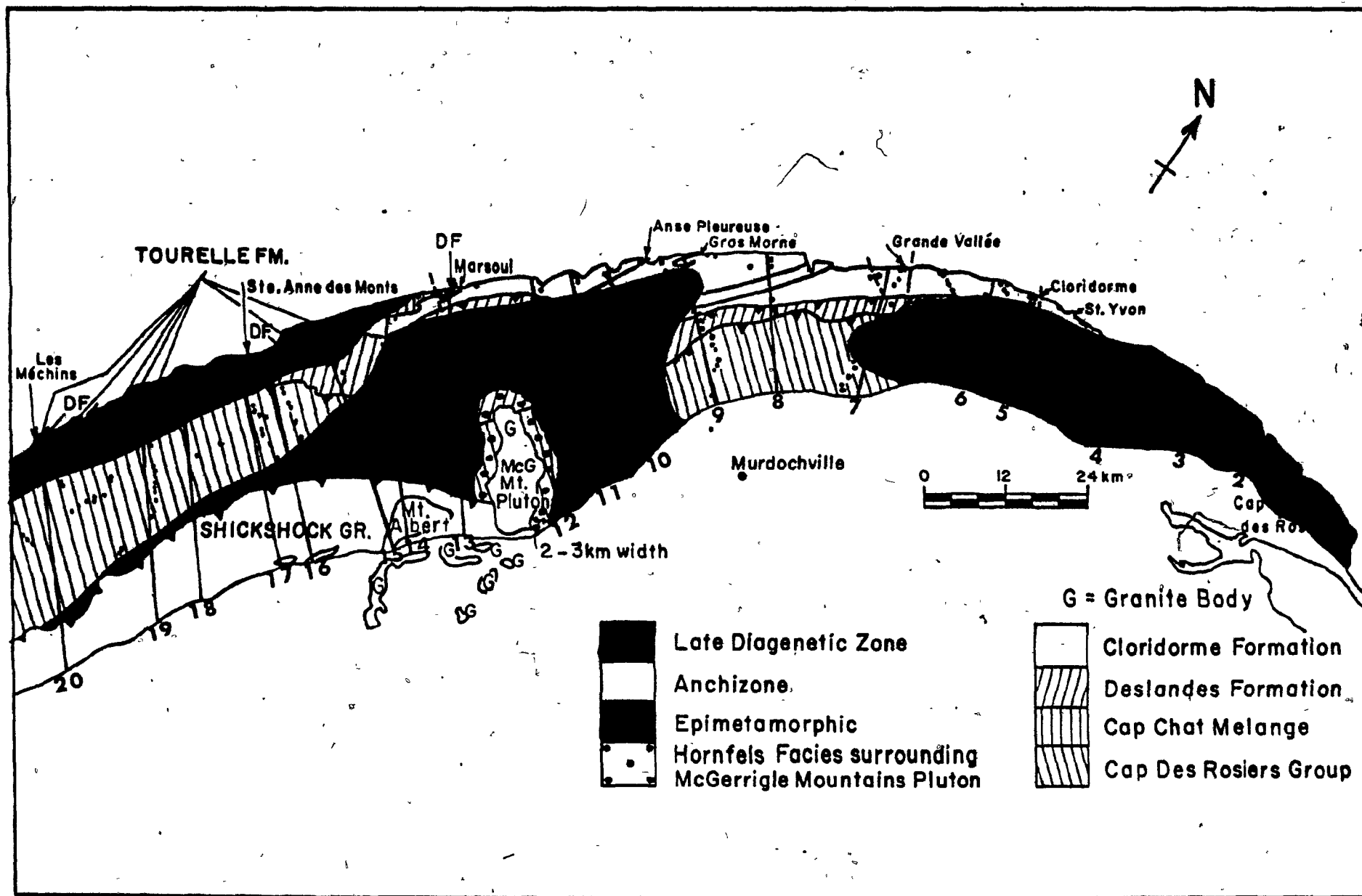


FIGURE 10

Illite crystallinity values plotted along north-south cross sections in the study area. For location of sections see FIGURE 9. Sections 12 and 13 are located in the thermal dome. Sections 2, 4, 7 and 9 are located east of the thermal dome. Sections 15, 16, 19 and 20 occur west of the thermal dome. Each point in the section represents the average of up to five analyses.

CL = Cloridorme Formation

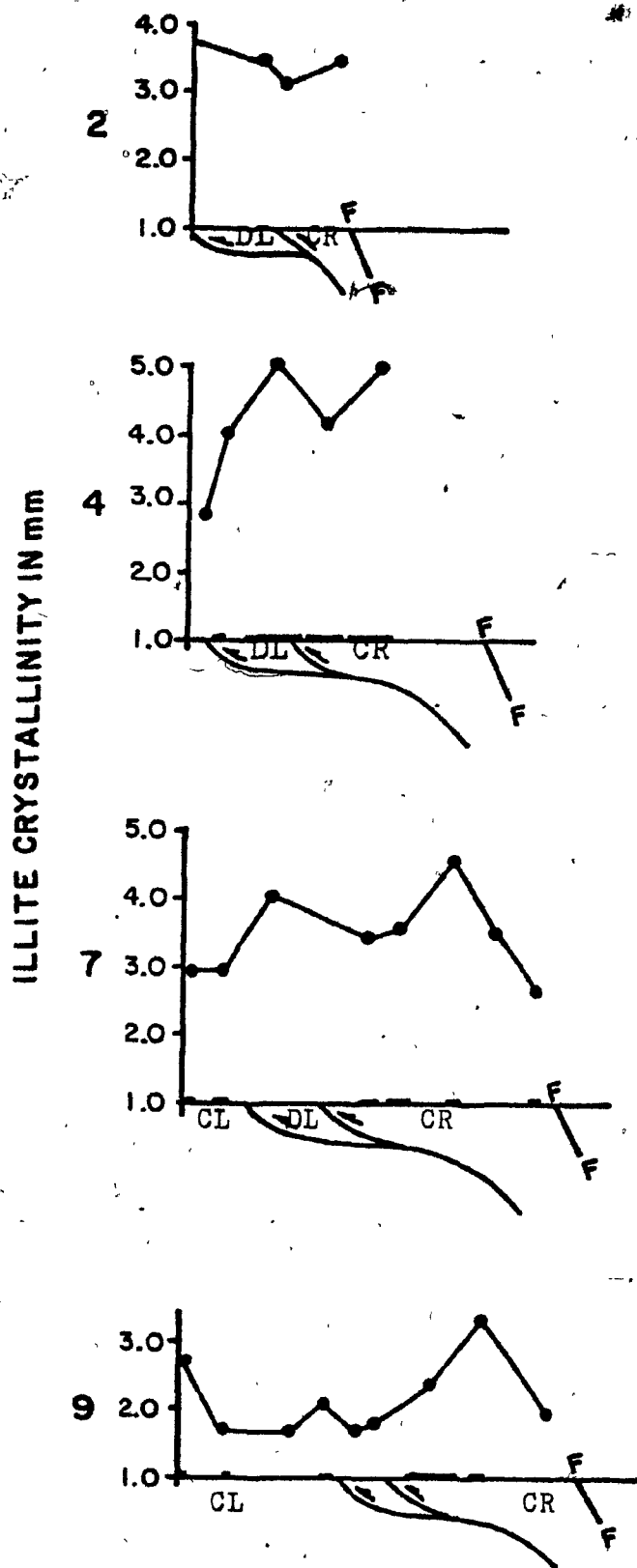
DL = Deslandes Formation

TR = Tourelle Formation

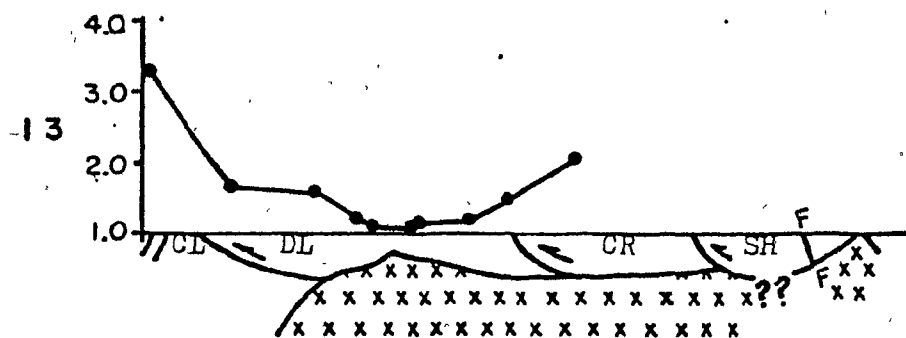
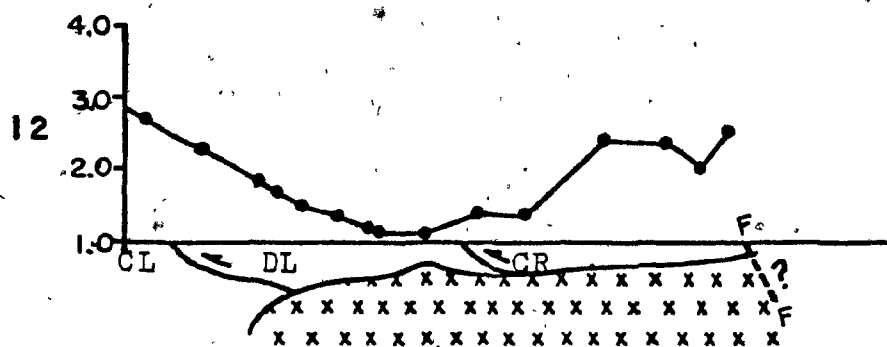
CM = Cap Chat Melange

CR = Cap-des-Rosiers Group

SH = Shickshock Gr.



ILLITE CRYSTALLINITY IN MM



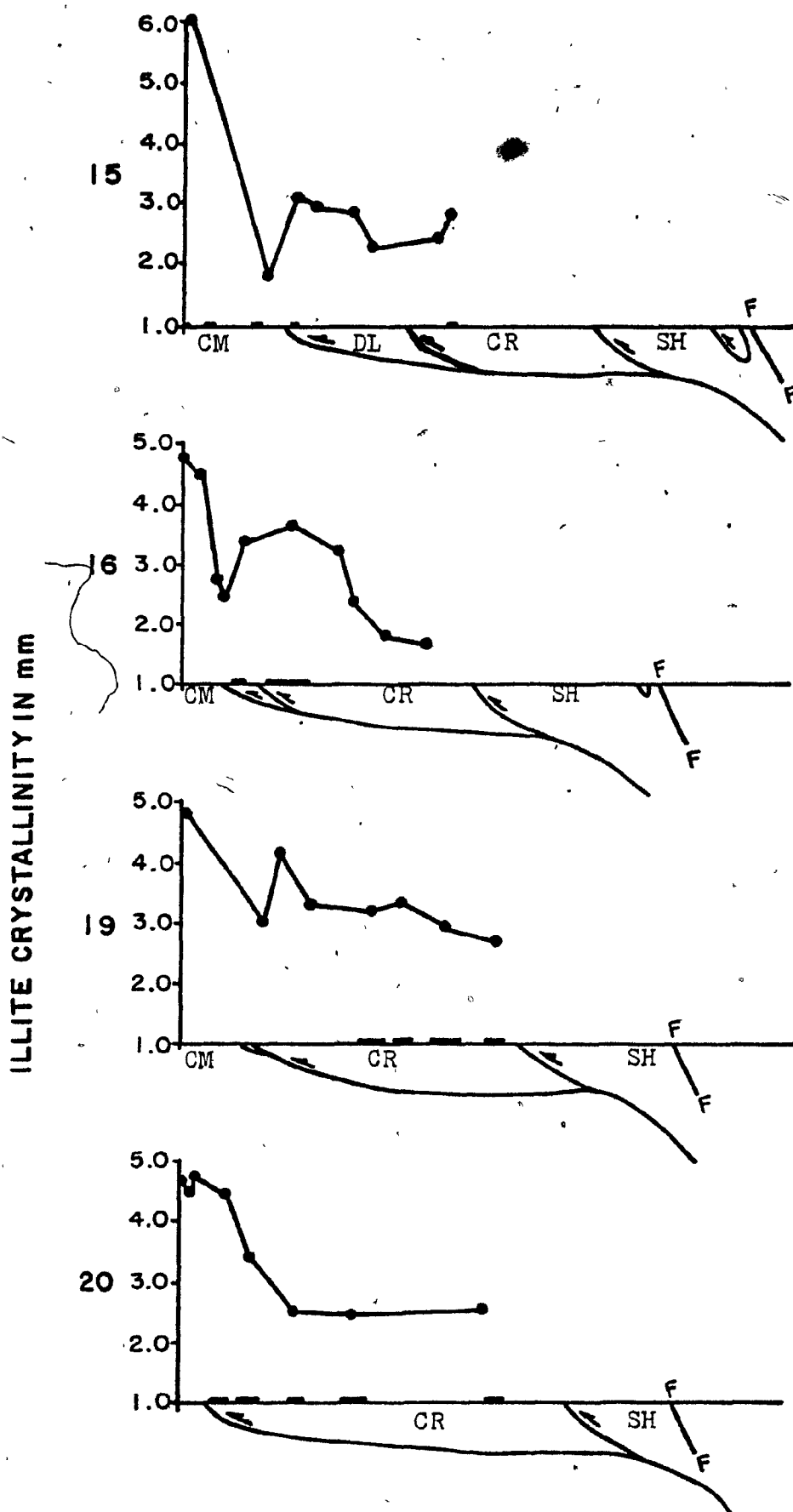


FIGURE 11

Illite crystallinity vs. illite 002/001 intensity ratio west of the thermal dome. Degree of thermal maturation increases from the younger sequences in the north (Deslandes Fm., Tourelle Fm., and Cap-Chat Melange) to older Cap-des-Rosiers Group in the south. Some samples in the Cap-des-Rosiers Group exhibit relatively poor crystallinity.

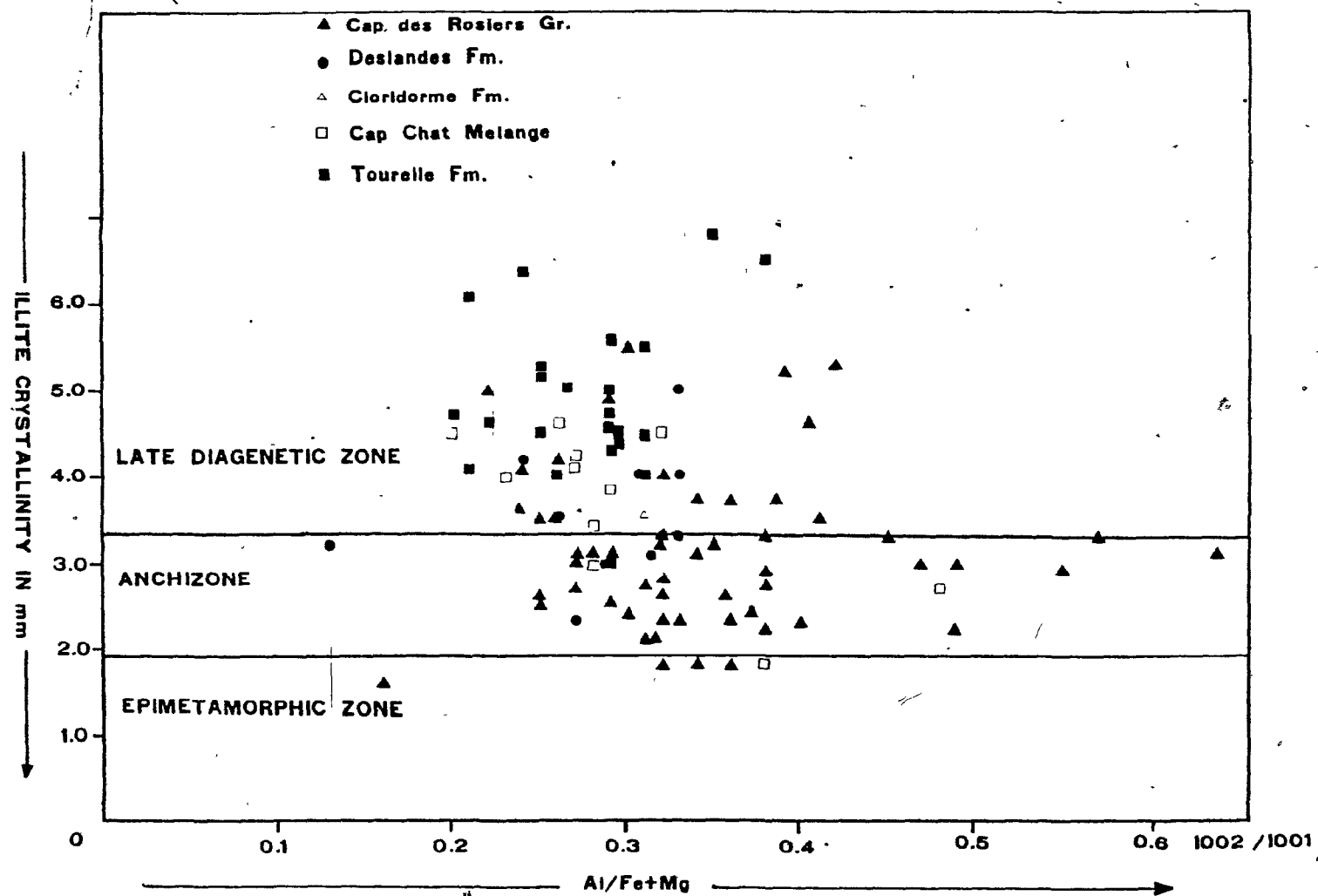


FIGURE 12

IC vs. illite 002/001 intensity ratio east of the thermal dome. Thermal maturation is highest in the youngest formation (Cloridorme Formation) thus contrasting with the results west of the thermal dome. Note that a few samples from the Cap-des-Rosiers Group show higher maturity.

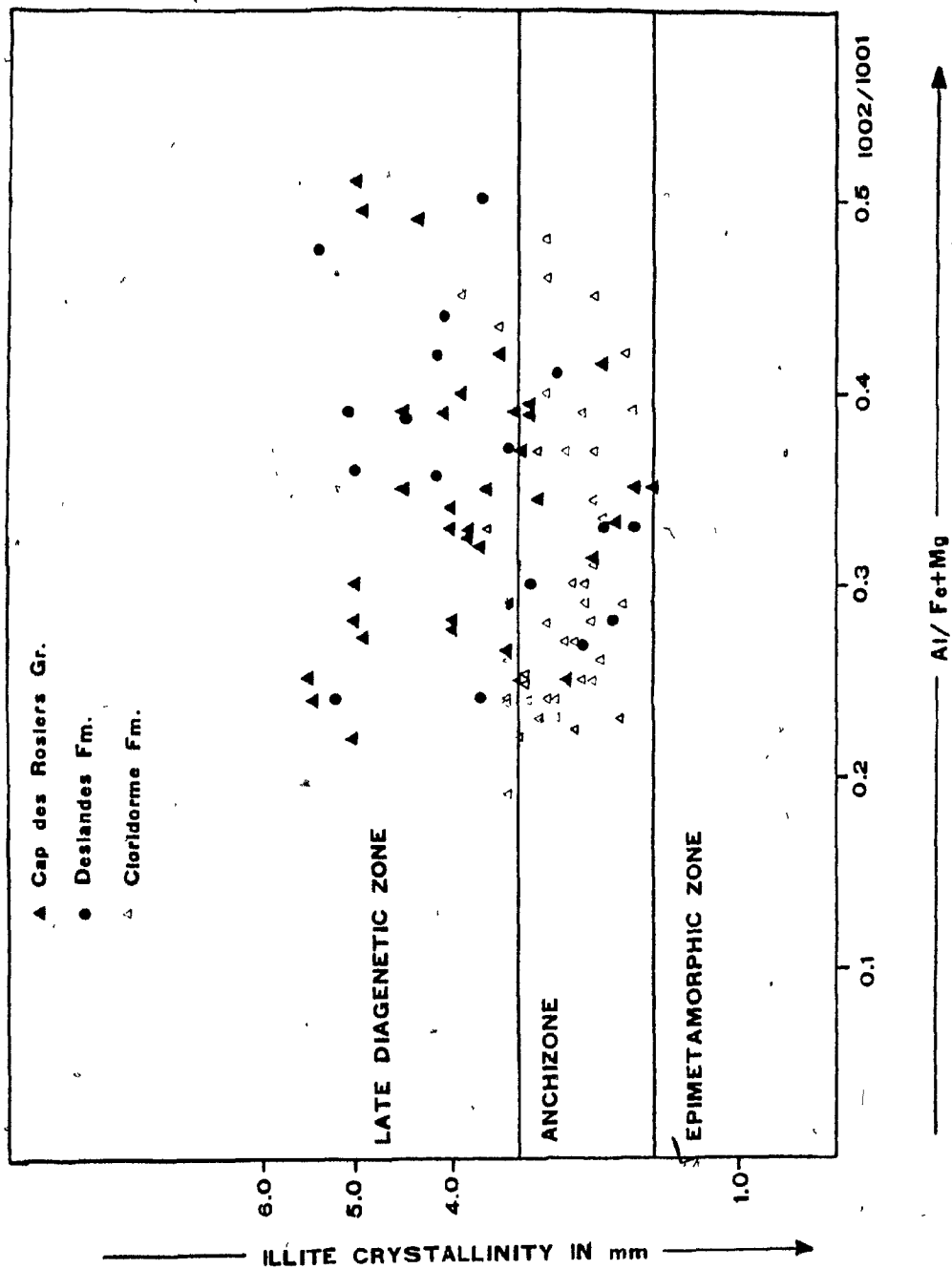


FIGURE 13

IC and illite 002/001 intensity ratio in the Tourelle Formation showing positive correlation (i.e. IC improves with increasing I002/I001 ratio).

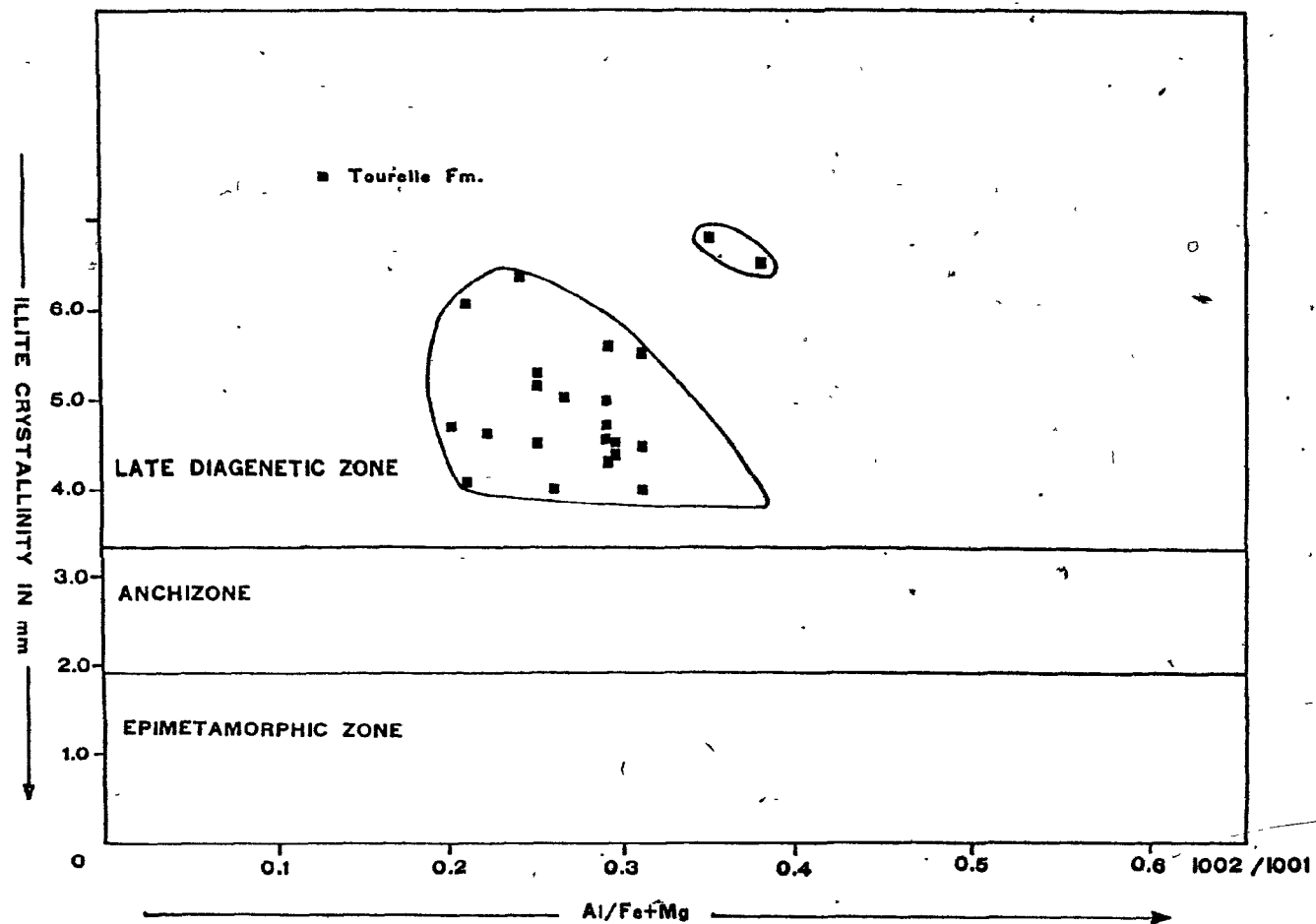
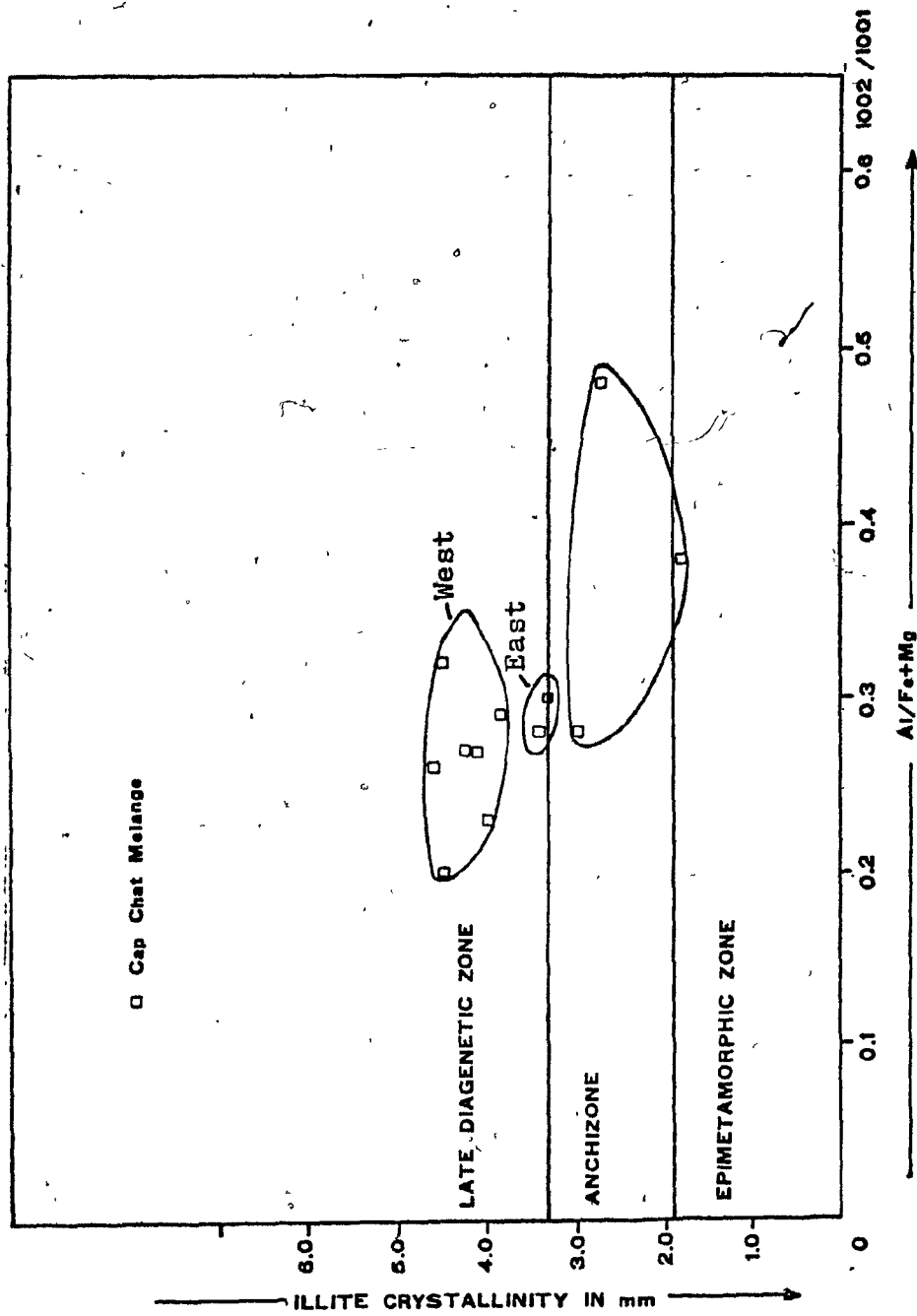


FIGURE 14

IC and illite 002/001 intensity ratio in the Cap-Chat melange. Illite crystallinity improves in the eastern outcrops (closer to pluton) compared to the western outcrops of the melange. However, best crystallinity is observed in the immediate vicinity of thrust boundary.



section (6.5 to 1.8mm) to the western Cap-Chat II section (5.5 to 2.6mm) (Fig. 10, Section 16, 19). Also from the former towards the latter section the epizone gradually disappears. Oval or egg-shaped local anomalies of improved crystallinity were observed in some green and red shales and with samples in the vicinity of the thrust separating the Cap-Chat Melange and Tourelle Formation from the Cap-des-Rosiers Group (Fig. 10, Sections 16, 19). Similar small anomalies were noted in some of the carbonate and organic matter rich black shales (Fig. 10, Section 16).

In the late diagenetic zone and anchizone east of the thermal dome, isopleth patterns show a thermal trough with a central thermal low. As an example, in the Grande Vallée section illite crystallinity improves from 5.0 - 4.0mm (Cap-des-Rosiers Group) to 2.5mm (Cap-des-Rosiers Group) in the south and 2.7 to 3.4mm (Cloridorme Formation) in the north (Fig. 10, Section 7). However, a number of complexities in the maturation trend are indicated by illite crystallinity data for this region. This produces rapid local variations, which have been plotted as oval-shaped anomalies on Fig. 8.

PYROBITUMEN REFLECTANCE

Pyrobitumen reflectance values of 95 samples were used to construct the isopleth map shown in Fig. 15, in order to corroborate the maturation patterns established

on the basis of illite crystallinity. The pattern of the reflectance isopleth lines is nearly identical to that produced by illite crystallinity values. Maximum reflectance observed is 6.06% in the Deslandes Formation (Mont Louis section). The minimum is 1.56% (Tourelle Formation, Cap-Chat section).

In the central thermal dome, reflectance values distinctly repeat the north-easterly bulge of the epizone shown on the illite crystallinity map. The anchizone in the thermal dome which lies north of the epizone is characterized by a uniform level of maturation of $\bar{R}_O = 3.7$ to 4.0% (Cloridorme Formation). In the east, \bar{R}_O increased to 4.41% near Anse-Pleureuse while in the west reflectance abruptly decreases at Logan's Line, i.e. from \bar{R}_O of 4.0% measured in the γ -4 member of the Cloridorme Formation east of Logan's Line to $\bar{R}_O = 2.96\%$ in the outlier of the Deslandes Formation to the west (Fig. 16, section 9, 13).

In the late diagenetic zone and anchizone west of the thermal dome reflectance values show fewer anomalies than the illite crystallinity values for the same area. Along the coast, reflectance values are uniform ($\bar{R}_O = 1.6$ to 1.7%). Towards the interior reflectance values increase from approximately 1.7% in the north to 5.0% in the south. West of the Tourelle section (15) the width of the anchizone increases markedly at the expense of the epizone. This is indicated by the reflectance and illite crystallinity maps. The epizone still continues westward with a width

of approximately 1km. This westward extension of the epizone is not seen on the illite crystallinity map. Across the thrust fault separating the Tourelle Formation and Cap-Chat Melange from the Deslandes Formation and Cap-des-Rosiers Group there is a jump in reflectance from values of $\bar{R}_0 = 2.0\%$ (Cap-Chat Melange) to 2.9% (Deslandes Formation) in the Ste-Anne-des-Monts I section and from \bar{R}_0 1.7% (Tourelle Formation, and Deslandes Formation) to 2.30% (Cap-des-Rosiers Group) in the Las Mechins section (Fig. 16, sections 16, 20). In the late diagenetic and anchizone east of the thermal dome reflectance isopleths show a thermal trough or lunate pattern exhibiting a thermal low. However, towards more easterly sections, such as Rivière-au-Renard (2) and Fame Point (4) the trough seems to disappear. East of the thermal dome, changes in reflectance values in each of the sections are distinct and more systematic than those recognized by illite crystallinity data.

FIGURE 15

Isopleth map of pyrobitumen reflectance of the Taconic Belt, Gaspé Peninsula.

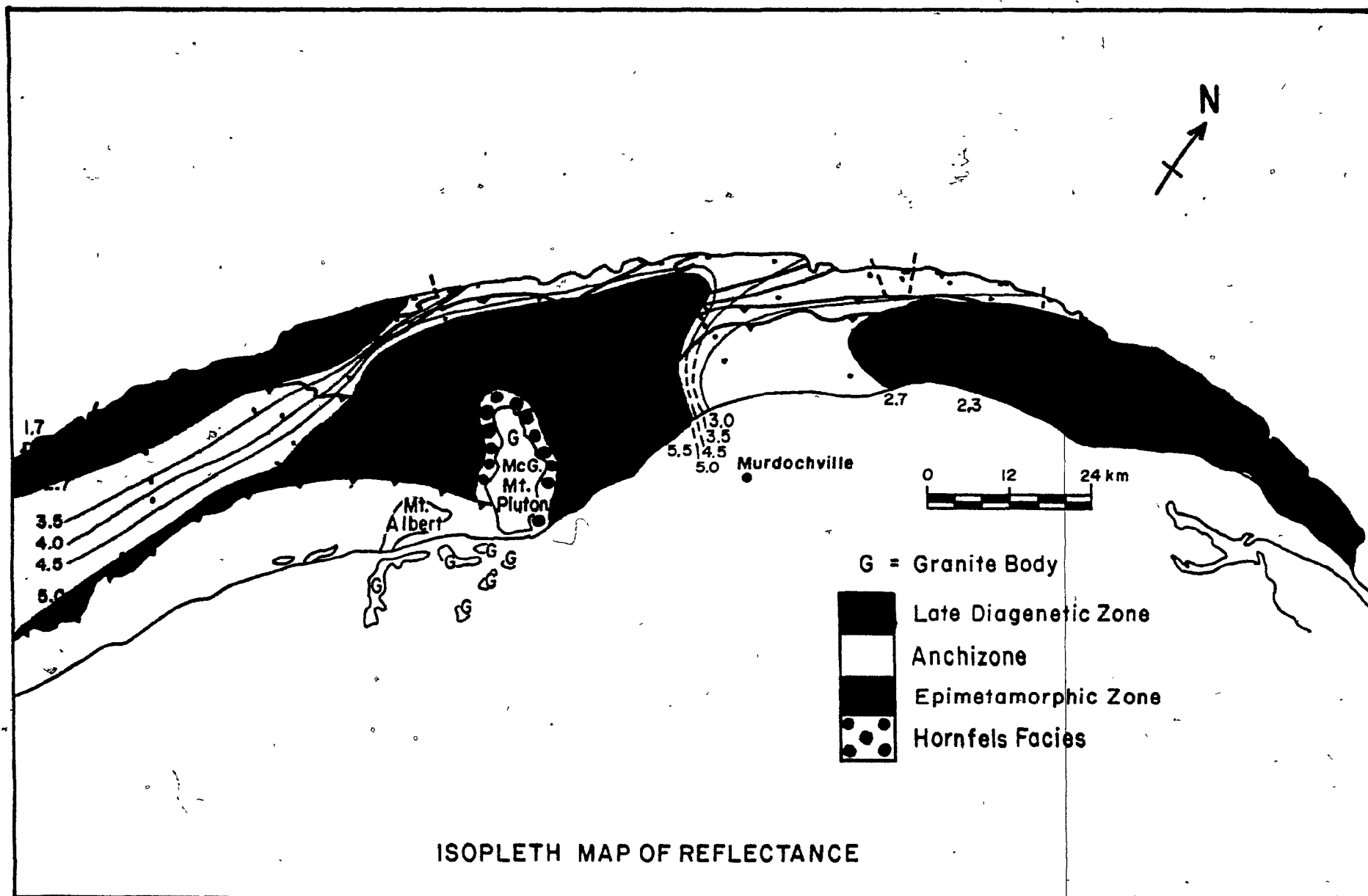


FIGURE 16

The following are north-south cross sections showing plotted values of pyrobitumen reflectance in the study area. For location of sections see FIGURE 9. Each point in the section represents one to three values.

CL = Cloridorme Formation

DL = Deslandes Formation

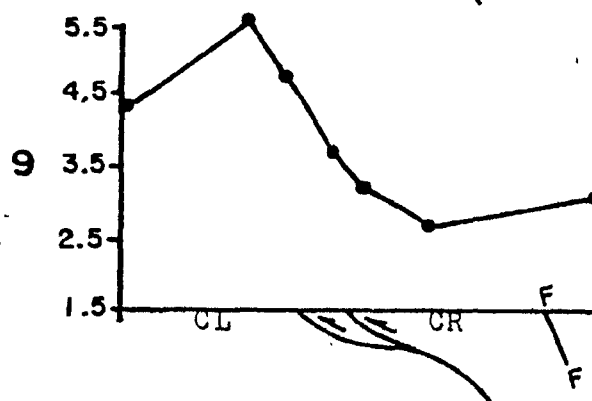
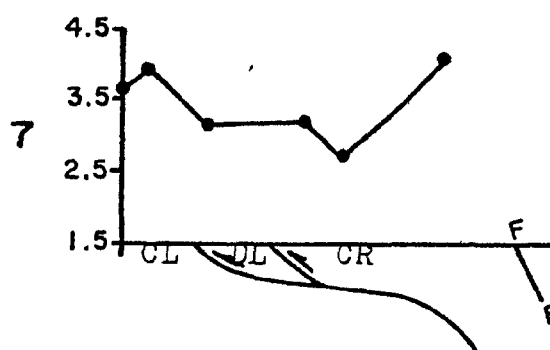
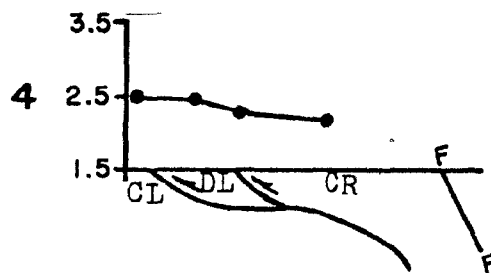
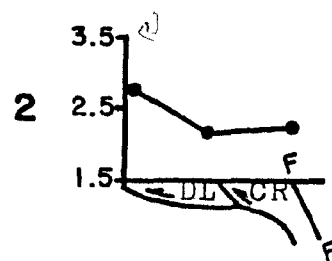
TR = Tourelle Formation

CM = Cap Chat Melange

CR = Cap-des-Rosiers Group

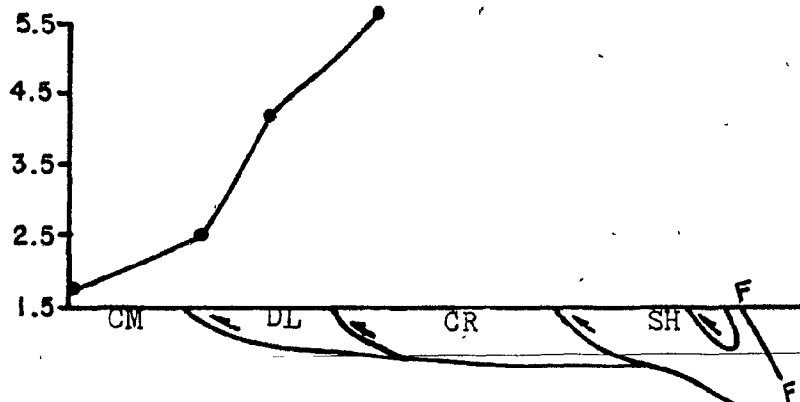
SH = Shickshock Gr.

% Ro (mean)

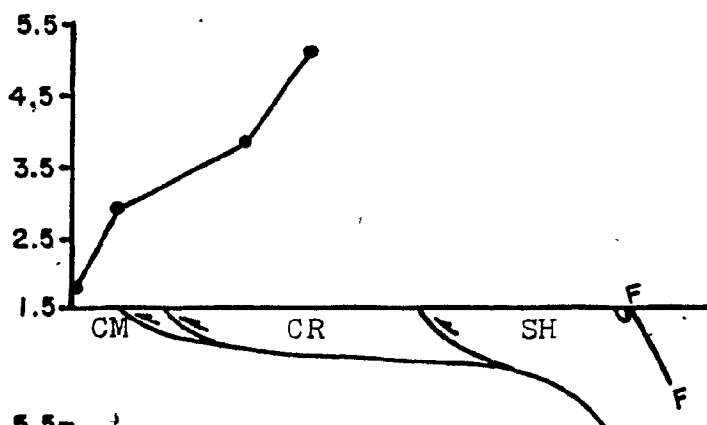


%Ro (mean)

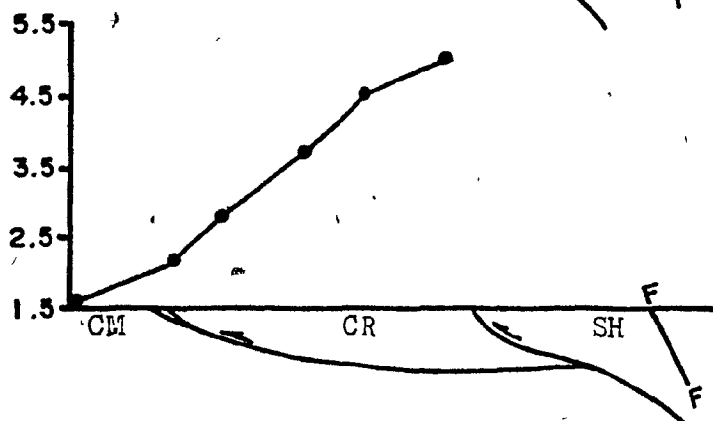
15



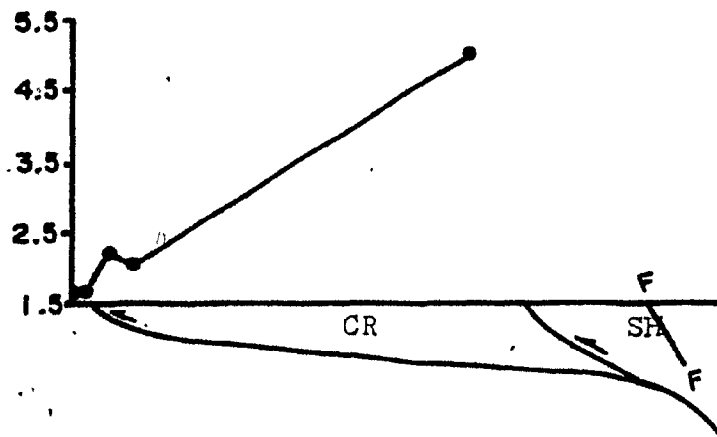
16

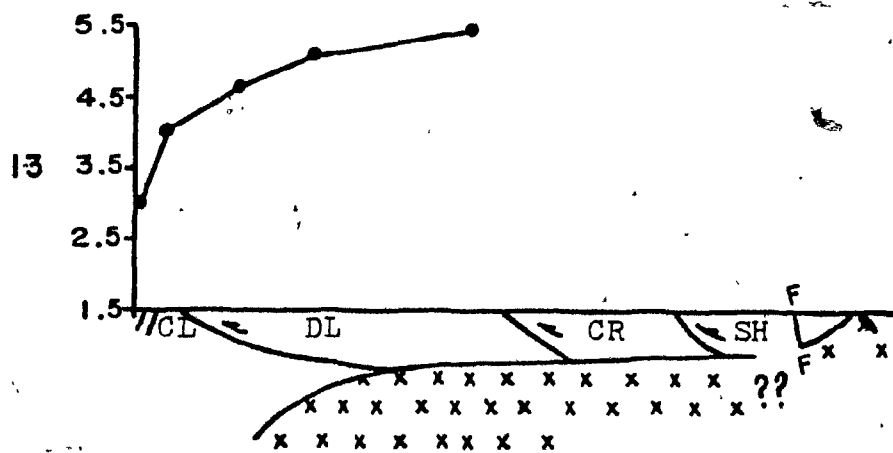
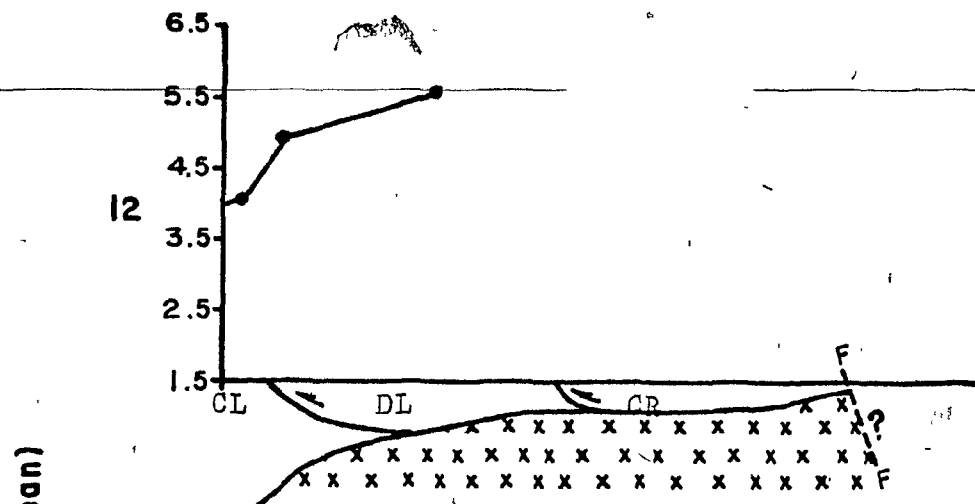


19



20





CHAPTER FIVE

INTERPRETATION

Isopleth maps of illite crystallinity and organic matter reflectance provide a framework for understanding the formation and spatial distribution of various regional diagenetic and metamorphic facies. Metamorphism due to depth of burial should increase downward in response to the normal gradients of temperature and pressure. However, this relationship does not seem to apply in many orogenic belts and the same is true here. The maturation patterns in the study area pose several questions as to the source of heat. How is the central thermal dome, which is unusually wide for a contact metamorphic zone, related to the McGerrigle Mountains pluton? How can the anomalously poor illite crystallinity in the immediate contact zone east of the pluton be explained? Are the "thermal slope" in the west and the "thermal trough" in the east related to the maximum depth of sedimentary burial at the original site of deposition or to regional heating associated with the Taconic Orogeny? Did the Murdochville intrusive bodies in the Acadian belt, south of the study area, also have an effect on the thermal maturation in the Taconic belt, at least in the south? How can other local maturation anomalies besides the ones mentioned above both for illite crystallinity and reflectance, be explained? In attempting to answer these questions the results of this study are dis-

cussed beginning with the most highly matured rocks of the central thermal dome.

The concentric configuration of isopleths about the McGerrigle Mountains pluton indicates that the pluton is the focus of heating during metamorphism. The effect of the intrusion is seen in a zone (epizone and higher metamorphic grade) three to five times the width of the intrusion. Factors controlling the extent to which sediments are affected by contact metamorphism include (1) pluton size, width, the depth of emplacement, permeability, and rate of cooling, (2) temperature differences between the intrusion and intruded rocks, (3) the composition and permeability of sediments, and (4) net motion of H_2O .

From the study of small dykes and sills it is known that the contact metamorphic effects of an intrusion may extend from about half the width of the intrusion (Bostic 1971; Perregaard and Schiener 1979; Peters et al. 1978) to twice (Dow 1977), or even more than four times this distance (Degens et al. 1978). On the other hand, the effects of large intrusive bodies on organic matter are noticeable over distances of several thousands of meters. The sensitivity of coaly material to heating is well exhibited by the aureoles of high rank coal around the deep-seated plutonic intrusion in the Bramscher Massif in North-West Germany (Stadler and Teichmüller, 1971 in: Teichmüller and Teichmüller, 1978). In the vicinity of plutonic intrusions, convective heat transfer by the circulation of fluids may

predominate over conductive heat transfer thereby affecting sediments to several kilometers (Norton and Knight, 1977).

The unusually large width of the epizone around the McGerrigle Mountains plutons is easiest to explain by the extension of the pluton beneath the thermal dome at shallow sub-surface levels. The bulging of the epizone toward north-east may reflect a subsurface trend of the intrusive body in that direction. The isolated plutons of Hog's Back, Mont-Valliers-de-St.-Real etc. in the Siluro-Devonian rocks are all located along this trend line but south-west of the main intrusion. These plutons are thought to have been emplaced at the same time as the McGerrigle Mountains pluton (de Römer, 1977).

West of the thermal dome, the trend from less mature, younger rocks in the tectonically deeper units to the north to more mature overlying older rocks in the south suggests that the maximum level of maturation in this area may have been achieved by burial. Thus it may have occurred before nappe transport as in the thrust imbricated zone and the outer belt of zone of nappes in the Québec City area (Ogunyomi et al., 1980). The younger Tourelle Formation shows an R_0 range from 1.56 to 1.70% and IC range from 6.6 to 4.1mm. For the Cap-Chat Melange R_0 ranges from 2.2 to 1.7% and IC ranges from 4.6 to 2.7mm. In the older Cap-des-Rosiers Group, reflectance values range from 2.2 to 5.0% and illite crystallinity ranges from 4.4 to 1.9mm. A systematic increase in maturation level with increasing

age of the sediments suggests that the rocks attained their maximum maturation during sedimentary burial, and were subsequently transported with the nappes. Further support for this idea is supplied by the fact that the isopleths closely follow tectonic boundaries. The phenomenon of 'transported diagenesis' has also been reported from the Swiss Alps (Frey et al, 1980; Kübler et al, 1979; Mullis, 1979) and the Appenines (Reutter et al, 1978).

In the late diagenetic and anchizone east of the thermal dome, the central east-west elongated thermal trough in the older Cap-des-Rosiers Group is puzzling. Northward from this thermal low there is a progressive increase in maturation in the younger Deslandes and Cloridorme Formations. Since the level of thermal maturation increases northward with decreasing age, it is unlikely to be induced by stratigraphic burial and is possibly syn- to postorogenic in nature. This enhanced thermal maturation north of the trough may be due to a continuation of the McGerrigle Mountains pluton trend and to heat generated by tectonic burial of older units. Oxburgh and Turcotte (1974) have demonstrated from their study in the Alps that in thrust belts there are thermal effects associated with tectonic movements which could account for regional metamorphism of younger rocks under thrust planes. This anomalously high metamorphism occurs despite the fact that the main post-thrusting restoration of thermal equilibrium takes millions of years. South of the central thermal trough the increase in thermal maturation may be

related to post-orogenic activities. In the Acadian belt (south of the study area), there are several Devonian igneous intrusives around Murdochville which may have supplied the heat necessary for this anomaly. In the far eastern part of the study area, the central trough becomes less distinct. This may be due to the absence of igneous activity in the Acadian belt south of the study area or to the limited width of outcrop area.

BURIAL DEPTH

If pre-orogenic levels of diagenesis have been preserved then the thickness of tectonic or stratigraphic units can be worked out using organic matter reflectance. This problem can be tackled in two stages. The first stage involves the determination of paleotemperature. Reflectance values can be related to temperature provided the effective heating time is known. Effective heating time is defined as the time during which the temperature is within 15°C of the maximum attained (Karweil, 1956). The second step is the determination of the actual geothermal gradient of the basin. Lack of conclusive information on both geothermal gradients and effective heating times for the Taconic belt makes burial depth estimates for any tectonic unit rather speculative. The regional maturation pattern reveals that the study area in general has been affected by additional heat from igneous intrusions and dynamothermal metamorphism during and after the Ordovician

Taconic Orogeny. The north-western and south-eastern thermal lows in the late diagenetic zone appear to be unaffected by external heat sources, however. Therefore an attempt has been made to arrive at some burial depth estimates for the rocks in these areas.

Geothermal gradients vary from place to place throughout the world, depending upon the geological environment. Geologically active regions give rise to diverse regional metamorphic environments because the Earth's thermal structure is disturbed in these regions. In the high-temperature/low pressure metamorphic belts of mobile regions, the heat flow is $\geq 40^{\circ}\text{C}/\text{km}$ (Fyfe, 1973). Conversely, areas near active trenches are characterized by a low gradient, caused by the downward deflection of isothermal surfaces (McKenzie, 1969; Minear and Tozsöz, 1970; Oxburgh and Turcotte, 1970). The presence of plutonic intrusions is usually inferred where isothermal surfaces form "dome-like" thermal surfaces (Turner 1968).

Ogunyomi et al. (1980) estimated the maximum burial temperatures and corresponding depths from the reflectance values in the Québec Appalachians, in the vicinity of Québec City, assuming a paleogeothermal gradient of $30^{\circ}\text{C}/\text{km}$, which is equal to present day average continental gradients. Hadrynian rifting has initiated the development of an Early Paleozoic Atlantic-Type continental margin in the Québec Appalachians where thick sequences of Cambro-Ordovician rocks were deposited. The lower Ordovician Tourelle For-

mation has been interpreted to have been deposited in the foredeep trough during the period of subduction (Hiscott, 1980). The upper Cambrian to lower Ordovician Cap-des-Rosiers Group, on the other hand, appears to be related to deposition on a subsiding passive continental margin (Fig. 18). In the Internal Domain, the Eastern Townships ophiolite complex near Québec City and the ultramafic bodies of Mount Albert and Mount Serpentine in the Gaspé Peninsula provide evidence that a cycle of ocean growth and destruction was involved in the evolution of the Appalachian System. The close analogy between the Early Paleozoic continental margin in the Québec City area and that in the current study area justifies the assumption of a paleogeothermal gradient of $30^{\circ}\text{C}/\text{km}$ for the study area. Calculations using geothermal gradients of 20°C and $40^{\circ}\text{C}/\text{km}$ are also presented (Fig. 19) for purposes of comparison. The effective heating time has been assumed, in this study, for the Tourelle Formation, to be 35Ma. This is based on several lines of reasoning.

(1) The age of regional metamorphism in the area has been dated at 443 ± 18 and 438 ± 20 Ma (K-Ar determination) from hornblende in amphibolites of Mount Albert and Mount Serpentine, respectively (Wanless et al., 1973, 1972, quoted in St. Julien and Hubert, 1975). Muscovite from a brecciated granite which is probably associated with the serpentine found in the western part of the Magereau Group, yielded a K/Ar date of 442 ± 20 Ma. These dates on the metamorphosed

rocks which overlie the sialic crust in the Internal Domain demonstrate that the dynamothermal metamorphism must have been completed in earliest Silurian time. From these data the peak of the regional metamorphism in the study area is estimated to be 440 Ma.

(2) Nappe transport must have occurred before metamorphism because the tectonic elements of the late diagenetic zone have escaped the regional, synorogenic thermal event.

(3) The denudated top of the Tourelle Formation is about 475 Ma (Fig. 17). Hence, nappe transport should have occurred between 475 and 440 Ma. This gives a timespan of 35 Ma for the maximum heating time. As sedimentation continued beyond 475 Ma, the time available for the maximum heating time should be less than the proposed 35 Ma. Also, effective heating time could be considerably shorter because the time of regional metamorphism can not be dated exactly. For our purpose we have taken 25 Ma as the maximum effective heating time. For comparison purpose, estimates of heating time are presented in the Fig. 19. With an effective heating time of 25 Ma and measured mean reflectance of 1.5% near the base of the Tourelle Formation, a maximum paleotemperature of 171°C is estimated from the diagrams prepared by Karweil (1956) and Hood et al (1975). These paleotemperature values correspond to a depth of burial of approximately 5.7 km for the Tourelle Formation. The present stratigraphic thickness has been estimated to be approximately one kilometer for this formation (Hiscott, 1977). The burial figure implies that about 5 km of overlying younger sediments have been eroded. This figure would

FIGURE 17

Stratigraphic table of various Cambrian and Ordovician stratigraphic units in the Taconic Belt of Gaspé Peninsula.

1. Parautochthon; 2 to 6 separate thrust sheets. Structural unit 4 is the Rivière Ste-Anne nappe. The Cap-Chat Melange is lithologically identical to the upper part of the Cap-des-Rosiers Group (Modified from Hiscott, 1977).

		base → top					
my.	Structural units	1	2	3	4	5	6
ORDOVICIAN	Ashgillian	AGE	↑ OF	REGIONAL	↑	METAMORPHISM	
	Caradocian	CLORIDORME FM	25 Ma. Effective maximum heating time		↓		
	Llandeirian	?		DESLANDES FM	40 Ma. Effective maximum heating time		
	Llanvirnian		?				
	Arenigian	D	TOURELLE FM				
		C	CAP CHAT MÉLANGE		CAP DES ROSIERS GROUP		
	Tremadocian	B					
CAMBRIAN	Upper				?		
	Middle					SHICKSHOCK GROUP	
	Lower						
	PRECAMBR.						

↑
?
↓
ULTRAMAFIC ROCKS (K/Ar)

FIGURE 18

The upper Cambrian to lower Ordovician Cap-des-Rosiers Group, is related to rifting on a passive continental margin. The lower Ordovician Tourelle Formation is deposited in the foredeep trough during the period of subduction (Modified after Hiscott, 1977).

NW

SE

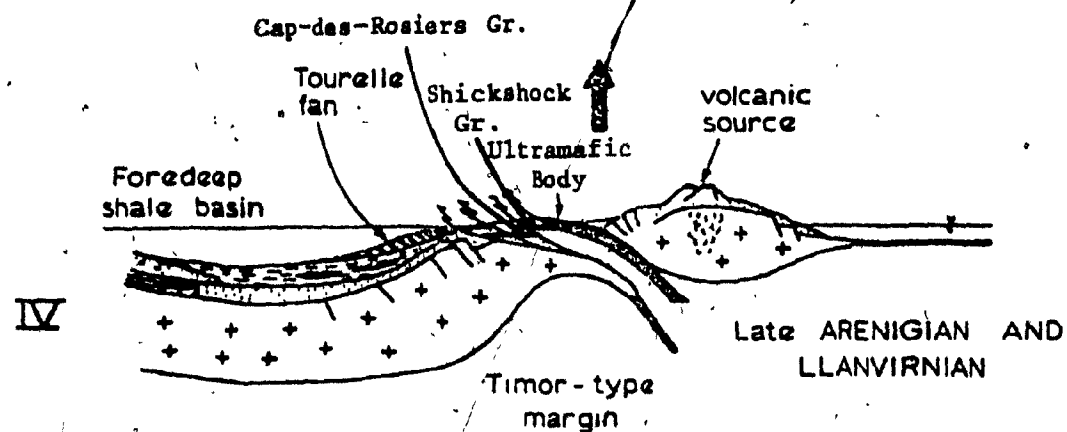
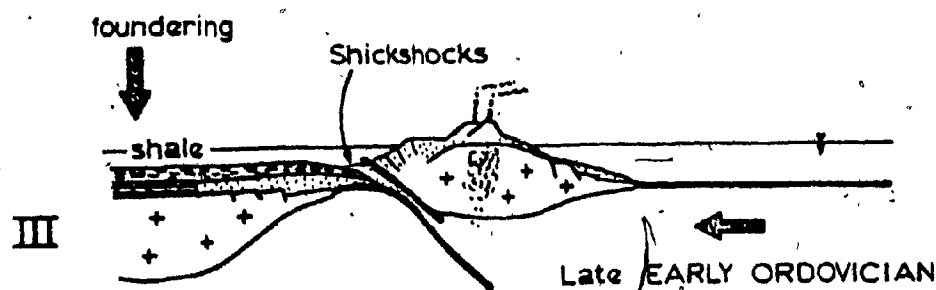
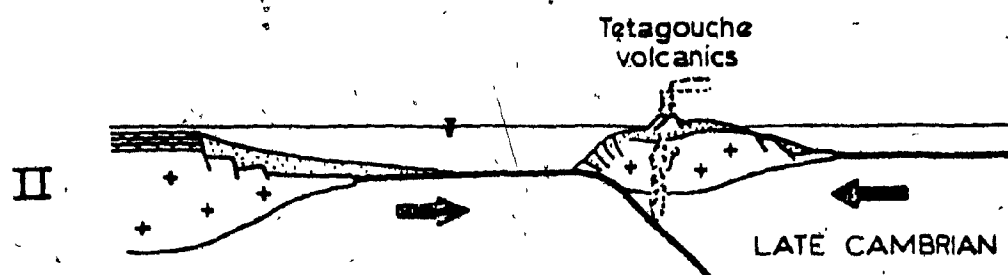
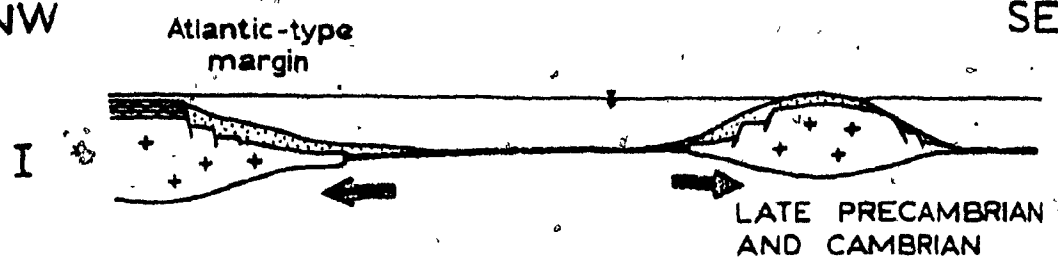


FIGURE 19

Estimates of temperatures and burial depths for the Tourelle Formation and the Cap-des-Rosiers Group. Assumed paleogeothermal gradient $30^{\circ}\text{C}/\text{km}$.

• Base of Tourelle Formation \bar{R}_0 (mean) 1.50%

Estimated Effective Heating Time in M. Yrs.	Assumed Paleo-Geothermal Gradient °C/km	Estimated Paleo-temperature in °C		Estimated Depth of Burial in km	
		After Karweil (1956)	After Hood et al. (1975)	After Karweil (1956)	After Hood et al. (1975)
25	20	170	173	8.5	8.6
25	30	170	173	5.7	5.8
25	40	170	173	4.2	4.3
35	20	154	155	7.7	7.8
35	30	154	155	5.1	5.2
35	40	154	155	3.8	3.9

Base of Cap-des-Rosiers Group
 \bar{R}_0 (mean) 2.20%

30	20	190	186	9.5	9.3
30	30	190	186	6.3	6.2
30	40	190	186	4.7	4.6
40	20	180	182	9.0	9.1
40	30	180	182	6.0	6.1
40	40	180	182	4.5	4.6

FIGURE 20

Relationship between reflectance, time and temperature.
Modification of Karweil's nomogram (1956) using Teich-
müller's (1971) reflectance values. Vertical dashed lines
indicate the reflectance values from which the maximum
temperatures were obtained for the Tourelle (TR) Formation
and the Cap-des-Rosiers (CR) Group by using various
effective heating time curves.

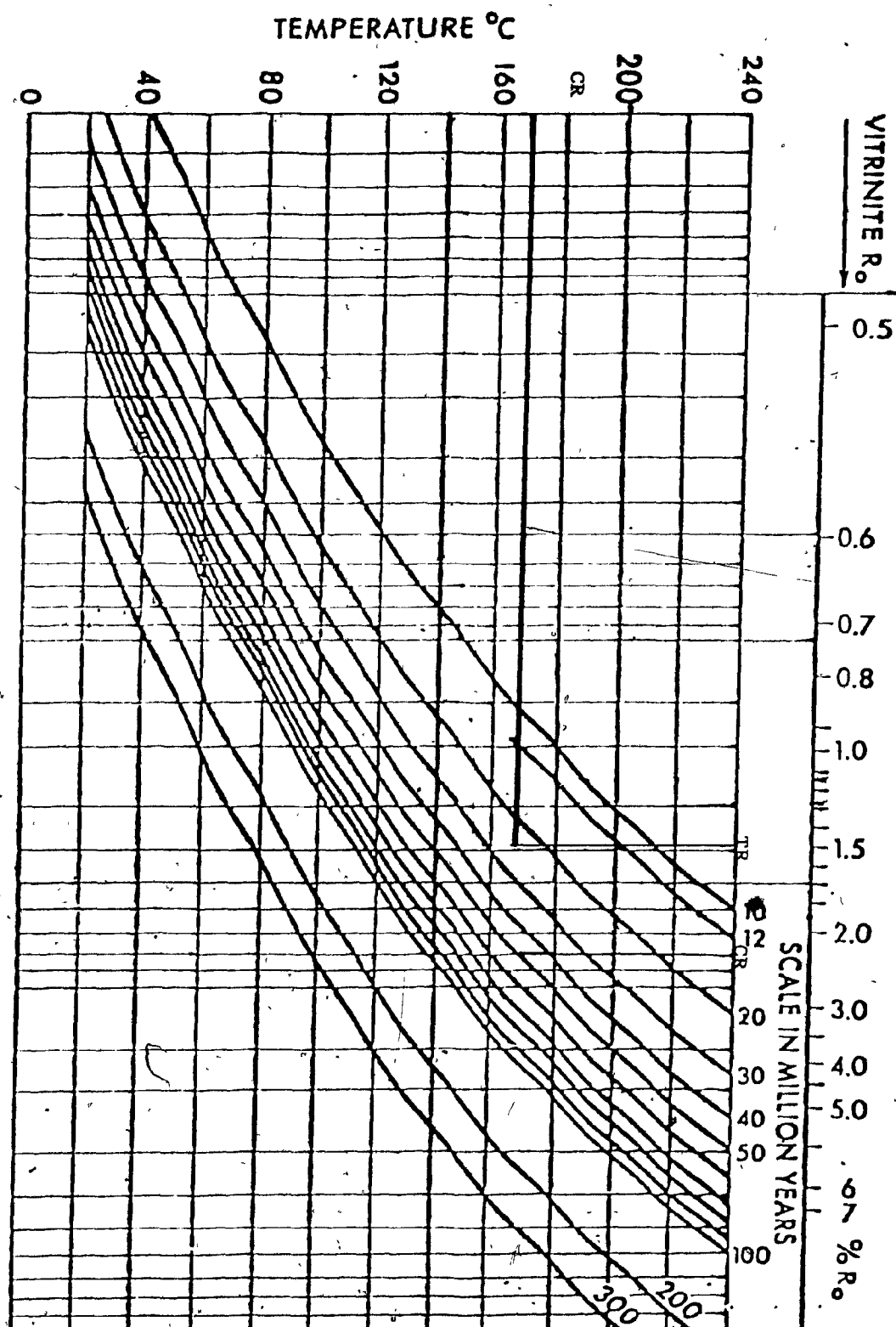
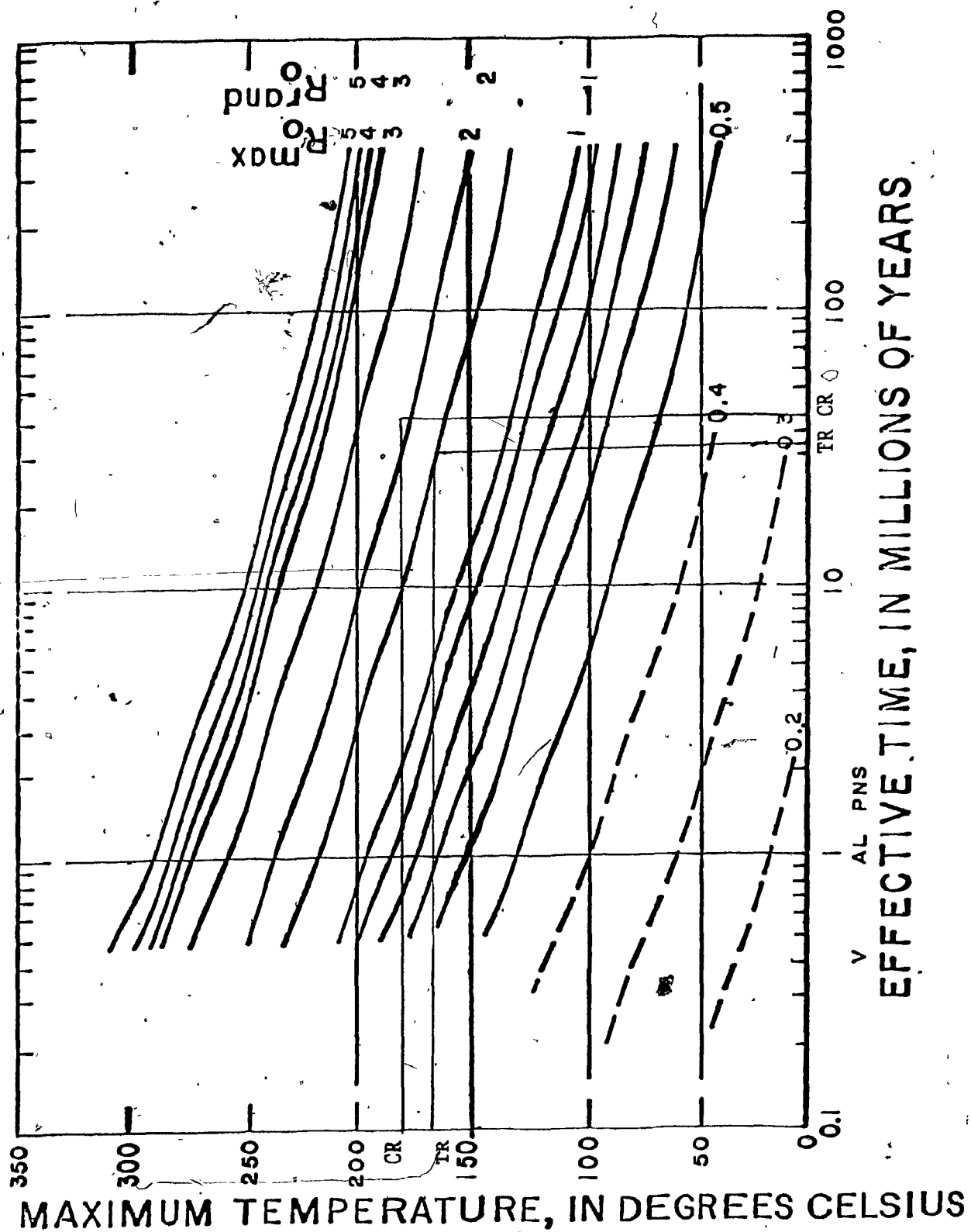


FIGURE 21

The relationship between reflectance (R_0), maximum rock temperature and burial time from Hood et al (1975).

"Effective time" means the duration of burial of a rock within 15°C of the maximum temperature in its history.

TR = Tourelle Formation, CR = Cap-des-Rosiers Group.



change significantly if there were a change in either paleogeothermal gradient or effective heating time (Fig. 19).

An effective heating time of 40 Ma has been estimated for the base of the Cap-des-Rosiers Group. This figure is based on the fact that sedimentation of this formation ceased around 480 Ma (Fig. 17) and that, as already mentioned, the age of the dynamothermal metamorphism is taken to be 440 Ma. From the mean reflectance value of 2.2% and an effective heating time of 40 Ma, the maximum temperature to which the base of this group may have been subjected is estimated to be approximately 180°C from the curve of Karweil (1956) and from Hood et al (1975). If the average geothermal gradient is taken to be 30 C/km a burial depth of 6 km is calculated for the base of the group. Structural complexities and a lack of detailed geological mapping in the area, make the actual thickness of the Cap-des-Rosiers Group unknown. Field observation suggests a thickness of 6 km for the Cap-des-Rosiers Group is reasonable.

EFFECT OF FOLDING ON ILLITE CRYSTALLINITY

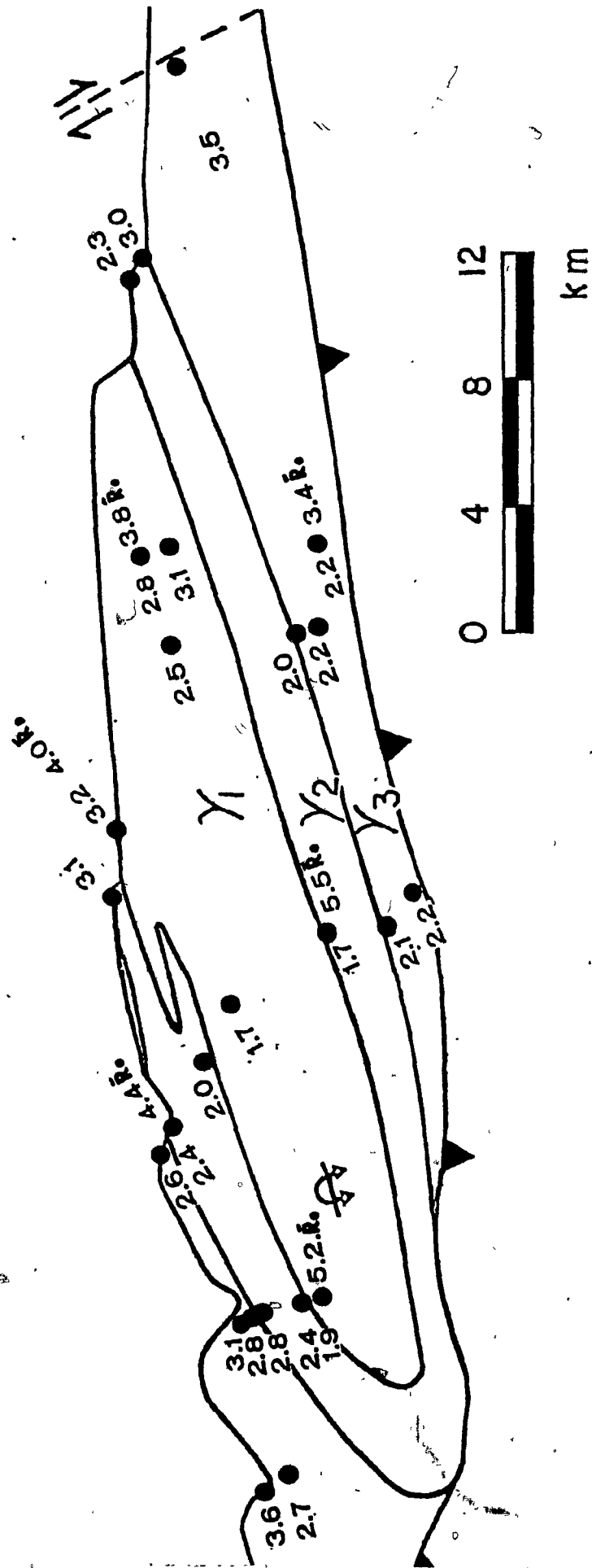
In the main anticlinorium of eastern Sauerland, in the Variscan fold belt of Germany, tectonic deformation has little effect on coalification but illite crystallinity increases from the flanks to the hinges of anticlines suggesting syndeformational recrystallization (Kalkreuth, 1979). On the other hand, Kübler (1967b) and Gruner (1976)

found no correlation between illite crystallinity and schistosity and folding. Teichmüller et al. (1979) noted that the time relationship between temperature increase and deformation determines whether illite crystallinity will be affected by deformation or not.

An attempt was made to evaluate the possible effect of folding and faulting on illite crystallinity in the Cloridorme Formation in order to be able to interpret some local anomalies. In the western tectonic block of the Cloridorme Formation, the γ -members are tightly folded forming a major asymmetrical anticline (appr. 40km in length) extending from the Madeleine River in the east to Mont St. Pierre in the west (Fig. 22; Biron, pers. comm., 1980). In the Anse Pleureuse section, better illite crystallinity was observed in the hinge (1.7mm) than in either limb of the anticline (2.6 to 2.0 northern and 2.2 to 1.7mm southern limb, respectively). A similar trend was determined in the Mont Louis section. Insufficient reflectivity data are available to construct a profile from hinge to limbs. On the southern limb the reflectivity increases from 4.9% (γ_3 -member) to 5.5% at the base of the γ_2 -member. It is possible, therefore, that illite crystallinity is, in part, controlled by varying stress regimes in different parts of the fold. However, regional maturation studies in this region (p. 78) suggest that much of the maturation might be due to high heat flow from the inferred subsurface igneous intrusion, and this may have been channelled into anticlinal crests. Increasing burial depth may also account

FIGURE 22

Effect of folding on illite crystallinity (IC), Cloridorme
Formation (γ -members).



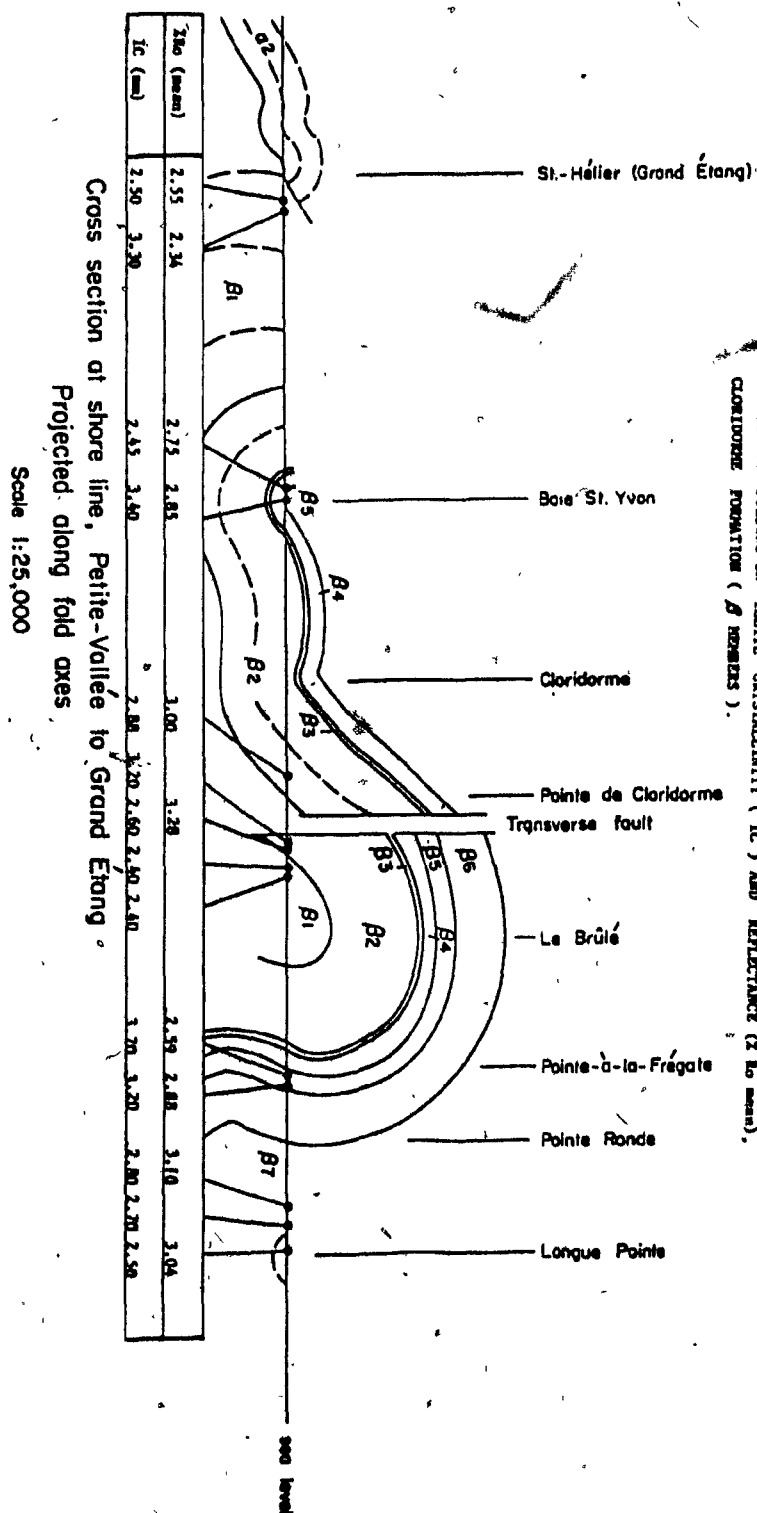
for this higher maturation from limbs to hinge. Synclines showing a similar trend of improved crystallinity from limbs to hinge would support the idea that folding enhances illite crystallinity, since the hinge of a syncline is at a shallower burial depth than the limbs.

Fig. 23 illustrates a syncline near Pointe Seche, Baie St. Yvon; an anticline with the northern limb overturned and southern limb steeply dipping (dip 70°) near Le Brule; and an overturned syncline with its hinge at Longue Pointe, west of Petite-Vallée (Enos 1965). These structures are well exposed along the coast of the St. Lawrence River. The maturation level of the area lies within the anchizone. The results from each of these folds are discussed separately as along the projected cross section ($\approx 20\text{km}$) there is considerable variation in maturation levels. Near Le Brule, illite crystallinity is best developed in the hinge (2.4mm) of the anticline in the β_1 -member. Crystallinity decreases towards the eastern limb from 2.6mm (β_3) to 3.2mm (β_3) at distances of 150 and 250 meters, respectively, from the hinge. A similar result is obtained from an overturned syncline at Longue Pointe where crystallinity becomes less well developed from the hinge (2.5mm, β_7 -member) at a distance of about 300 meters. Reflectance values remain almost the same from the hinge ($\bar{R}_0 = 3.05\%$) to the limb ($\bar{R}_0 = 3.10\%$). This suggests that illite crystallinity is, in part, controlled by varying stress regimes in the different parts of a fold, while reflectivity values are not

FIGURE 23

Effect of folding on illite crystallinity (IC), and
reflectance (% R_0 mean), Cloridorme Formation (β -members).

EFFECT OF FOLDING ON ILITE CRYSTALLINITY (IC) AND REFLECTANCE (R₀ max).
CLORIDORME FORMATION (β MEMBERS).



affected. However, at the Baie St. Yvon syncline, the crystallinity trend is reversed. Illite crystallinity improves from the hinge (3.4mm, β_5 member) within a distance of 100m towards the eastern limb (2.45mm, β_4 member). Here during folding, stress may not have been sufficient to enhance illitization.

In the late diagenetic zone west of the central thermal dome, illite crystallinity improves near the thrust separating the Cap-Chat Melange and the Cap-des-Rosiers Group (Ste-Anne-des-Monts I and Les Machins sections, Fig. 10, sections 16, 19). Illitization can be accelerated by the shear stress and concentrated frictional heat generated during faulting. Thus, to evaluate the causes of local variation in illite crystallinity, the contribution of each of the factors such as folding, tectonic activities, intrusions, etc. should be considered.

CORRELATION BETWEEN ILLITE CRYSTALLINITY AND REFLECTANCE

The best correlation coefficients (-1.0) are achieved when illite crystallinity and reflectance are affected primarily by temperature. Linear correlation coefficients between mean reflectance and illite crystallinity were determined for the following:

- (1) Different zones of maturation within a formation.
- (2) Formations as a whole.

(3) Alteration zones as a whole.

Figures 24 to 26 illustrate these relationships. Illite crystallinity vs. reflectance plots show significant variations in correlation coefficients for the different maturation zones within a formation. Large variations also exist for a given maturation level in different formations. In the late diagenetic zone, good correlation exists within the Cap-Chat Melange ($r = -0.91$) and Tourelle Formation ($r = -0.69$). Correlation is poorer in the Cap-des-Rosiers Group ($r = -0.34$) and coefficients show no significant correlation in the Deslandes ($r = -0.07$) and Cloridorme ($r = +0.16$) Formations. The reason for the lack of correlation in the Cloridorme and Deslandes Formations may be the high carbonate content in many shale samples. This is indicated by X-ray analysis of the 2 to 16 μm fraction. An insufficient supply of potassium and aluminium in the calcareous shales along with low porosity may have inhibited the process of illitization. Alternatively, it may be that either organic compounds or metals have acted to block off the open sheets of illite or swelling clay minerals. Also, black shales are generally rich in organic matter. The oxidation of organic matter in black shales can create a weakly acidic environment which is unfavourable for illitization. In a previous study in the Quebec City area (Ogunyomi, 1980) correlation coefficients of -0.56 and -0.83 between illite crystallinity and mean reflectance have been established for the middle and late diagenetic zones, respectively.

In the anchizone, a good correlation exists for the Deslandes Formation ($r = -0.65$) whereas correlation is poorer in the Cap-des-Rosiers Group ($r = -0.24$) and Cloridorme Formation ($r = -0.14$). The reasons for these wide variations in correlation between illite crystallinity and reflectance are manifold. In the Cloridorme Formation, illite crystallinity and reflectance may have been influenced in a different way by differential stress during folding (as discussed on page 98) which could be responsible for poor correlation. A poor correlation ($r = -0.057$) in the anchizone has been reported from the Quebec Appalachians (Ogunyomi, 1980). Frey et al. (1980) reported poor correlation between illite crystallinity and reflectance from very low-grade metamorphic rocks of the external parts of the Central Alps. Poor correlations have been attributed to the influence of lithology (1) on illite crystallinity, (2) differential tectonic stress on illite crystallinity, (3) the presence of mixed-layer muscovite/paragonite which causes a broadening of the 10\AA peak, and (4) the increase of reflectance anisotropy by shear stress at the beginning of the anthracite stage ($R_{\text{mean}} = 2.5\%$). The absence of paragonite from the study area suggests a different mode of mineralogical transformation compared with that seen in the Central Alps. As such, it is difficult to compare these two areas.

Since the correlation coefficients in the late diagenetic zone ($r = -0.37$) and anchizone ($r = -0.31$) are not very

good, the positive correlation in the epizone is surprising. This correlation may be due to the anisotropy of the organic matter reflectance, i.e., higher deviation of the mean from minimum and maximum reflectance values. A few irregularities in the illite crystallinity (retardation or even retrogradation due to hydrothermal fluids) could also be a factor. The overall correlation ($r = -0.67$) in the study area is reasonably good.

FIGURE 24

Correlation coefficient of IC vs. mean reflectance for
different formations and zones.

FORMATIONS	CORRELATION COEFFICIENTS (r)				
	LATE DIAGENETIC ZONE	ANCHIZONE	EPIMETAMORPHIC ZONE	FOR EACH FORMATION	FOR THE STUDY AREA
CLORIDORME	+0.16	-0.14	—	-0.42	-0.67
DESLANDES	-0.066	-0.65	+0.36	-0.78	
TOURELLE	-0.69	—	—	-0.69	
CAP-CHAT-MELANGE	-0.91	—	—	-0.41	
CAP-DES ROSIERS	-0.34	-0.24	—	-0.59	
r FOR EACH ZONE	-0.37	-0.31	+0.26		

CORRELATION COEFFICIENTS (r) IN DIFFERENT MATURATION ZONES IN DIFFERENT FORMATIONS.

FIGURE 25

Correlation of illite crystallinity (IC) and mean
reflectance (% R_0 mean) in different formations.

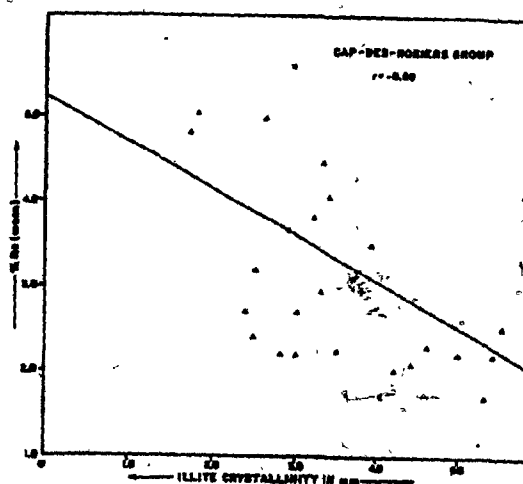
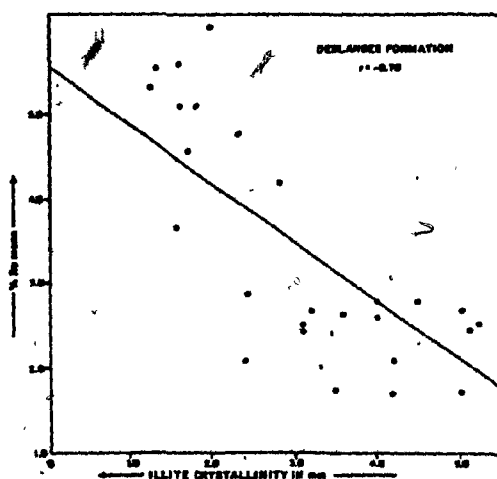
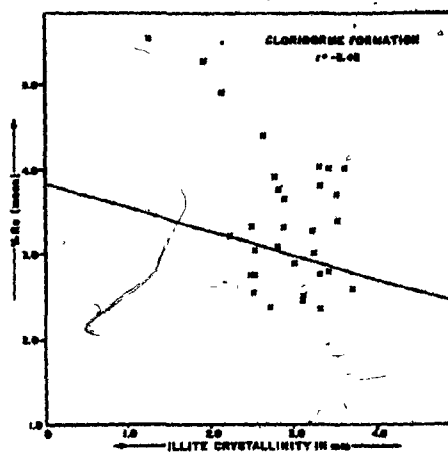
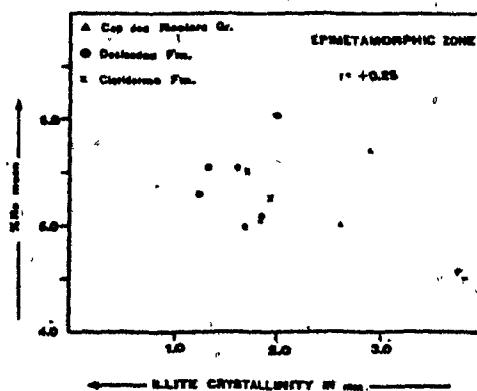
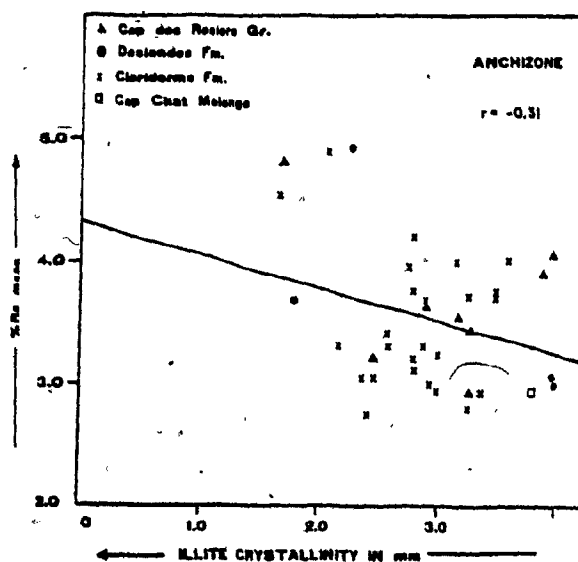
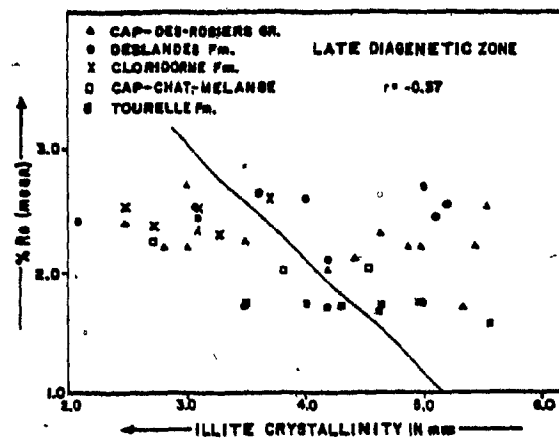


FIGURE 26

Correlation of illite crystallinity (IC) vs. mean
reflectance (% R_0 mean) in different maturation zones.



CHAPTER SIX

DIAGENESIS OF CARBONATE CONCRETIONS

Although emphasis in this study has been on the evolution of late diagenesis, anchi- and epimetamorphism in deep water shales of the Taconic belt, some information on early diagenetic reactions related to the breakdown of organic matter has been obtained from carbonate concretions. The precipitation of carbonate concretions is a function of temperature, pressure, pH, P_{CO_2} , and ionic concentrations. Carbonate concretions consist of an authigenic cementing fraction and a detrital component related to the original host sediment. Low magnesian calcite, dolomite, siderite and rhodochrosite are the most common carbonate cements in concretions, although vaterite has recently also been discussed for Ordovician concretions in Québec (Fong et al., 1981).

It is argued that the volume percent of the authigenic fraction of the concretion is related to the host-sediment porosity at the time of concretion growth (Lippmann, 1955; Raiswell, 1971, 1976; Oertel and Curtis, 1972). Thus various stages of concretion formation may be related to progressive compaction of the host-sediment with increasing burial based on the proportion of cement materials.

Close association of certain black shales and carbonate concretions suggest that the decomposition of organic matter plays a significant role in the concretion-forming

process by providing the carbonate alkalinity ($\text{HCO}_3^- + 2\text{CO}_3^{2-}$) necessary for the inorganic precipitation of carbonates. Carbonate alkalinity is defined as the total concentration of the dissolved bicarbonate plus twice the concentration of the dissolved carbonate species (Berner et al, 1970). Development of a high bicarbonate concentration may be seen as an intermediate step toward carbonate precipitation as long as the bicarbonate can later be dissociated. A relatively high pH is required for the dissociation of bicarbonate into H^+ and CO_3^{2-} but the exact numerical value depends on temperature. Weeks (1957) suggested that the decomposition of organisms produced ammonia as the tissue decayed, creating a microenvironment with relatively high pH. Such an increase in pH would precipitate calcium carbonate from the pore fluids and form a nodule around the organic matter. Later works by Raiswell (1976), Dickson and Barber (1976) and Hudson (1978) also recognized the importance of an isolated microenvironment with high pH producing CO_3^{2-} ions, from which carbonate can precipitate. Recently, Fleet (1980) from the study of carbonate nodules at DSDP Site 503 in the eastern Equatorial Pacific Ocean concluded that the nodules probably formed from the decay of organic matter which was concentrated in burrows.

Commonly recognized depth-related reaction zones involving breakdown of organic matter are as follows:

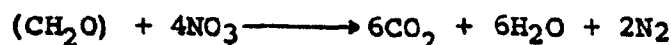
- (1) Bacterial degradation proceeds quickly and efficiently

in aerobic oxygen bearing water. An equation for this reaction is:



where the first term represents organic matter.

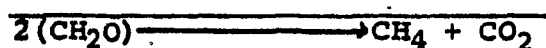
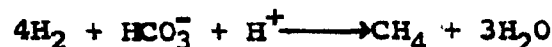
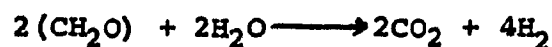
- (2) When the dissolved oxygen becomes exhausted, oxidation of organic matter by anaerobic bacteria using nitrate as a source of oxygen (electron acceptor) takes over according to the generalized formula:



- (3) Once nitrate has been depleted, degradation of organic matter continues by anaerobic bacteria using sulphates as the oxidant. The reaction can be represented by the equation:



- (4) The next step in the oxidation of organic matter is achieved by carbonate reduction:

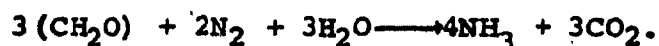
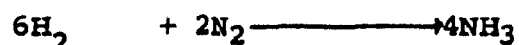


- (5) After inorganic compounds (O_2 , NO_3^- , SO_4^{2-} , and HCO_3^-) are exhausted, degradation of organic matter is achieved by methanogenic bacterial fermentation:



Organic matter degradation by bacterial fermentation is accelerated by removal of hydrogen, which in turn depends on availability of suitable electron acceptors,

such as CO_2 , NH_3 . If there is sufficient organic matter (i.e. more than 0.5% organic carbon) and there is no significant biogenic CO_2 production then methane production tends to raise the pH (by using H^+) and thus favours precipitation of carbonates. Carbonate precipitation is also favoured by the increase in pH due to the release of NH_3 during fermentation (Gieskes, 1975). An equation for this is:



The above early diagenetic reactions involving organic matter can affect the source rock potential for the generation of hydrocarbons. At deeper zones, thermally induced organic matter degradation occurs at least in two stages: (6a) dehydration, decarboxylation; (6b) cracking to produce hydrocarbons.

During biological fractionation, isotopic composition of the pore water varies greatly so that specific source reactions can be identified in certain cases. As for example, unlike at other stages, CO_3^{2-} produced at the fermentation stage is characterized by heavy carbon isotopes (up to +15% PDB). Here the lighter carbon isotope is removed in methane at a faster rate resulting in a marked C^{13} enrichment in the residual interstitial water bicarbonate. An example of this kind has been documented by Rosenfeld and Silverman (1959) from an anoxic fjord of British Columbia,

where during methane formation, $\text{HC}^{12}\text{O}_3^-$ is removed at a rate of 7% faster than $\text{HC}^{13}\text{O}_3^-$.

FIELD DESCRIPTIONS

Ellipsoidal shaped carbonate concretions with average diameters of 50 to 200cm are embedded in organic matter rich black shales of the Cloridorme and Deslandes Formations. Sometimes two or more concretions are connected by a small neck during growth but still retaining their ellipsoidal shape. The concretions consist of micritic dolomite and are dark in color. Their length is usually 3 to 4 times their width. The long axis of these concretions lies in the bedding plane. The shale beds containing these concretions have a thickness of 1.2 to 1.5m, and often grade into silty dolomite to graywacke. The cores of the concretions often contain abundant shrinkage cracks. These fracture planes are often filled by calcite and/or quartz.

SAMPLING:

A total of 6 carbonate concretions was sampled in the β - and γ -members of the Cloridorme Formation (Fig. 27). From each concretion five samples were taken for petrographic and isotopic analyses as indicated in Fig. 28.

RESULTS:

The concretions consist of ~~ferroen~~ dolomite. They

FIGURE 27

**Locations of carbonate concretion samples, Cloridorme
Formation.**

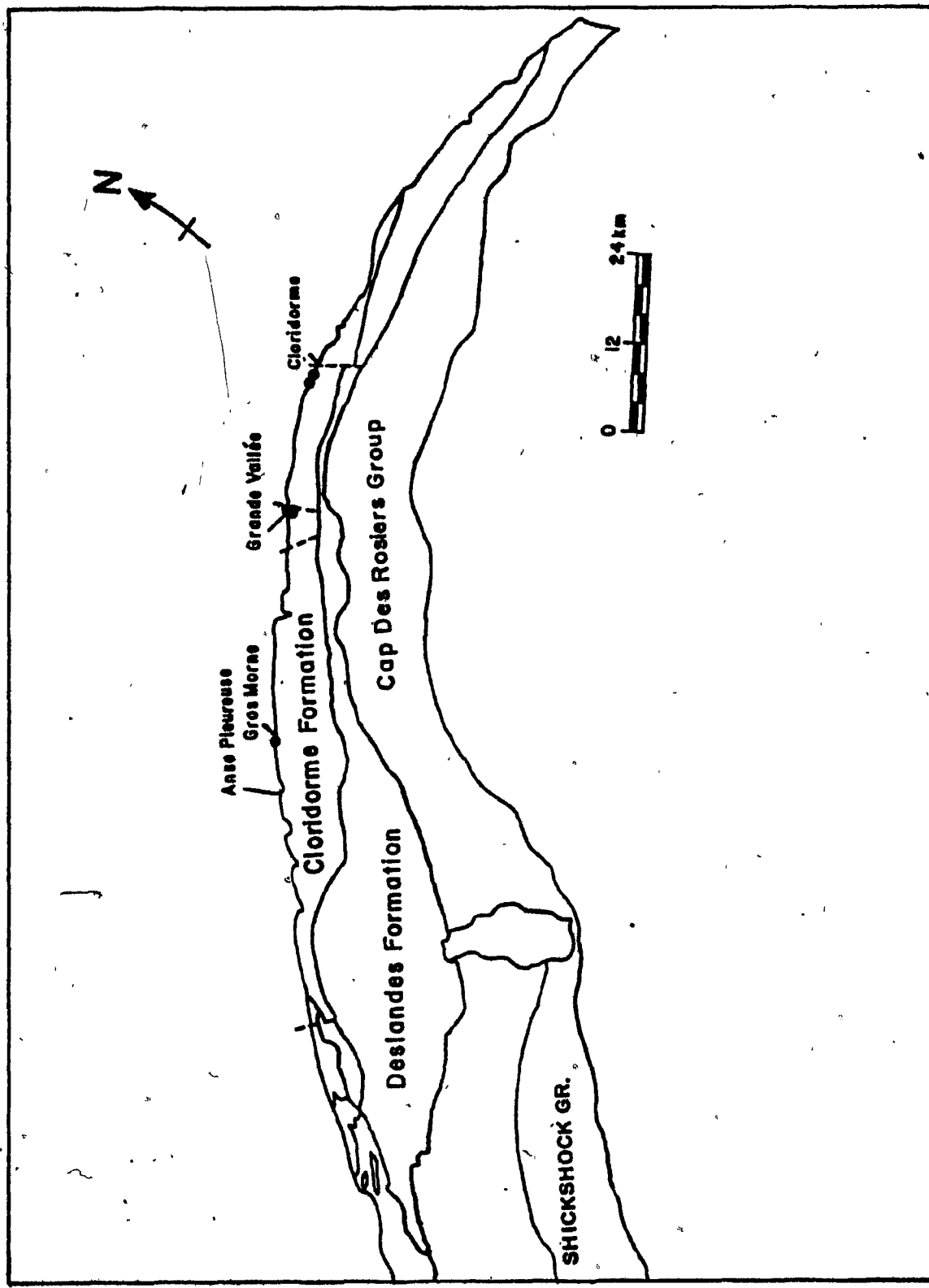
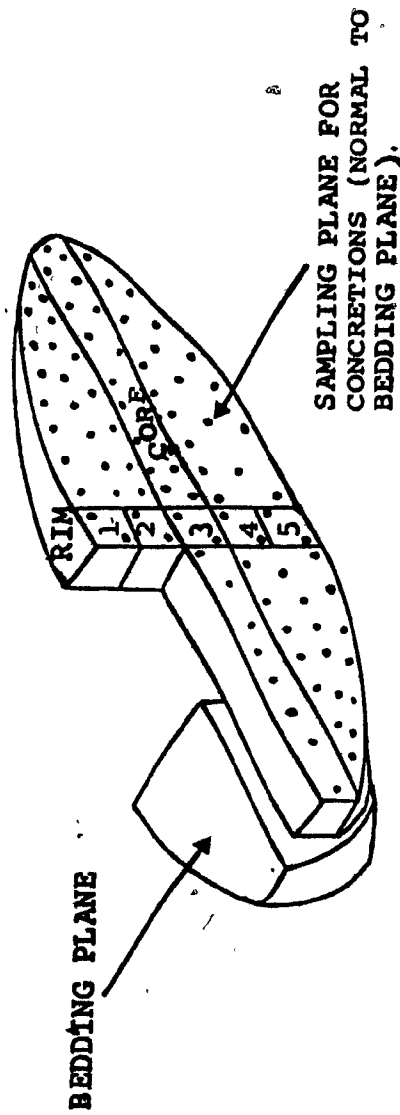


FIGURE 28

The sampling pattern of concretions for laboratory studies.



react very weakly to HCl and display a brown weathering surface indicating the presence of small amounts of Fe in solid solution. X-ray diffraction values for the principal $\delta_{(211)}$ -peak range from 2.884 to 2.902 Å, as compared with 2.886 Å for an ideal dolomite. This discrepancy can be explained by both partial replacement of Mg^{++} by Fe^{++} and excess of Ca^{++} in the structure (Lippman, 1973). Upon staining with potassium ferrocyanide, a typical light blue color develops, indicating their ferroan nature (Friedman, 1971).

Fig. 29 shows the percent of total carbon, carbonate carbon, organic carbon, and carbonates in the various parts of each concretion. With few exceptions the percentages of the above constituents show a decrease from the core to the periphery of each concretion.

CARBON AND OXYGEN ISOTOPES

During the last decade, various workers began to appreciate the potential value of isotopic analyses of carbonate concretions to monitor some of the changes in the interstitial water composition of the sediments as the concretions grew and the timing of concretion growth. Isotopic compositions of diagenetic carbonates in sediments reflect the variation of the isotopic composition of CO_3^{2-} in pore water during diagenesis (Galimov et al. 1968; Murata et al., 1972; Pearson, 1974; Irwin et al., 1972; Curtis, 1980).

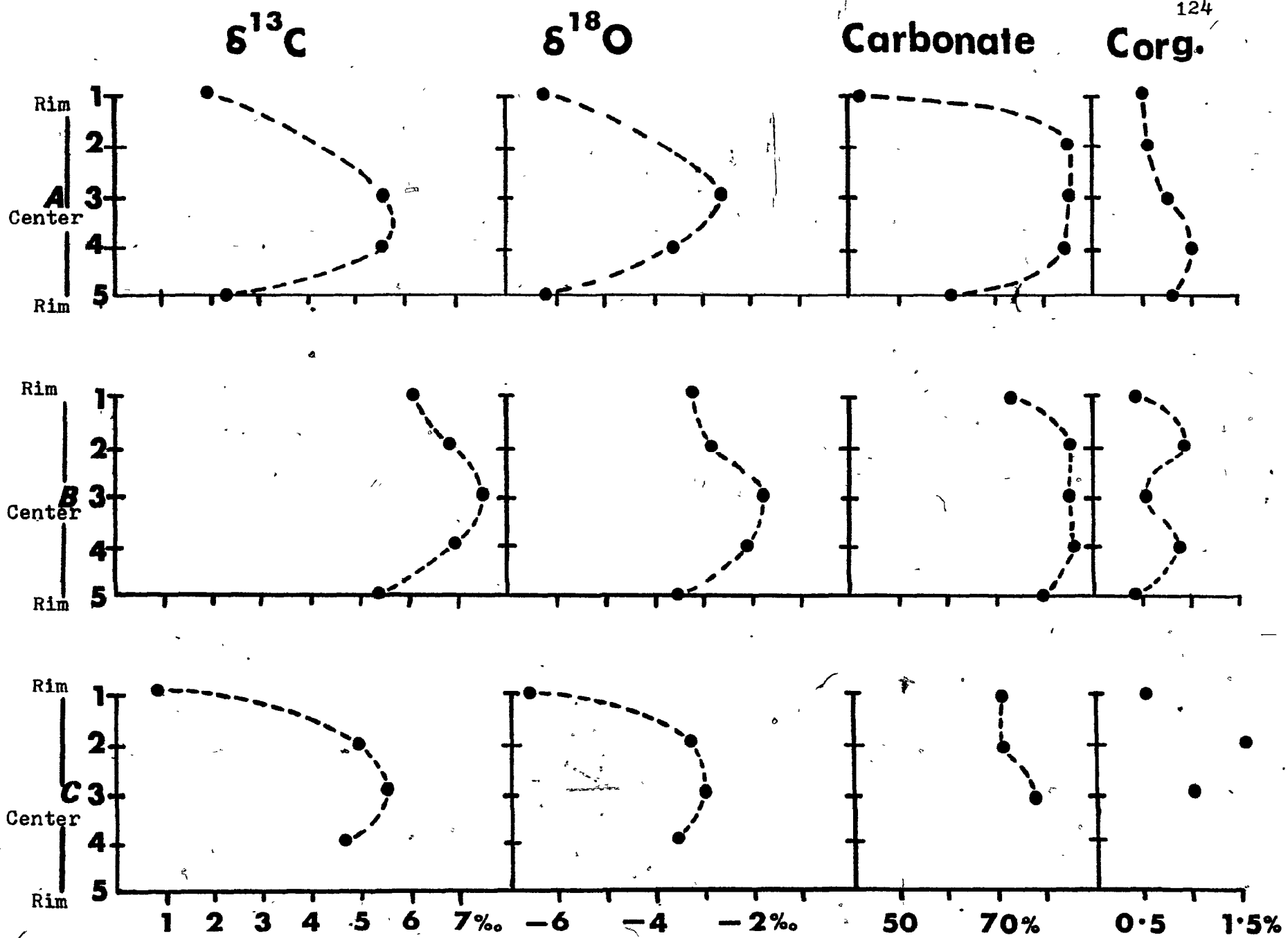
The analytical results of C and O isotope studies

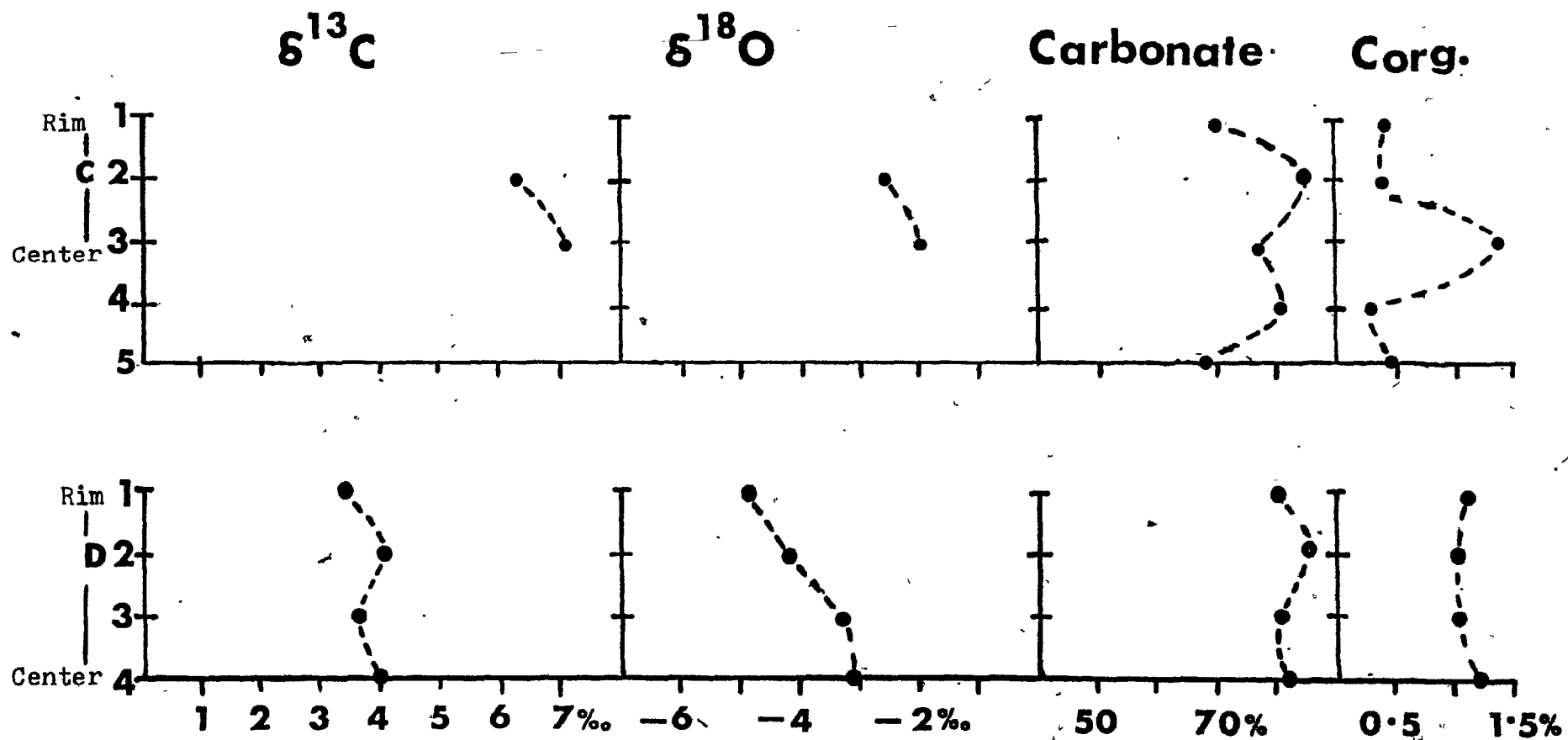
Table 3. Percentage of carbon and oxygen isotopes,
and carbonate and organic carbon content of the concretions.

CLORIDONNE FORMATION	MEMBER	SAMPLE NUMBER	TOTAL CARBON %	CARBONATE CARBON %	CARBONATE %	ORGANIC CARBON %	$\delta^{13}C$ ‰ (PDB)	$\delta^{18}O$ ‰ (PDB)
	B_7	A - 1 (Top)	5.72	5.19	42.58	0.53	2.11	-6.22
		A - 2	11.03	10.20	86.82	0.57	-	-
		A - 3 (Cent.)	11.29	10.46	86.82	0.83	5.58	-2.60
		A - 4	11.38	10.35	85.90	1.03	5.65	-3.64
		A - 5 (Btm.)	8.23	7.42	61.59	0.81	2.35	-6.016
	B_6	B - 1 (Top)	9.20	8.80	73.04	0.40	6.10	-3.22
		B - 2	11.44	10.57	87.73	0.87	6.84	-2.79
		B - 3 (Cent.)	10.88	10.32	85.66	0.56	7.57	-1.76
		B - 4	12.00	11.20	89.60	0.80	6.91	-2.07
		B - 5 (Btm.)	10.27	9.77	81.09	0.48	5.46	-3.49
	B_2	C - 1 (Top)	9.00	8.50	70.55	0.50	0.88	-6.61
		C - 2	10.09	8.50	70.55	1.59	4.88	-3.31
		C - 3 (Cent.)	10.40	9.40	78.02	1.00	5.51	-3.02
		C - 4					4.62	-3.57
	B_2	D - 1 (Top)	8.80	8.35	69.30	0.45		
		D - 2	10.80	10.40	86.32	0.40	6.62	-2.55
		D - 3 (Cent.)	10.72	9.30	77.19	1.42	7.02	-2.00
		D - 4	10.40	10.10	83.83	0.30	-	-
		D - 5 (Btm.)	8.69	8.28	68.72	0.41	-	-
	γ_1	E - 1 (Top)	11.14	9.77	81.09	1.37	3.30	-4.89
		E - 2	11.52	10.48	86.98	1.04	3.99	-4.19
		E - 3	10.96	9.83	81.59	1.13	3.67	-3.29
		E - 4 (Cent.)	11.52	9.98	82.83	1.54	3.97	-3.19

FIGURE 29

Variations of carbon and oxygen isotopes, and carbonate
and organic carbon content of the concretions.





are conventionally reported in the "delta" (δ) notation as per mil deviation from a standard.

$$\delta_{\text{sample}} = \left[\frac{R_{\text{sample}}}{R_{\text{standard}}} - 1 \right] 10^3$$

where R is the ratio of mass of 46 to 44 + 45 in the case of ^{18}O and the ratio of mass 45 to 44 in the case of ^{13}C .

Stable carbon isotope values ($\delta^{13}\text{C}$) vary from +7.57 to +0.88‰ (PDB) from the core to the rim of the concretions suggesting simultaneous CO_2 and CH_4 production by bacterial fermentation of organic matter. This fermentation zone is Zone III of Irwin et al. (1977). It corresponds to the carbonate reducing and bacterial fermentation zones of Claypool and Kaplan (1974). According to Irwin et al. (1977) this bacterial fermentation is characterized by production of heavy carbon having $\delta^{13}\text{C}$ values up to +15‰ compared to -25‰ at shallower zones (bacterial oxidation and sulphate reduction zones) and -10 to -25‰ (PDB) in deeper abiotic reaction zones. However, they ignore the possibility of carbon fractionation between methane and carbonate at depth. Claypool and Kaplan (1974) suggest that sulphate reduction and methane production are, to a large degree, mutually exclusive. According to these authors when sulphate concentration goes to zero, the onset of methane production is reflected in decreased titration alkalinity and increased $\delta^{13}\text{C}$ values of total dissolved CO_2 . During this early stage of methane production, commonly observed changes are a decrease in dissolved bicarbonate from 30 to 5 mmol/kg

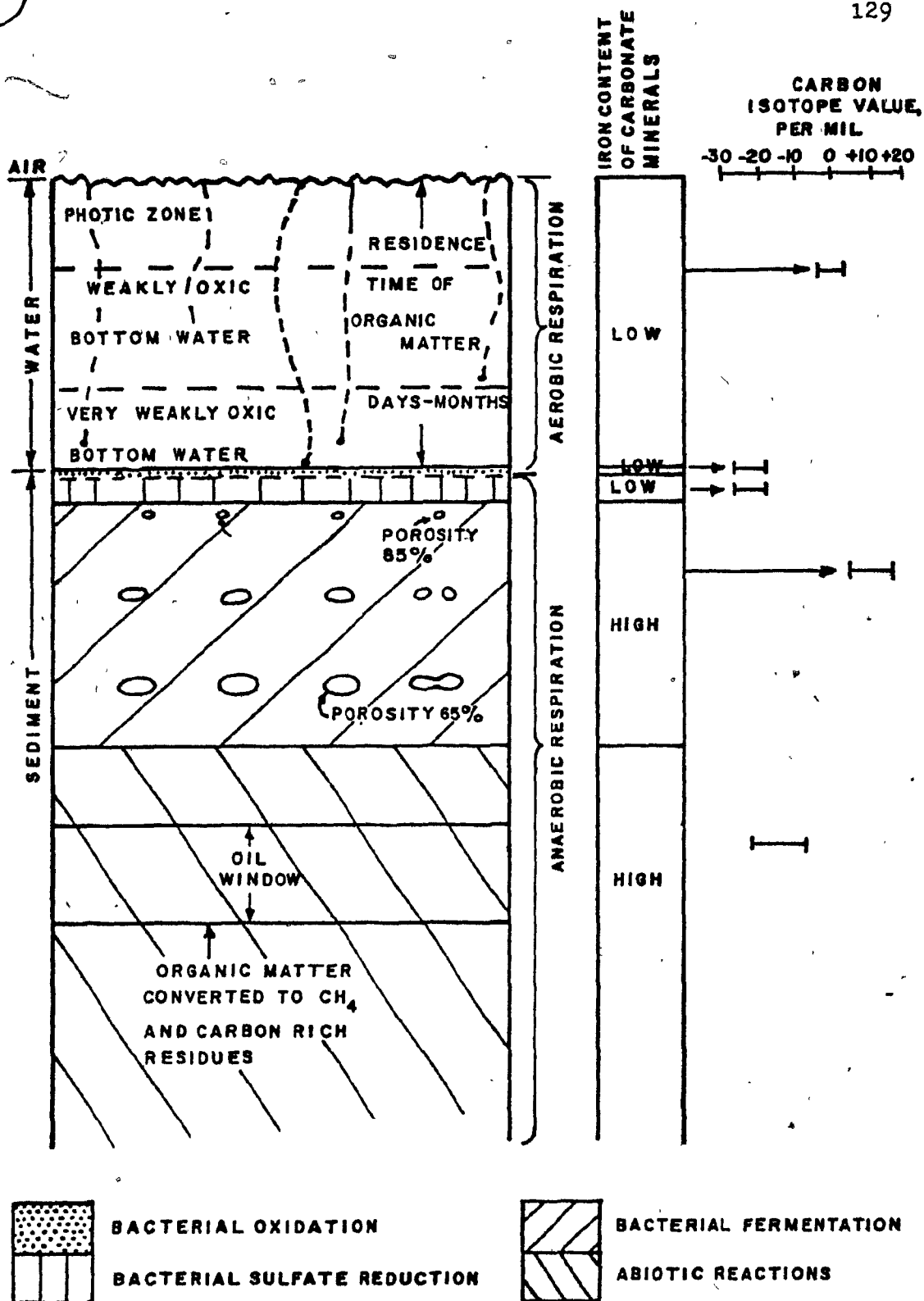
and an increase in $\delta^{13}\text{C}$ from -23 to about +5% (Claypool and Kaplan, 1974). The $\delta^{13}\text{C}$ values in this study average close to +3%. This implies that decay of organic matter by microbial oxidation and methane production may be responsible for the carbonate in the concretions.

Oxidation of organic matter after burial in the sediment provides a ^{12}C -enrichment of dissolved carbon (av. of -28%, Holser et al. 1979) which may contribute to lighter $\delta^{13}\text{C}$ cements. Organic material can also produce substances such as $\text{C}_2\text{H}_5\text{OH}$, CS , NO_2 , and C_3H_8 , which have molecular masses in the same range as the important isotopic species of carbon dioxide (mass 44-46) and thus produce a molecular mass ratio which does not reflect the isotopic composition of CO_2 (Urey, 1947). Studies by Scholle and Arthur (1980) reveal that carbonate carbon to organic carbon ratios of less than 7:1 in the interstitial sediment may lead to unreliable results. Table 3 shows that the ratios of carbonate carbon to organic carbon in the concretions are greater than 7:1. Thus the possible contamination due to the presence of organic matter (0.41 to 1.59% of organic carbon) in the samples is insignificant. If there is contamination by organic carbon then the carbonate $\delta^{13}\text{C}$ values would be more positive than the present value obtained without prior removal of C_{org} . Thus the precipitation of the concretions is interpreted to be due to bacterial fermentation.

The oxygen isotope values for all concretion samples

FIGURE 30

Schematic diagram showing depth-related reaction zones involving breakdown of organic matter in an area of fairly rapid deep water sedimentation where organic matter is little affected by aerobic and sulphate reduction zone processes (modified after Claypool and Kaplan, 1974; Coleman et al, 1979; Demaison and Moore, 1980; Curtis, 1980).



are distinctly negative (Table 3). The values range from -1.74 to -6.61‰ $\delta^{18}\text{O}$ (PDB). Oxygen isotope values become increasingly lighter from the centre to the periphery of the concretions. This trend is interpreted as reflecting a continuous post-depositional equilibration of the precipitated carbonates with isotopically lighter fluids and possibly higher temperature pore waters at depth. The major isotopic effect of diagenesis on pore water is depletion of ^{18}O associated with formation of diagenetic minerals enriched in that isotope. The concentration of O^{18} (δO^{18}) in carbonates is controlled by the $\text{O}^{18}:\text{O}^{16}$ ratio in the fluids and the temperature at which reaction occurs. However, temperatures of carbonate precipitation derived from ^{18}O values may not always fit into the geologic history of a given rock sequence (e.g. Yeh and Savin 1977; Walls et al, 1979; Dickson and Coleman 1980). In this study the estimated porosity of the host sediment at the time of concretion growth decreases from 85 (core) to 65% (rim); depth and temperature most likely increases simultaneously.

Thus, the carbon isotope values and porosity data suggest that decay of organic matter may be responsible for the carbonate in the concretions. These concretions are multigeneration products. Probably they began to develop just below the sediment-water interface and continued to grow at greater depth with sedimentation.

CHAPTER SEVEN

CONCLUSIONS

The study area has been sub-divided into three diagenetic and low-grade metamorphic zones on the basis of asphalitic pyrobitumen reflectance (95 samples) and illite crystallinity (350 samples): (i) Epimetamorphic zone (mean reflectance $\gg 5.0\%$; illite crystallinity $\leq 1.9\text{mm}$); (ii) Anchizone ($2.7 \leq \bar{R}_0 \leq 5.0\%$; $1.9 \leq I_c \leq 3.3\text{mm}$); (iii) Late diagenetic zone ($R_0 < 2.7\%$, $I_c > 3.3\text{mm}$). Two processes account for this regional variation in maturation: (1) maturation during pre-orogenic burial and (2) thermal maturation associated with syn- and post-orogenic activities. The most striking aspect of the study area is a thermal zone of epimetamorphic and higher grade conditions which forms a halo around the Devonian McGerrigle Mountains pluton. Since the epimetamorphic halo around this pluton is more than twice as wide (16-20km) as the pluton itself, the igneous rocks probably extend over a much larger area in the subsurface. The bulging (30km) of the epizone toward north-east probably reflects a subsurface continuation of the intrusive body in that direction. The isolated plutons of Hog's Back, Mont-Valliers-de-St-Real and others in the Siluro-Devonian rocks which lie along a line to the south-west suggest a NE-SW line of intrusives. Just east of the McGerrigle Mountains pluton, an anomaly in the illite crystallinity values is observed.

This retardation in crystallinity may be attributed to hydrothermal fluids.

West of the thermal dome, less mature, younger rocks occur in the tectonically deeper units. Within individual nappes, the degree of thermal maturation increases with increasing stratigraphic age. Isopleths, here, closely follow tectonic boundaries. These observations suggest that the pre-orogenic grade of maturation reached during sedimentary burial, has been subsequently preserved in the transported nappes.

In the late diagenetic zone and anchizone east of the thermal dome an east-west elongated thermal trough is noted. North of this trough maturation is "upside down" since it increases with decreasing age. This maturation pattern suggests syn- to post-orogenic origin. South of the thermal trough, the increase in thermal maturation might be attributed to post-orogenic igneous activities around Murdochville.

Correlation of illite crystallinity and reflectance data shows a wide range of values within and among formations. A similar range is also observed among maturation zones. The best correlation coefficient (-0.78) has been noted in the Deslandes Formation. This is followed by the Tourelle Formation (-0.69), the Cap-des-Rosiers Group (-0.59), the Cloridorme Formation (-0.42), and the Cap-Chat melange (-0.41). As for maturation zones, the late diagenetic zone has a correlation coefficient of -0.37,

which gets poorer in the anchizone (-0.31) and epizone (+0.25). These wide variations in correlation coefficients of illite crystallinity and reflectance data suggest that illite crystallinity and reflectance values are influenced by different factors. These factors probably include tectonics, plutonic activities, lithology, organic matter content etc. Each is important to a greater or lesser extent.

A depth of burial of 5km for the lower Ordovician Tourelle Formation has been estimated assuming a normal geothermal gradient of 30°C/km. This implies that about 4km of the Tourelle Formation or younger units have been eroded. On the other hand, burial depth of 6km for the Cap-des-Rosiers Group appears reasonable from the field observation.

Carbon isotope values ($\delta^{13}\text{C}$) of ferroan dolomite concretions vary from +7.57 to +0.88‰(PDB) from the core to the rim, suggesting simultaneous CO_2 and CH_4 production by bacterial fermentation of organic matter. Oxygen isotope values becomes increasingly lighter from the centre (-1.74‰ $\delta^{18}\text{O}$ (PDB)) to the periphery (-6.61‰ $\delta^{18}\text{O}$ (PDB)) of the concretions. This trend is interpreted as reflecting a continuous post-depositional equilibration of the precipitated carbonates with isotopically lighter fluids and possibly higher temperature pore water at depth. Porosity decrease of the host sediment from 85% at the beginning to 65% at the end of concretion growth implies depth and temperature to increase together. Thus the carbon isotope

values and porosity data suggest that decay of organic matter by methane producing bacteria may be responsible for the carbonate concretions. Probably they began to develop just below the sediment-water interface and continued to grow at greater depth with sedimentation.

CHAPTER 8

SUGGESTIONS FOR FUTURE WORK

During the last decade thermal maturation studies of pelitic rocks have elucidated many aspects of diagenesis and low-grade metamorphism but at the same time have opened up some new questions. From the results of the present study the following suggestions are made for future work:

- (1) The orogenic belt of the Canadian Appalachians has numerous intrusive bodies. Detailed studies of organic matter reflectance and illite crystallinity surrounding these bodies may exhibit the extent and possibly subsurface trends and intensity of contact metamorphism on the host rock. This may have significant implications in the exploration of base metals.
- (2) Fluid inclusion studies from quartz veins should be helpful to verify the temperatures obtained from reflectance studies and to determine paleopressures. Accurate determinations of paleotemperatures and paleopressures during thermal maturation provides a means of assuming paleogeothermal gradients and thus of establishing actual burial depths and delineating boundaries between various stages of diagenesis and low-grade metamorphism.
- (3) Presently correlation between the thermal maturation characteristics of pre-Devonian asphaltic pyrobitumen and those of vitrinite in younger rocks has only tentatively been established. South of the study area, the Devonian

Acadian belt of Gaspé Peninsula presumably contains both types of organic matter. Coal macerals can be characterized by their maturation pathways. Thus reflectance studies on each of the pyrobitumen type (elaterite, wurtzilite, albertite, impsonite, ingramite, anthraxolite) or organoclasts (chitinozoans, graptolites, acritarchs, etc.) could give some insight about their individual maturation pathways.

(4) At higher maturation levels ($\bar{R}_o \gg 2.0\%$) anisotropy of organic matter becomes significant because of complete disappearance of aliphatic carbon chains, the beginning of an ordering of basic kerogen units and a rapidly increasing production of high temperature methane. The anisotropy of the organic matter if related with their structural changes may provide additional information in defining various maturation levels.


(5) Correlation between illite crystallinity and organic matter reflectance should be carried out in different parts of Québec Appalachians to evaluate the effect of structural complexities, igneous intrusions and lithologic differences.

(6) To my knowledge, the determination of progressive sandstone diagenesis as a function of maturation levels established by reflectance, illite crystallinity and fluid inclusions has not yet been carried out anywhere. This type of study would give valuable further insight into the post-depositional history of sedimentary basins.

(7) Thermal maturation studies of the organic matter in

in carbonate concretions should be carried out in order to compare it with the organic matter in shales.

(8) Finally isopleth maps of illite crystallinity and organic matter reflectance should be constructed for the Québec Appalachians. This would give a quantitative picture of the regional heat source and mechanisms of thermal maturation. Regional thermal maturation trends if incorporated into the findings from the plate-tectonic studies would lead to a better understanding of the tectonics of this region. Thus studies of this kind may provide a useful means of solving some of the problems mentioned above.



REFERENCES CITED

- Abraham, H., 1960, Asphalts and allied substances: Van Nostrand, New York, v. 1, p. 1-326.
- Ammosov, I.I., Babashkin, B.G. and Sharkova, L.S., 1975, Bituminiy nizhnnekembriyskikh otlozheniy Irkutskoy neftegazonosnoy oblasti (Bituminite of Lower Cambrian deposits in the Irkutsk oil and gas region): in Yeremin, I.V. (ed.), Paleotemperature Zon nefteobrazovaniya: Moscow, Nauka Press, p. 25-29.
- Bell, K.G. and Hunt, 1963, Native bitumens associated with oil shales: Internat. Ser. Mon. Earth Sci., v. 16, p. 333-366.
- Berner, R.A., Scott, M.R. and Thomlingson, 1970, Carbonate alkalinity in the pore waters of anoxic marine sediments: Limnol. Oceanogr., v. 15, p. 544-549.
- Bird, J.M. and Dewey, J.F., 1970, Lithosphere plate continental margin tectonics and the evolution of the Appalachian Orogen. Geol. Soc. Am. Bull., v. 81, p. 1031-1060.
- Biron, S., 1971, Géologie de la rive du St-Laurent de Cap-Chat à Gros Morne; Rapport préliminaire, DP-240, Min. Rich. Nat. Québec.
- Biron, S., 1973, Géologie de la région de Marsoui; Rapport préliminaire, DP-244, Min. Rich. Nat. Québec.
- Biron, S., 1974, Géologie de la région des Mechins: Québec Dept. Nat. Resources, Preliminary Rept., open file.

Boles, J.R. and Franks, S.G., 1979, Clay diagenesis in Wilcox Sandstones of Southwest Texas: Implications of smectite diagenesis on sandstone cementation: Jour. Sed. Pet., v. 49, p. 55-70.

Bostic, N.H., 1971, Thermal alteration of clastic organic particles as an indicator of contact and burial metamorphism in sedimentary rocks: Geoscience and Man, v. 3, p. 83-92.

Bostic, N.H., 1979, Microscopic measurement of the level of catagenesis of solid organic matter in sedimentary rocks to aid exploration for petroleum and to determine former burial temperatures - A review; SEPM Special Publication No. 26, p. 17-43.

Brass, M.S. and Williams, G.L., 1973, Palynology and nanofossil processing techniques: Geol. Surv. Can., Paper 73-26, 25p.

Brindley, G., 1961, Chapters 5 and 6, in Brown, G. (ed.), The X-ray identification and crystal structures of clay minerals: (2nd edition): Mineral. Soc., London, Jarrold and Sons Ltd., 544p.

Brown, G., 1961, The X-ray identification and crystal structures of clay minerals (2nd edition): Mineral. Soc., London, Jarrold and Sons Ltd., 544p.

Cady, W.M., 1972, Are the Ordovician Northern Appalachians and the Mesozoic Cordilleran System Homologous? Jour. Geophys. Res., 77, p. 3806-3815.

Carroll, D., 1970, Clay minerals: A guide to their X-ray identification: Geol. Soc. Am. Spec. Paper 126, 80p.

- Claypool, G.E. and Kaplan, I.R., 1974, The origin and distribution of methane in marine sediments: in I.R. Kaplan (ed.): Natural gases in marine sediments: Mar. Sci., v. 3, p. 99-139.
- Coleman, M.L., Curtis, D.C. and Irwin, H., 1979, Burial rate a key to source and reservoir potential, World Oil, p. 83-92.
- Correia, M., 1967, Relations possibles entre l'état de conservation des éléments figurés de la matière organique (microfossiles palynoplanctologiques) et l'existence de gisements d'hydrocarbures: Rev. Inst. France. Pétrole, v. 22, p. 1285-1306.
- Curtis, C.D., 1980, Diagenetic alteration in black shales, J. Geol. Soc., London, v. 137, p. 189-194.
- Degens, E.T. et al., 1978, Varve chronology: estimated rates of sedimentation in the Black Sea deep basin: Initial Rept. Deep Sea Drilling Project, v. 42, pt. 2, p. 499-508.
- Demaison, G.J. and Moore, G.T., 1980, Anoxic environments and oil source bed genesis: Amer. Assoc. Petrol. Geol. Bull., v. 64, p. 1179-1209.
- Dewey, J.F. and Kidd, W.S.F., 1974, Continental collisions in the Appalachian - Caledonian orogenic belt: variations related to complete and incomplete suturing: Geology, v. 2, p. 543-546.
- Dickson, J.A.D. and Barber, C., 1976, Petrography, chemistry and origin of early diagenetic concretions in the

Lower Carboniferous of the Isle of Man: Sedimentology, v. 23, p. 189-211.

Dickson, J.A.D. and Coleman, 1980, Changes in carbon and oxygen isotope composition during limestone diagenesis: Sedimentology, v. 27, p. 107-118.

Dow, W.G., 1977, Kerogen studies and geological interpretations, Jour. Geochem. Explor., v. 7, p. 79-99.

Dow, W.G., 1978, Petroleum source beds on continental slopes and rises, Amer. Assoc. Petrol. Geol. Bull., v. 62, p. 1584-1606.

Dunoyer, de Segonzac, G., 1970, The transformation of clay minerals during diagenesis and low-grade metamorphism: A review: Sedimentology, v. 15, p. 281-346.

Enos, P., 1965, Anatomy of a flysch - Middle Ordovician Cloridorme Formation, Northern Gaspé Peninsula: Ph.D. Thesis, Yale Univ., New Haven, Connecticut.

Enos, P., 1969, Cloridorme Formation, Middle Ordovician flysch, Northern Gaspé Peninsula, Québec: Geol. Soc. Am. Spec. Paper 117, 66p.

Epstein, A.G., Epstein, J.B. and Harris, L.D., 1977, Conodont color alteration - an index to organic metamorphism, Geol. Surv. Prof. Paper 995, p. 1-27.

Esquevin, J., 1969, Influence de la composition chimique des illites sur leur cristallinité: Bull. Centre Rech. Pau, v. 3, p. 147-154.

Fawcett, J.J. and Yoder, H.S., 1966, Phase relationships of chlorites in the system $MgO - Al_2O_3 - SiO_2 - H_2O$:

Am. Mineral., v. 51, p. 353-380.

Fleet, A.J., 1980, The nature and genesis of deep-sea carbonate nodules from DSDP SITE 503, Eastern Equatorial Pacific, Geol. Soc. Amer., (Abt.), Annual Meeting, v. 12(7), p. 427, Atlanta, Georgia.

Fong, C., Hesse, R., Islam, S. and Polan, K., 1981, Mineralogy and isotopic composition of carbonate concretions, Québec Appalachians: Record of early and middle diagenetic shale maturation, Geol. Assoc. Canada, Abs., v. 6, A-18.

Foscolos, A.E. and Kodama, H., 1974, Diagenesis of clay minerals from Lower Cretaceous shales of North Eastern British Columbia: Clays and Clay Minerals, v. 22, p. 319-335.

Foscolos, A.E. and Stott, D.F., 1975, Degree of diagenesis, stratigraphic correlations and potential sediment sources of Lower Cretaceous shale of Northeastern British Columbia: Geol. Surv. Can. Bull., v. 250, 46p.

Foscolos, A.E., Powell, T.G and Gunther, P.R., 1976, The use of clay minerals and inorganic and organic geochemical indicators for evaluating the degree of diagenesis and oil generating potential of shales: Geochim. Cosmochim. Acta, v. 40, p. 953-966.

Frey, M., 1978, Progressive low-grade metamorphism of a black shale formation, Central Swiss Alps, with special reference to pyrophyllite and margarite bearing assemblages: Jour. Petrology, v. 19, p. 95-135.

- Frey, M., Teichmüller, M., Teichmüller, R., Mullis, J.,
Künzi, B., Breitschmid, A., Gruner, U. and Schwizer,
B., 1980, Very low-grade metamorphism in external
parts of the Central Alps: Illite crystallinity,
coal rank, and fluid inclusion data: *Eclog. Geol.*
Helv., v. 73(1), p. 173-203.
- Friedman, G.M., 1971, Staining, in R.E. Caryer, (ed.), *Pro-
cedures in sedimentary petrology*, John Wiley and
Sons, New York, p. 511-530.
- Fyfe, W.S., 1973, The generation of batholiths, *Tectono-
physics*, v. 17, p. 273-283.
- Galimov, E.M., Girin, Y.P. and Vernadskiy, 1968, Variation
in the isotopic composition of carbon during the
formation of carbonate concretions: *Geochem. Int.*,
v. 5, p. 178-182.
- Gieskes, J.M., 1975, Chemistry of interstitial waters of
marine sediments: *Ann. Rev. Earth Planet. Sci.*,
v. 3, p. 433-453.
- Gruner, U., 1976, *Geologie des Falknis - Glegghorn - Gebietes
(W - Rhätikon)*. - Liz. - Arbeit Univ. Bern.
- Gutjahr, C.C.M., 1966, Carbonization measurements of pollen
grains and spores and their application: *Leidse
Geol. Meded.*, v. 38, p. 1-29.
- Harwood, R.J., 1977, Oil and gas generation by laboratory
pyrolysis of kerogen: *Amer. Assoc. Petr. Geol. Bull.*,
v. 61, p. 2082-2102.

Harrassowitz, H., 1927, Anchimetamorphose, das Gebiet zwischen Oberflächen-und Tiefenumwandlung der Erdrinde. Ber. oberhess Nat.-u. Heilk, v. 112, p. 9-15.

Harrassowitz, H., 1928, Anchimetamorphose, Zweite Mitteilung. Ber. oberhess. Ges. Nat.-u. Heilk.

Heroux, Y., Chagnon, A. and Bertrand, R., 1979, Compilation and correlation of the major thermal maturation indicators: Am. Assoc. Petrol. Geol. Bull., v. 63, p. 2128-2144.

Hiscott, R.N., 1977, Sedimentology and regional implications of deep-water sandstones of the Tourelle Formation, Ordovician, Quebec, Ph.D. Thesis, McMaster, Univ. Hamilton, Ontario.

Hiscott, R.N., 1978, Provenance of Ordovician deep-water sandstone, Tourelle Formation, Quebec, and implications for initiation of the Taconic orogeny, Can. J. Earth Sci., v. 15, p. 1579-2597.

Hiscott, R.N., 1980, Depositional framework of sandy mid-fan complexes of Tourelle Formation, Ordovician, Quebec, Amer. Assoc. Petrol. Geol. Bull., v. 64, p. 1052-1077.

Holser, W.T., Kaplan, I.R., Sakai, H. and Zak, I., 1979, Isotope geochemistry of oxygen in the sedimentary sulfate cycle: Chem. Geol., v. 25, p. 1-17.

Hoschek, G., 1969, The stability of staurolite and chloritoid and their significance in metamorphism of

politic rocks: Contr. Mineral. Petrol., v. 22, p. 208-282.

Hower, J., Eslinger, E.V., Hower, M.E. and Perry, E.A., 1976, Mechanism of burial metamorphism of argillaceous sediment - I. Mineralogical and chemical evidence: Geol. Soc. Am. Bull., v. 87, p. 725-737.

Hudson, J.D., 1978, Concretions, isotopes and the diagenetic history of the Oxford clay (Jurassic) of central England: Sedimentology, v. 25, p. 339-370.

Hunt, J.M., 1977, Distribution of carbon as hydrocarbons and asphaltic compounds in sedimentary rocks: Am. Assoc. Pet. Geol. Bull., v. 61, p. 100-104.

Irwin, H., Curtis, C. and Coleman, M., 1977, Isotopic evidence for source of diagenetic carbonates formed during burial of organic rich sediments: Nature, v. 269, p. 209-213.

Jones, R.W. and Edison, T.A., 1978, Microscopic observations of kerogen to geochemical parameters with emphasis on thermal maturation: in Oltz, D.F. (ed.), Symposium in Geochemistry: Low temperature metamorphism of kerogen and clay minerals: Pacific Section, Soc. Econ. Paleotol. Mineral., Los Angeles, p. 1-12.

Kalkreuth, W., 1979, Coalification of Paleozoic sediments in the region of East Sauerland Anticline (Rhenohercynicum) with special regard to trend-surface analysis Fortschr. Geol. Rheinl. Westf., v. 27, p. 277-321, (in German).

- Karweil, J., 1956, Die Metamorphose der Kohlen vom Standpunkt der physikalischen Chemie (The metamorphism of coal from the standpoint of physical chemistry): Zeitschr. Deutsche Geol. Gesell., v. 107, p. 132-139.
- Kisch, H.J., 1975, Coal rank and very low stage metamorphic mineral facies in associated sedimentary rocks; an introduction: in A. Alpern, (ed.), Pétrographie de la Matière Organique des Sédiments, Relations avec la Paléotempérature et la Potentiel Pétrolier, Centre natn. Rech. Sci., p. 117-122.
- Kisch, H.J., 1980, Incipient metamorphism of Cambro-Silurian clastic rocks from the Jamtland Supergroup, Central Scandinavian Caledonides, Western Sweden: illite crystallinity and vitrinite reflectance: Jour. Geol. Soc., London, v. 137, p. 271-288.
- Kossovskaya, A.G. and Shutov, V.D., 1958, Zonality in the structure of terrigene deposits in platform and geosynclinal regions: Eclog. Geol. Helv., v. 51, p. 656-666.
- Kübler, B., 1967a, La cristallinité de l'illite et les zones tout à fait supérieures du métamorphisme. Colloq. Etages tectoniques, Neuchâtel, 1967, p. 105-122.
- Kübler, B., 1967b, Anchimétamorphisme et schistosité. Bull. Centre Rech. Pau., v. 1, p. 259-278.
- Kübler, B., 1968, Evaluation quantitative du métamorphisme par la cristallinité de l'illite: Cent. Rech. Pau-

S.N.P.A., v. 2, p. 385-397.

Kübler, B., Heroux, Y., Pittion, J.L., Charollais, J. and Weidmann, M., 1979, Sur le pouvoir réflecteur de la vitrinite dans quelques roches du Jura, de la molasse et des nappes préalpines, helvétiques et penniques (Suisse Occidentale et Haute-Savoie): *Eclogae Geologicae Helvetiae*, v. 72, p. 347-373.

Landes, K.K., 1967, Eometamorphism, and oil and gas in time and space. *Bull. Am. Assoc. Petrol. Geol.* v. 51, p. 828-841.

Laurent, R., 1975, Occurrences and origin of the ophiolites of Southern Québec, Northern Appalachians, *Can. J. Earth Sci.*, v. 12, p. 443-455.

Laurent, R., 1978, The ophiolites of Southern Québec: Oceanic crust of Belts Cove type: Discussion, *Canad. Jour. Earth Sci.*, v. 15(11), p. 1880.

Liard, P., 1972, Géologie de la région de Mont-Joli-Matane; Rapport préliminaire, DP-202, Min. Rich. Nat. Québec.

Lippmann, F., 1955, Ton, Gerdien und Minerale des Barreme von Hoheneggelsen. *Geol. Rundsch.*, v. 43, p. 475-503.

Lippmann, F., 1973, *Sedimentary Carbonate Minerals*, Springer-Verlag.

Logan, W.E., 1863, *Geology of Canada: Geol. Surv. Can.*, Rept. Prog., p. 1843-1863.

Maxwell, D.T. and Hower, J., 1967, High-grade diagenesis and low-grade metamorphism of illite in the Precam-

brian Belt Series: Am. Mineralogist, v. 52,
p. 843-857.

McCrea, J.M., 1950, The isotopic chemistry of carbonates
and a paleotemperature scale. Jour. Chem. Phys.,
v. 18, p. 849-857.

McGerrigle, H.H., 1959, La régions de Tourelle et de cour-
cellette, Rapport géologique 62, Min. des Mines
du Québec.

McKenzie, D.P., 1969, Speculations on the consequences and
causes of plate motions. Geophys. Jour. R. Astron.
Soc., v. 18, p. 1-32.

Miner, J.W. and Toksöz, M.M., 1970, Thermal regime of a
downgoing slab and new global tectonics: Jour.
Geophys. Res., v. 75, p. 1397-1419.

Mullis, J., 1979, The system methane-water as a geologic
thermometer and barometer from the external part
of the Central Alps: Bull. Mineral., v. 102,
p. 526-536.

Murata, K.J., Friedman, I. and Cremer, 1972, Geochemistry of
diagenetic dolomites in Miocene marine formations
of California and Oregon: U.S. Geol. Survey Prof.
Paper 724-e, 12p.

Norton, D. and Knight, J., 1977, Transport phenomena in hy-
drothermal systems: cooling plutons: Am. Jour.
Sci., v. 277, p. 937-981.

- Oertel, G. and Curtis, C.D., 1972, Clay ironstone concretion preserving fabrics due to progressive compaction: Bull. Geol. Soc. Am., v. 83, p. 2597-2606.
- Ogunyomi, O., 1980, Diagenesis and deep-water depositional environments of Lower Paleozoic continental margin sediments in the Québec City area, Canada, Ph.D. Thesis, McGill University, Montréal, Québec.
- Ogunyomi, O., Hesse, R. and Heroux, Y., (in press): Pre- and synorogenic diagenesis and achimetamorphism in Lower Paleozoic continental margin sequences of the Northern Appalachians in and around Québec City, Canada, Bull. Canad. Petroleum Geol., v.27(4).
- Oxburgh, E.R. and Turcotte, D.L., 1970, Thermal structure of island arcs: Geol. Soc. Am. Bull., v. 86, p. 1665-1688.
- Oxburgh, E.R. and Turcotte, D.L., 1974, Thermal gradients and regional metamorphism in overthrust terrains with special reference to the Eastern Alps: Schweiz. Mineral. Petrogr. Mitt., v. 54, p. 641-662.
- Pearson, M.J., 1974, Sideritic concretions from the Westphalian of Yorkshire: a chemical investigation of the carbonate phase: Min. Mag. v. 39, p. 696-699.
- Perry, E.A. and Hower, 1970, Burial diagenesis in Gulf Coast pelitic sediments: Clays and Clay Minerals, v. 18, p. 165-177.
- Peters, K.E., Simoneit, B.R.T., Brenner, S. and Kaplan, I.R.,

1978, Vitrinite reflectance - temperature determinations for intruded Cretaceous black shale in the Eastern Atlantic, Soc. Econ. Paleont. Mineralogists, Symposium in Geochemistry, The Pacific section, Los Angeles, California.

Perregaard, J. and Schiener, E.J., 1979, Thermal alteration of sedimentary organic matter by a basalt intrusive (Kimmeridgian shales, Milne Land, East Greenland) Chem. Geol., v. 26, p. 331-343.

Poole, W.H., 1976, Plate tectonic evaluation of the Canadian Appalachian region: Geol. Surv. of Canada, Paper 76-1B, p. 113-126.

Raiswell, R., 1971, The growth of Cambrian and Liassic concretions in the Upper Lias of England: Chem. Geol., v. 18, p. 227-244.

Raiswell, R., 1976, The microbiological formation of carbonate concretions in the Upper Lias of England: Chem. Geol., v. 18, p. 227-244.

Rast, N., Kennedy, M.J. and Blackwood, R.F., 1976, Comparison of some tectonostratigraphic zones in the Appalachians of Newfoundland and New Brunswick: Can. Jour. Earth Sci., v. 13, p. 868-875.

Reutter, K.J., Teichmüller, M., Teichmüller, R. and Zanzucchi, G., 1978, Coalification studies in the Northern Apennines and paleogeothermal implications: in Closs, H., Roeder, D. and Schmidt, K. (eds.),

- Alps, Apennines, Hellenides: Inter-Union Comm. on Geodynamics, Scientific Report No. 38, p. 261-265.
- Reynolds, R.C. and Hower, J., 1970, The nature of interlayering in mixed layer illite-montmorillonites. *Clays and Clay Minerals*, v. 18, p. 25-36.
- Riva, J., 1968, Graptolite faunas from the Middle Ordovician of the Gaspé North Shore; *Naturaliste Can.*, v. 95, p. 1379-1400.
- Roberts, A.A., Palacas, J.G., and Frost, I.C., 1973, Determination of organic carbon in modern carbonate cements: *Jour. Sed. Petrology*, v. 43, p. 1157-1159.
- Robert, P., 1973, Analyse microscopique des charbons et des bitumens dispersés dans les roches et mesure de leur pouvoir reflecteur, in *Advances in organic geochemistry: Sixth Intl. Congr. Organic Geochemistry*, Rueil-Malmaison, France, p. 549-569.
- Rodgers, J., 1968, The eastern edge of the North American continent during the Cambrian and Early Ordovician; In: Zen et al., eds., *Studies of Appalachian Geology, Northern and Maritime*, p. 141-150.
- Rogers, M.A., McAlary, J.D. and Bailey, N.J.L., 1974, Significance of reservoir bitumens to thermal-maturation studies, Western Canada Basin Amer. Assoc. Petrol. Geol. Bull., v. 58, p. 1806-1824.
- Römer, H.S. de., 1977, Région des Monts McGerrigle area, Min. des Rich. Nat. Que., Rapport Géologique - 174.

- Rosenfeld, W.D. and Silverman, S.R., 1959, Carbon isotope fractionation in bacterial production of methane: Science, v. 130, p. 1658.
- Ruitenberg, A.A., Fyffe, R.L., McCutcheon, S.R., Irrinki, C. and Vengopal, R., 1977, Evolution of pre-Carboniferous tectonostratigraphic zones in the New Brunswick Appalachians, Geoscience Canada, v. 4, p. 171-181.
- Rupke, N.A. and Stanley, D.J., 1974, Distinctive properties of turbiditic and hemipelagic mudlayers in the Algero-Balearic Basin, Western Mediterranean Sea: Smithsonian Contr. to Earth Sci., n. 13, p. 1-40.
- Schenk, O.E., 1978, Synthesis of the Canadian Appalachians: Geol. Surv. Can. Paper 78-13, p. 111-136.
- Scholle, P.A. and Arthur, M.A., 1980, Carbon isotope fluctuations in Cretaceous pelagic limestones: Potential stratigraphic and petroleum exploration tool: Amer. Assoc. Petr. Geol. Bull., v. 64, p. 67-68.
- Sikander, A.H. and Pittion, J.L., 1978, Reflectance studies on organic matter in Lower Paleozoic sediments of Québec: Can. Soc. Petrol. Geol. Bull., v. 26, p. 132-151.
- Stach, E., et al., 1975, Stach's textbook of coal petrology, 2nd ed.: Berlin, Gebrüder Borntraeger.
- St. Julien, P. and Hubert, C., 1975, Evolution of the Taconian Orogen in the Québec Appalachians: Am. Jour.

Sci., v. 275-A, p. 337-362.

Teichmüller, M., 1971, Anwendung kohlenpetraphischer Methoden bei der Erdöl - und Erdgasprospektion: Erdöl u. Kohle, v. 24, p. 69-76.

Teichmüller, M., 1974, Entstehung and Veränderung bituminöser Substanzen in Kohlen in Beziehung zur Entstehung und Umwandlung des Erdöls. Fortschr. Geol. Rheinld, Westf., v. 24, p. 65-112.

Teichmüller, M. and Teichmüller, R., 1978, Coalification studies in the Alps: In: Cloos et al. (eds.): Alpes, Apennines, Hellenides. Schweizerbart, Stuttgart, p. 49-55.

Teichmüller, M., Teichmüller, R. and Weber, R., 1979, Inkohlung und Illitkristallinität: Vergleichende Untersuchungen im Mesozoikum und Paläozoikum von Westfalen. Fortschr. Geol. Rheinld. Westf., v. 27, p. 201-276.

Tissot, B., Durand, B., Espitalie, J. and Combaz, A., 1974, Influence of nature and diagenesis of organic matter in formation of petroleum: Am. Assoc. Petrol. Geol. Bull., v. 58, p. 499-506.

Tissot, B.P. and Welte, D.H., 1978, Petroleum formation and occurrence: Springer-Verlag, Berlin, 538p.

Tissot, B., Demaison, G., Masson, P., Delteil, J.R., and Combaz, A., 1980, Paleoenvironment and petroleum potential of Middle Cretaceous black shales in

- Atlantic basins: Amer. Assoc. Petr. Geol. Bull.,
v. 64, p. 2051-2063.
- Turner, F.J., 1968, Metamorphic Petrology, McGraw-Hill
Book Co., New York.
- Urey, H.C., 1947, The thermodynamic properties of isotope
substances, Jour. Chem. Soc., p. 502-581.
- Van Krevelen, D.W., 1961, Coal-petrology, chemistry, physics,
constitution: New York, Elsevier Publ. Co., 514p.
- Vassoyevich, N.B., Korchagina, U.I., Lopatin, N.V. and
Chernyshev, V.V., 1970, Principal phase of oil
formation: Moskov, Univ. Vestnik, No. 6, p. 3-24.
(English Translation Intern. Geology Rev., v. 12,
p. 1276-1296).
- Vine, J.D. and Tourtelot, E.B., 1970, Geochemistry of black
shale deposits - a summary report: Econ. Geol.,
v. 65, p. 253-272.
- Walls, R.A., Mountjoy, E.W. and Fritz, P., 1979, Isotopic
composition and diagenetic history of carbonate
cements in Devonian Golden Spike reef, Alberta,
Canada: Geol. Soc. Am. Bull., v. 90, p. 963-982.
- Warshaw, C.M. and Roy, M., 1961, Classification and a scheme
for the identification of layer silicates: Geol.
Soc. Am. Bull., v. 72, p. 1455-1492.
- Weaver, C.E., 1958, Geologic signification of argillaceous
sediments, 1. Origin and significance of clay mine-
rals in sedimentary rocks; 2. Clay petrology of

- Upper Mississippian - Lower Pennsylvanian sediments of central United States: Bull. Am. Assoc. Petrol. Geologists, v. 42, p. 254-309.
- Weaver, C.E., 1960, Possible uses of clay minerals in the search for oil: Am. Assoc. Petrol. Geol. Bull., v. 44, p. 1505-1518.
- Weaver, C.E., 1961, Clay minerals of the Quachita structural belt and adjacent foreland: in Flawn, P.T. (ed.), The Quachita System: Bur. Econ. Geol., p. 147-160.
- Weber, K., 1972, Notes on determination of illite crystallinity: N. Jb. Miner. Mh., v. 1972, p. 267-276.
- Weeks, L.G., 1957, Origin of carbonate concretions in shales, Magdalena Valley, Columbia: Geol. Soc. Am. Bull., v. 68, p. 95-102.
- Williams, H., 1976, Tectonic-stratigraphic subdivisions of the Appalachian orogen: Geol. Soc. Amer., v. 8, p. 300, (abstr.).
- Williams, H., 1979, Appalachian orogen in Canada: Can. Jour. Earth Sci., v. 16, p. 792-807.
- Wilson, J.H., 1926, Lithologic character of shale as an index of metamorphism. Bull. Am. Ass. Petrol. Geol. v. 10, p. 625-633.
- Winkler, H.G.F., 1967, Petrogenesis of metamorphic rocks, 2nd edit., Springer-Verlag, New York-Berlin.
- Winkler, H.G.F., 1975, Petrogenesis of metamorphic rocks,

4th edit., Springer-Verlag, New York-Berlin.

Wolf, M., 1975, Über die Beziehungen zwischen illit-Kristallinität und Inkohlung: N. Jb. Geol. Paläont., v. 1975, Mh. 7, p. 437-447.

Yeh, H. and Savin, S., 1977, The mechanism of burial diagenetic reactions in argillaceous sediments:
3. Oxygen isotope evidence: Geol. Soc. America Bull., v. 88, p. 1321-1330.

Zen, E-an, 1967, Time and space relationships of the Taconic allochthon and autochthon: Geol. Soc. America Spec. Paper 97, 107p.

Zen, E-an, 1972, The Taconic zone and the Taconic orogeny in the western part of the northern Appalachian orogen: Geol. Soc. Amer., Spec. Paper 135, p. 72.

PLATE 1

Structure and Rock Types in the Taconic Belt, Gaspé Peninsula

- (a) Minor F1 fold overturned to the south. The axial plane of the minor fold is sub-horizontal. γ_2 member, Cloridorme Formation, Gros Morne.
- (b) Competent beds are chaotically folded, olistrostromes, West of Marsoui.
- (c) Alternation of black shales, graywacke, calcisiltite etc. characteristic of the Cloridorme Formation. Note the elipsoidal shaped carbonate concretion. β_2 member, Grande Vallée.



PLATE 2

Carbonate Concretions from the Cloridorme Formation, Gaspé Peninsula

- (a) Carbonate concretion embedded in shale with its long axis lying in the bedding plane(photo: R. Hesse)
- (b) Concretion showing shrinkage cracks in the core(photo: R.Hesse)
- (c) Plan view of the concretion(photo: R.Hesse)

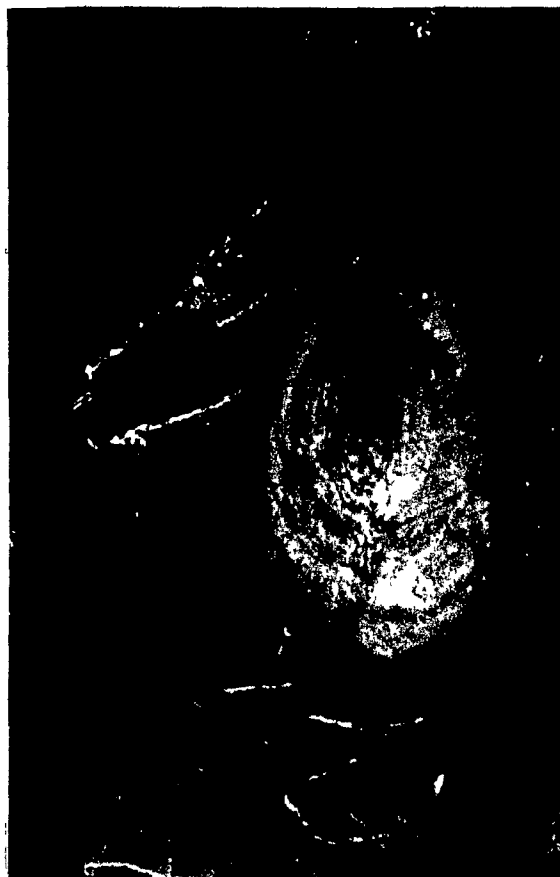


PLATE 3

Organic Matter in Transmitted and Reflected Light
from Cambro-Ordovician Shales of Gaspé Peninsula

- (a) Photomicrograph of amorphous organic matter from the Lower Ordovician Cap Chat Mélange in parallel polarized transmitted light. \bar{R}_o mean : 1.70%.
- (b) Photomicrograph of dispersed organic matter (Chitinozoan of the genus *Conochitina*; Graptolite periderm showing ornamentations) from the Lower Ordovician Tourelle Formation in parallel polarized transmitted light. \bar{R}_o mean : 1.70%.
- (c) Photomicrograph of asphaltic pyrobituman from the Middle Ordovician Cloridorme Formation under reflected light. \bar{R}_o mean : 3.20%
- (d) Photomicrograph of asphaltic pyrobitumen with framboidal pyrites from the Lower Ordovician Tourelle Formation under reflected light. \bar{R}_o mean : 1.69%.



150μ

b

50μ

a

APPENDIX 1

SAMPLE PREPARATION AND ANALYTICAL TECHNIQUES
FOR CLAY MINERALOGY

The samples were washed, dried and then crushed into small pieces (about 8mm) in an iron mortar. About 40g of the material is placed into 125ml plastic bottles and washed 2-3 times in distilled water. The samples are disintegrated by filling $\frac{2}{3}$ of the bottle with distilled water and shaking with small metal balls in a paint mixer for 7 minutes. The fine-grained suspended material is poured into 50ml test tubes and centrifuged for 7 minutes at about 1500 rpm. If the water is clear then it is thrown away without draining any of the finer particles. To prevent flocculation of the finer particles, a small spatula-full quantity of sodium hexametaphosphate is added and mixed thoroughly either by a mechanical mixer or by a hand stirrer. Samples were centrifuged for 5 minutes at 700 rpm after which only the less than 2μ m fraction remained in suspension. The process was repeated (normally 2-3 times) until all the particles less than 2μ m were extracted. This is confirmed by the appearance of clear water as a result of settling of the greater than 2μ m particles at the bottom of the test tube. About $\frac{2}{3}$ of this clear water is thrown away. The settled particles are then thoroughly mixed and the test tube is filled with distilled water. The test tube is allowed to stand for 5-7 minutes to con-

centrate the 2-16 μ m fraction in the upper half of the tube. Oriented samples of the less than 2 μ m and 2-16 μ m are prepared on glass slides using a pipette and subsequently air drying.

X-RAY DIFFRACTION

X-ray diffractograms were run on all samples with a Phillips PW 1060 diffractometer using a Hewlett-Packard XY' recorder. The characteristics and the settings of the system are the following:

X-rays : CuK_{α} , 50KV and 32Ma.
Slits : 1° - 0.2, Ni, 1° .
Discrimination : attenuation 1, height 1560 (counter)
Threshold: 1.65V, Channel 3V.
Time constant : 0.4 seconds.
Goniometer speed : $2.4^{\circ}/\text{min}$.
Recorder
Y sensitivity : position 2, potentiometer 4.31.
X sensitivity : 4×10^3 (PW 4620), 1mV/cm.

All samples were scanned unglycolated through 2θ angles of 2° to 33° .

APPENDIX 2

SAMPLE PREPARATION AND PROCEDURE FOR
REFLECTANCE MEASUREMENTS

Palynologists were the first to process shales to isolate organic matter. A flow chart for the isolation of organic matter is shown in Fig. 31, which is a modification from Brass and Williams (1973). One hundred and forty-five black shales were analyzed. In 90 samples, the amount of organic matter was sufficient, in 12 samples fair to good and 43 samples contained insufficient amounts of organic matter.

The samples are first washed, dried and crushed to chips of about 1cm diameter. Samples (150 to 200gms) are placed in 1000ml plastic beakers to be treated with 300 to 400ml of HCl (10%) for the removal of carbonates. Occasional agitation with a polypropylene stirring rod will allow the acid to penetrate the entire sample. After 3 hours the HCl is carefully decanted to avoid any escape of fine particles. The residue is neutralized by washing 3 to 4 times with water, allowing the residue to settle for an hour, and decanting as much water as possible. It is important to neutralize the sample, otherwise calcium fluoride crystals will form in the sample on addition of hydrofluoric acid. About 200ml of HF (70%) is added and stirred occasionally with a polypropylene rod. Since some residues react violently at this stage, the acid is added in 100ml portions. The HF breaks down the residues by removing

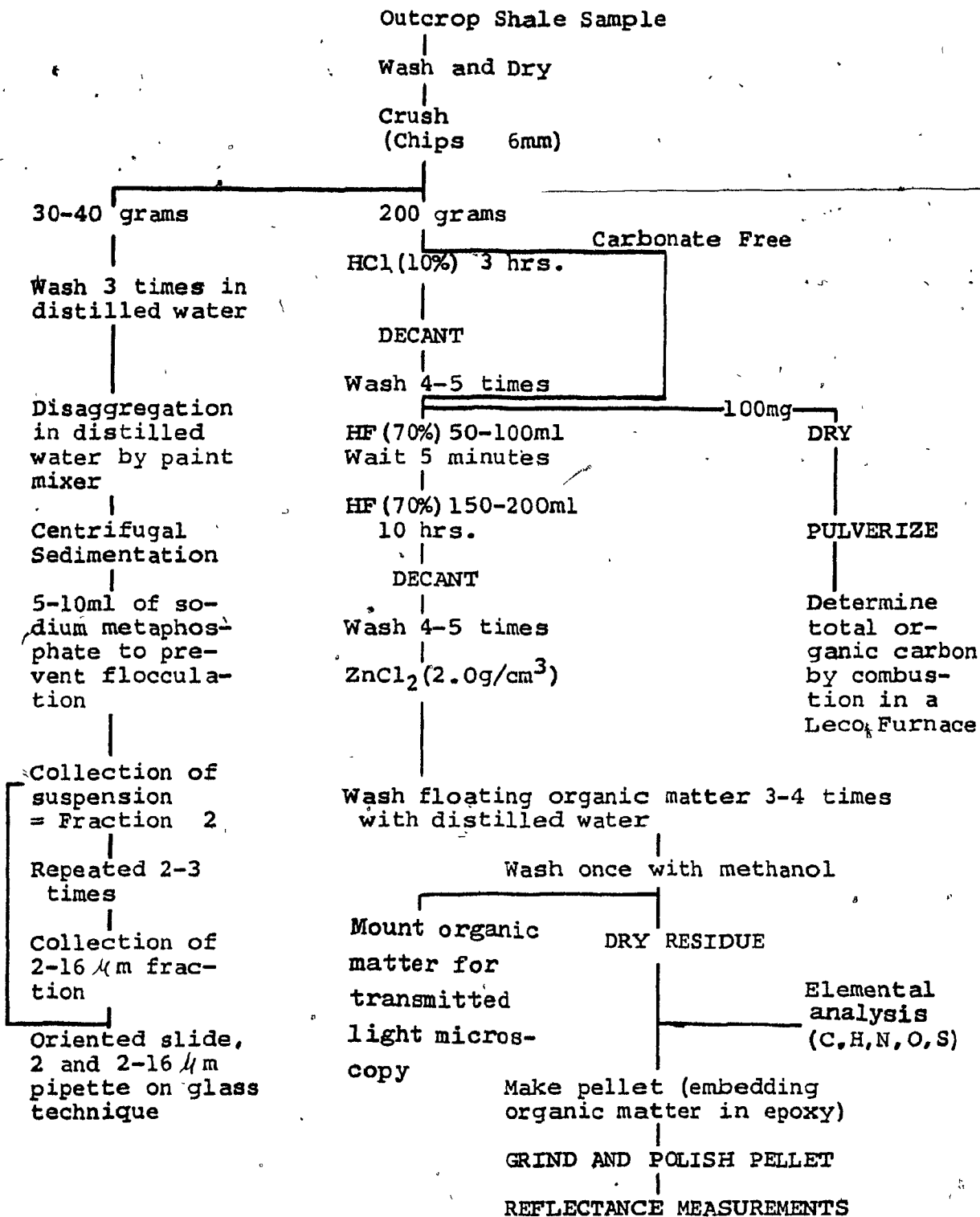
the silicates. The mixture is left at least eight hours. Upon complete breakdown of the sample materials, the acid is decanted and the residue washed until neutral to litmus paper (3 to 5 times). The residue is then transferred to two 50ml centrifuge tubes. Centrifuging is carried out for 5 minutes at 1500 rpm. The clear water is drained out as much as possible. The residue is thoroughly mixed with zinc chloride (sp. gr. = 2.0g/cm^3) for the separation of organic and inorganic material. Upon centrifugation at 1000 rpm for 12 minutes in flexible plastic tubes, separation into two fractions is achieved. The organic matter will be present in the supernatant. The nonorganics will settle-out. The supernatant, with the organic matter, is removed by pinching the tube with pliers. The organic matter is thoroughly washed (3 to 4 times) with distilled water to remove traces of ZnCl_2 . Finally the organic matter is washed twice with methanol and dried.

Organic matter is embedded in epoxy-resin mixed with hardener (5:1 ratio) and formed into a cylindrical pellet. Care is taken to concentrate the organic matter on one face of the pellet by centrifuging at high speed (20,000 rpm) for about 12 minutes. The pellet is allowed to harden for 6 hours at room temperature.

The sample mount is then polished with 600 grit in water on a carbomet surface followed by $6\mu\text{m}$ and $1\mu\text{m}$ diamond powder on a texmet surface mounted on a slowly revolving automatic polishing lapidary wheel. The final polishing

FIGURE 31

Flow chart for organic matter and clay mineral analyses. 164



is done with 0.05 μ m alumina powder. Polishing compounds are removed by gentle ultrasonic treatment between the polishings. The final polish is very important. The sample must be highly polished, free of scratches. After the final polish, the sample is dried at room temperature for 6 hours and is then ready for reading.

This process leads to the recovery of the main part of the organic matter, but the disadvantage is that the particles are finely comminuted, so that the organic particles may disintegrate, resulting in difficulty of diagnosis.

REFLECTANCE MEASUREMENTS

Reflectance is measured with a Zeiss photomicroscope II equipped with a voltage stabilizer, RCA1 - P28 model photomultiplier, HTV R-446 model microphotometer and a Zeiss digital display unit. Other characteristics of the microscope are:

Objective : X40 epiplan oil immersion objective.

Optovar : 1.25

Diaphragm : 160 microns

Diameter of measuring aperture: approximately 3 microns.

Light and Filter: Tungsten 3050°K, 546mm wavelength

Vertical illuminator type H.P. Pol Zeiss.

Immersion oil: Cargill oil, refractive index, $n = 1.515$.

For standardization of the photomultiplier, glass standards with refractive indices of 1.694 and 1.856

(1.02% R_0) were used. After standardizing the photomultiplier

traverses spaced 1mm apart were made on polished surface selecting and measuring 50 grains of asphaltic pyrobitumen per sample. After 25 measurements, the photomultiplier was restandardized. The random (unrotated) reflectance was recorded. Statistical parameters like mean, standard deviation and skewness of the reflectance data were calculated for each sample with the aid of a computer. The data are presented in Appendix 8.

APPENDIX 3

DETERMINATION OF TOTAL ORGANIC CARBON

In shales the element carbon usually occurs as carbonate carbon; solid insoluble carbon (kerogen); carbon in organic bases, humic materials, or bitumens; in liquid hydrocarbons; and gases (CO_2 , CH_4). The insoluble organic carbon is mainly kerogen. Roberts et al. (1973) showed that 9 to 17% (or more depending on acid strength and temperature) of the organic carbon in modern carbonate sediments can be solubilized and lost during mild acid treatment. The more thermally matured samples probably show lesser effects of non-kerogen organic carbon because with increasing diagenesis there will be less volatile or soluble organic matter present.

Total carbon is determined by Leco apparatus, which combusts the sample in oxygen at about 1400°C . The carbon in the sample is converted to CO_2 . A catalyst in the furnace converts any CO to CO_2 . The CO_2 gas is measured by a highly acidic red solution in a buret by titration. As a gas is being analysed, and as gases change volume with temperature and pressure, a factor determined from the barometric pressure and gas temperature is multiplied by the final buret reading. This gives the amount of total carbon. Carbonate carbon is also determined by the same Leco apparatus which combusts the sample in oxygen at about 1400°C . Organic carbon by-difference is obtained by subtracting carbonate carbon

value from the total carbon value. The organic richness of rocks is customarily expressed in terms of weight percent organic carbon.

Fifteen shale samples (13 black, 3 red, 1 green) were initially analyzed quantitatively for their total organic carbon content (Table 4). A few samples are very poor in organic carbon (0.19 - 0.32%), however, on the average, the organic matter content (0.95%) is sufficient for reflectance studies.

Table 4. Organic carbon content of black, green and red shales, Taconic Belt, Gaspé Peninsula.

Sample	Total Carbon %	Organic Carbon %
PF 73 Black	1.08	0.37
FP 69 "	0.59	0.38
LE 67 "	2.23	1.86
AP 06 "	1.69	0.85
CM 10 "	2.30	1.75
GR 72 "	2.31	0.32
AP 06 "	1.69	0.85
MO 32 "	2.12	0.19
MO 07 "	2.01	1.37
FP 08 "	1.95	1.56
AP 59 "	2.40	2.06
AP 61 "	1.69	0.62
AM 93 "	2.31	0.32
		Av. 0.95
CM 10 Red	1.08	0.15
SAS 31 Green	1.06	0.21

APPENDIX 4

ANALYTICAL TECHNIQUES FOR ISOTOPIC ANALYSIS

The procedure followed for isotopic analysis is that outlined by McCrea (1950). Finely powdered samples were reacted with 100% phosphoric acid overnight. The evolved CO_2 was purified by passage through a dry-ice acetone trap. This was then analysed by mass spectrometer. All values are reported as parts per thousand.

APPENDIX 5

IDENTIFICATION OF CLAY MINERALS

The clay minerals are identified by x-ray diffraction analysis as described by Brown (1961), Warshaw and Roy (1961), and Carrol (1970). Illite (clay-sized minerals of mica group) is identified by 10, 4.96, and 3.34Å peaks on x-ray diffractograms of oriented slides. Samples with 10Å peak slightly skewed towards the lower angle ($2^\circ\theta$) may imply that illite/smectite mixed layering is associated with illite. Any change of this 10Å peak upon glycol saturation suggests the presence of mixed-layers (Reynolds and Hower, 1970). Chlorite is recognized by the 14.1Å (d_{001}), 7.08Å (d_{002}), 4.73Å (d_{003}), and 3.53Å (d_{004}) peaks. Chlorite can be confused with kaolinite on x-ray diffractograms because of d_{001} spacing of kaolinite (7.15Å) is close to the d_{002} spacing of chlorite, and the 3.5Å d-spacing in both the minerals is similar (Brindley, 1961). However, if heating of the sample up to 600°C followed by slow cooling does not result in destruction of this peak then kaolinite is not present. Chlorites consist naturally of Fe-chlorites, intermediate, and Mg-chlorites. Brindley concluded from the x-ray data that all chlorites have essentially the same type of layer structure and that compositional variations arise mainly from isomorphous substitution of cations. Works by Brindley and colleagues (Brindley, 1961) have shown that the relative intensities of diffraction peaks are related to the chemical

composition. The ratio of even reflection over the odd one enables to see if there is any variation in chemical composition of chlorites. Chlorites rich in iron give relatively weak (001), (003), and (005) reflections and strong (002) and (004) reflections. Magnesium chlorite (clinochlore) is stable up to temperatures of 670°C to 820°C over the range of PH_2O from 1 to 7 kbar (Fawcett and Yoder, 1965) and is more common in metamorphic rocks. On the other hand chlorites common to most pelitic rocks are rich in Fe^{2+} and Al^{3+} and disappear with progressive metamorphism at a temperature range of 580°C to 620°C at 4 kbar (Hoschek, 1969).

VARIATION IN ILLITE 002/001 PEAK INTENSITY RATIO

Two elements have a major role in the ordering of the illite lattice: the level of aluminium in the octahedral layer; and the level of interlayer sodium or potassium. As for the first one Esquevin (1969) used one intensity ratio of the 5Å and 10Å illite (002/001) peaks to indicate the chemical composition of the octahedral layer. He concluded that the 'crystallinity indices' of illite, and muscovite/phengites with high 002/001 ratios are better indicators of degree of maturation than those with low ratios. That is, aluminous illite is further recrystallized than ferromagnesian illite of same maturation grade. Dunoyer de Segonzac (1970) used the same technique and plotted illite

crystallinity versus illite 002/001 peak intensity ratio. This resulted in five types of relationships representing different stages of progressive maturation (Fig. 32). It is important to note that aluminous illites attain good crystallinity more rapidly than Mg-Fe rich illites provided the illite 002/001 peak intensity ratio is greater than 0.26.

APPENDIX 6

CLAY MINERALOGY

Clay mineral analyses were done on the less than 2 microns fraction (fine fraction) and on the 2 to 16 μ m fraction (coarse fraction). Samples were scanned unglycolated through 2 θ angles of 2° to 33°. Some samples were re-scanned after glycolation. All samples (2 μ m) investigated contain illite, chlorite, and quartz. Additionally calcite, dolomite, and feldspar were noted in most cases. The x-ray diffractogram of the coarser 2-16 μ m fractions help to detect the presence of the latter minerals.

PERCENT OF MIXED-LAYERS WITH ILLITE

The (001) diffraction-peak maxima of illite for the 2 μ m fractions are almost invariably located at 10-10.2 \AA . Some samples from late diagenetic and a few samples from the anchizone show slightly asymmetric peaks toward the higher d-spacing side. These tails are generally quite gradual, without marked shoulders, suggesting that the percent of 14 \AA layers in the mixed-layers is usually low. Glycolated samples were run which, however, do not show any significant shift in the 10 \AA peak towards higher side (Fig. 33). This suggests that the percent of mixed layers is negligible to zero.

CHLORITES

Relatively higher positive value of chlorite 002/001 peaks of $-2\mu\text{m}$ and 2 to $16\mu\text{m}$ fraction in the study area suggests that the chlorites are rich in iron.

ILLITE-CHLORITE RATIO

The illite/chlorite relative abundance ratio is based on a measure of the peak height ratios using 4.95\AA peak of illite (002) and the 3.53\AA peak of chlorite (004), Rupke and Stanley (1974). Nearly all the samples ($< 2\mu\text{m}$ fractions) exhibit these two characteristic illite (002) peak and chlorite (004) peak. The ratio greater than one means that chlorite is minor in amount. In the study area illite (002) and chlorite (004) peak ratio range from 0.20 to 4.1. However, no correlation exists between this illite/chlorite ratio and degree of thermal maturation.

Figure 32. Types of relation between illite crystallinity and illite intensity ratio ($I^*(002) / I(001)$) (from Dupoyer de Segonzac, 1970).

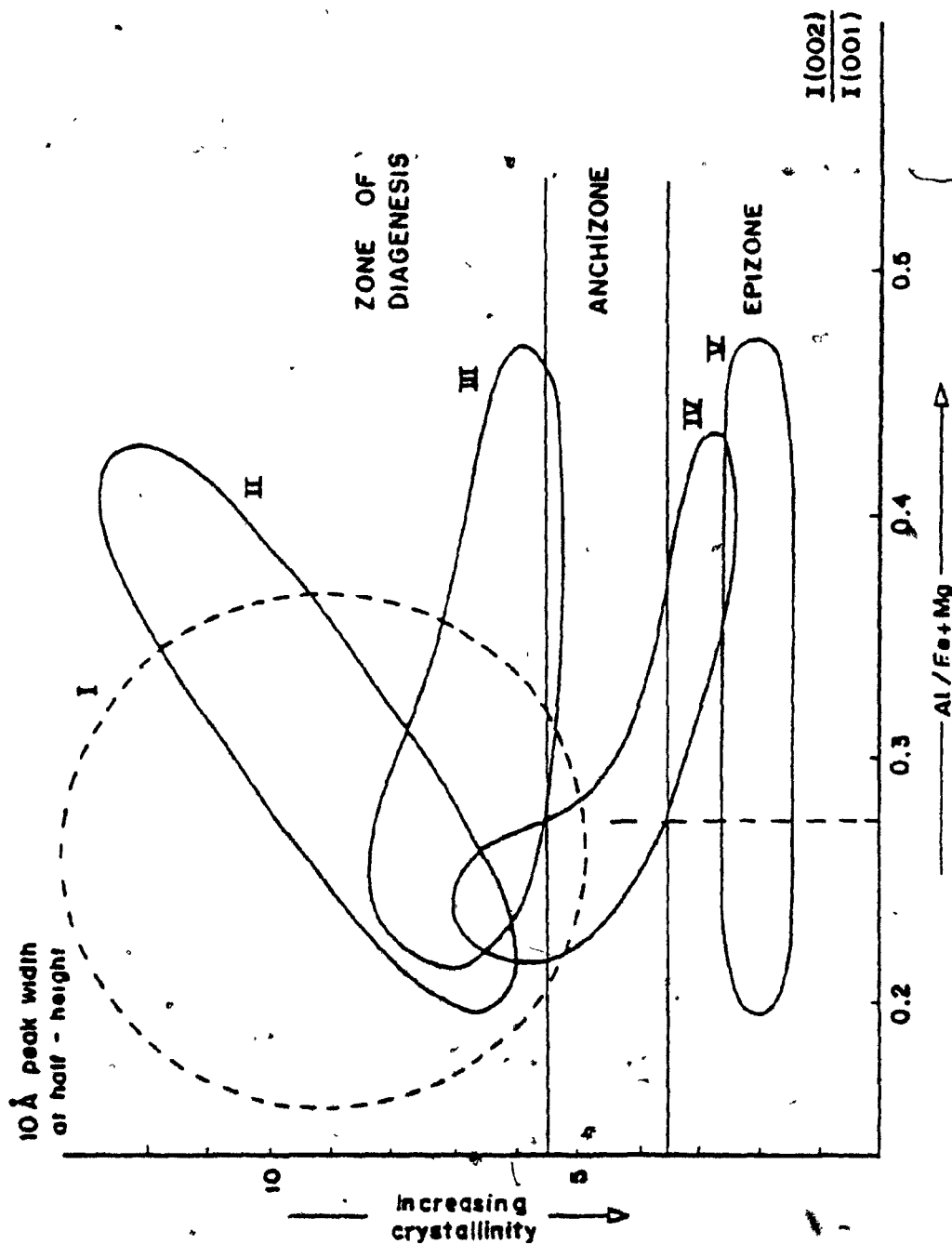


Figure 33. After glycol saturation (b) no shifting of the 10 Å peak (illite, 001) is observed, suggesting that the percent of mixed layers is zero. Note that the illite 001 peak is narrower (IC = 3.7 nm) in the coarser fraction, (2-16 μ m) compared to the finer fractions (2 μ m) (IC = 5.0 nm). Finer fractions represent authigenic illite. X-ray diffractogram of the coarser fractions help to detect the presence of carbonates (calcite, 104).

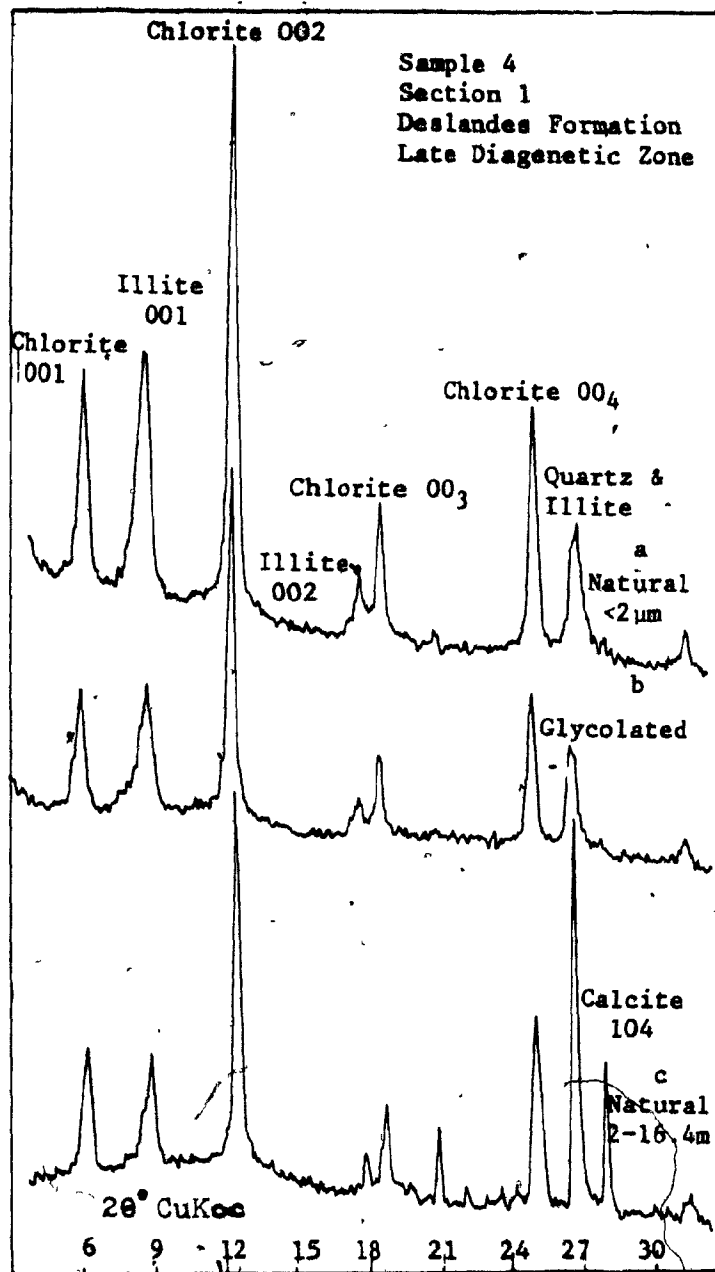


Figure 34. Natural sample (a) shows a slightly asymmetric 10\AA peak (illite 001) towards the higher d-spacing side. Glycolation of the same sample does not show any significant shift in the 10\AA peak suggesting that the percentage of mixed-layers is negligible.

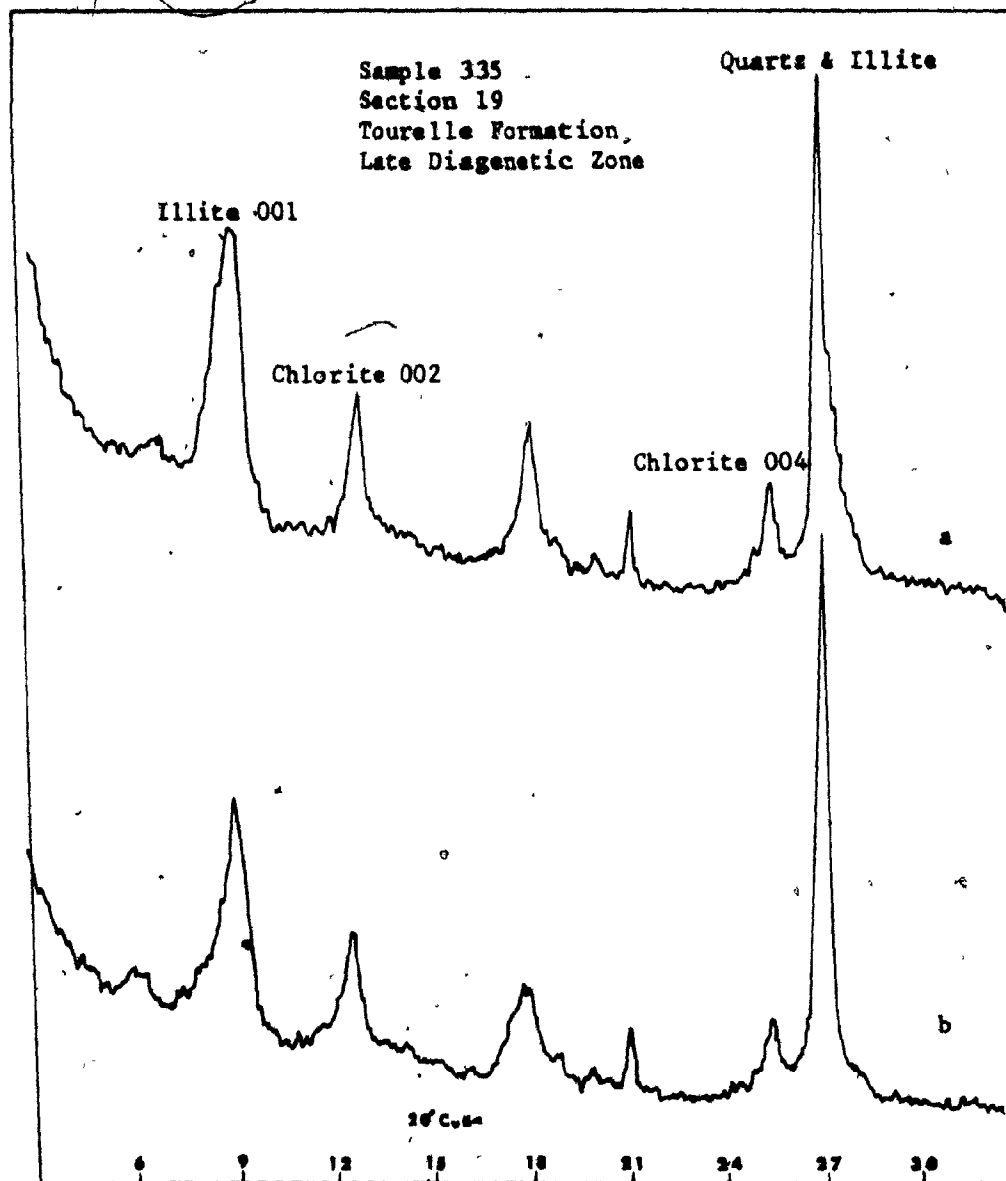
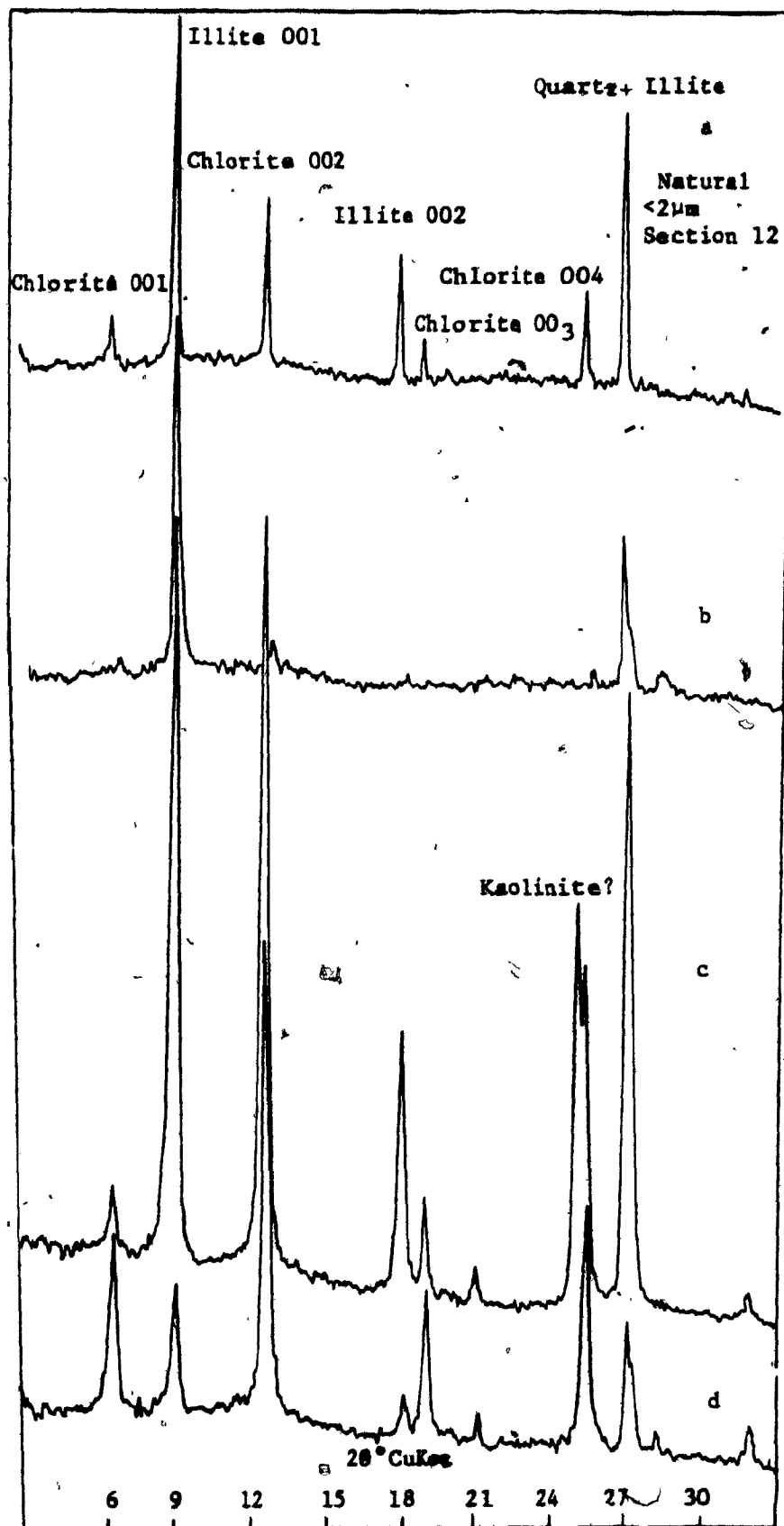


Figure 35. X-ray diffractograms of four samples immediately east of the McGerrigle Mountains pluton in the Riviere Claude Section (Section, 12). Sample (a) shows the best crystallinity ($1.0 \text{ nm} = 0.13^\circ 2\theta$) in the study area. South of it (e.g. b.c.d.) IC gets anomalously poorer. Note in the sample (b) chlorite is absent and in sample (c) there is a possible presence of Kaolinite.



APPENDIX 7

DIFFERENCES IN CRYSTALLINITY BETWEEN VARIOUS SIZE FRACTIONS

Interpretation of illite crystallinity data is difficult because of the possible inherited characteristics of illite. These characteristics need to be differentiated from the ones acquired after burial. To overcome this problem in some samples crystallinity indices are measured on the fine fraction ($< 2\mu\text{m}$) as well on the coarse fraction ($2-16\mu\text{m}$). The narrower peaks when present in the coarser fractions compared to finer fractions implies admixture of unweathered clastic mica of igneous and metamorphic origin. Finer fractions represent authigenic illite formed during diagenesis. The differences in crystallinity indices on these two size fractions which are noted in the late diagenetic zone, decrease markedly in the lower grades of the anchizone and ultimately disappear in the higher-grade anchizone and epimetamorphic zone, Table 5. Differences in crystallinity in the late diagenetic and early anchizone obviously indicate the persistence of coarse, relatively unaltered clastic micas in a fine authigenic matrix. It seems that in the late diagenetic zone the burial diagenesis phenomenon has not been sufficient enough to mask the effects of detrital material and this affects most of the material in the coarse fraction. In the 'higher grade' anchizonal samples the peak widths of coarser as well as finer fractions appears to be similar. This indicates the progressive

crystallinity increase of the fine authigenic micas, and the extension of the recrystallization process to the coarser clastic micas. Above observations suggest the presence of inherited illites in these samples. However, the crystallinity indices for both fractions indicates that the fine fraction illites have been more sensible to the diagenetic effects.

Table 5. Illite Crystallinity of natural
($<2\mu\text{m}$ and $2-16\mu\text{m}$) and
Glycolated ($<2\mu\text{m}$) Sample

Maturation Zone	Sample No.	Illite Crystallinity $<2\mu\text{m}$ mm	Illite Crystallinity $2-16\mu\text{m}$ mm	Illite Crystallinity $<2\mu\text{m}$ Glycolated mm
DIA GENETIC ZONE	DL 1-4	5.0	2.0	3.5
	DL 1-9	5.2	3.5	4.8
	DL 1-13	4.5	3.5	
	CL 5-65	3.5	1.5	
	CL 8-125	3.3	2.0	3.0
	CM 14-226	3.8	1.9	
	TR 20-341	5.0	3.5	
	TR 20-343	3.7	2.5	
ANCHIZONE	CL-5-69	2.6	2.0	
	CL-5-67	2.5	1.2	
	CL-7-113	2.8	1.5	
	DL-13-203	3.0	2.0	
	DL-13-212	1.2	1.2	
	DL-13-273	1.3	1.3	
	DL-13-219	1.2	1.2	
	DL-13-222	2.0	2.0	

APPENDIX 8

Reflectance Data and Calculated
Statistical Parameters.

In the sample number column first
number refers to section number.

CL = Cloridorme Formation

DL = Deslandes Formation

TR = Tourelle Formation

CM = Cap Chat Melange

CR = Cap-des-Rosiers Group

Sample Number	No. of observations	R_0 (mean)	Standard Deviation	Skewness Coefficient	Variation Coefficient	Standard Deviation of Mean	No. of Modes
CR-1-2	50	2.52	0.211	-0.248	0.083	0.030	1
DL-1-4	58	2.60	0.95	0.797	0.035	0.012	2
DL-1-5	53	2.70	0.123	-0.339	0.044	0.017	3
DL-1-10	9	2.24	0.493	0.916	-0.217	0.164	2
DL-2-21	33	2.66	0.154	0.269	0.058	0.027	2
DL-2-23	39	2.70	0.158	0.316	0.057	0.025	2
DL-2-25	4	2.10	-	-	-	-	-
CR-2-28	6	2.24	0.240	-2.091	0.107	0.107	1
CL-3-35	50	2.53	0.174	0.717	0.069	0.025	1
CL-3-36	49	2.44	0.466	1.731	0.190	0.066	1
DL-3-37	50	2.41	0.049	0.810	0.098	0.081	1
DL-3-42	50	2.62	0.144	0.739	0.055	0.020	1
CR-3-44	28	2.21	0.079	-0.177	0.036	0.015	2
DL-3-50	53	2.70	1.23	0.339	-0.044	0.017	3
CL-4-51	44	2.73	0.238	0.316	0.098	0.54	2
CL-4-54	23	2.38	0.180	0.773	0.078	0.038	1
DL-4-55	41	2.40	0.301	0.612	0.082	0.410	1
DL-4-59	47	2.45	0.234	0.494	0.047	0.055	1
CR-4-62	51	2.24	0.124	-0.160	0.055	0.017	2
CR-4-65	50	2.21	0.107	-0.231	0.05	0.015	2
CL-5-66	50	2.34	0.353	3.116	0.151	0.050	2
CL-5-67	52	2.55	0.282	0.757	0.110	0.039	1
CL-5-70	20	2.75	0.123	-0.171	0.072	0.081	1
CL-5-71	13	2.86	0.112	0.275	0.038	0.031	1

Sample Number	No. of observations	R_o (mean)	Standard Deviation	Skewness Coefficient	Variation Coefficient	Standard deviation of Mean	No. of Modes
CL-5-72	6	3.18	0.454	-0.458	0.128	0.203	
CL-5-73	53	2.98	0.265	0.248	0.088	0.036	1
CL-5-75	50	3.25	0.181	0.645	0.104	0.087	2
DL-5-80	58	2.64	0.270	0.583	0.102	0.035	1
CL-6-87	19	2.92	0.449	-0.352	0.15	0.103	2
CL-6-88	48	2.57	0.354	0.714	0.138	0.051	1
CL-6-90	49	2.72	0.234	0.494	0.086	0.033	2
CL-6-92	53	3.10	0.191	0.015	0.062	0.026	2
CL-6-93	48	3.04	0.116	0.107	0.070	0.041	2
CL-6-95	45	3.19	0.257	0.078	0.080	0.038	1
CR-6-98	7	2.40	0.060	1.071	0.25	0.030	1
CL-7-101	32	3.68	0.566	0.074	0.154	0.100	2
CL-7-102	50	3.28	0.475	-0.044	0.144	0.067	2
CL-7-104	50	3.85	0.387	0.044	0.103	0.055	2
DL-7-107	50	3.05	0.158	-0.070	0.052	0.032	2
CR-7-112	50	2.68	0.84	-0.220	0.031	0.012	1
CR-7-119	50	4.07	0.194	-0.088	0.047	0.027	3
CL-7-124	50	3.39	0.450	0.737	0.133	0.064	3
CL-8-126	12	3.77	0.529	0.699	0.167	0.093	2
CL-8-129	7	3.33	0.110	0.715	0.033	0.055	1
CL-8-132	49	3.80	3.03	0.111	0.080	0.043	3
CL-8-134	54	3.95	0.309	-0.387	0.078	0.042	1
CL-8-135	50	4.00	0.419	0.218	0.215	0.071	2

Sample Number	No. of observations	R_o (mean)	Standard Deviation	Skewness Coefficient	Variation Coefficient	Standard Deviation of Mean	No. of Modes
CL-9-136	53	4.41	0.558	1.235	0.127	0.077	3
CL-9-138	52	5.58	1.011	-0.807	0.176	0.140	2
CL-9-141	9	4.90	0.810	-0.151	0.201	0.093	1
DL-9-144	17	3.68	0.220	-0.688	0.059	0.053	1
CR-9-147	49	3.18	0.685	1.172	0.223	0.098	3
CR-9-149	50	2.73	0.133	0.645	0.049	0.019	1
CL10-151	54	4.09	0.361	0.876	0.088	0.049	2
CL10-155	48	4.11	0.411	0.819	-0.039	0.119	1
CL10-155	15	5.25	0.529	-0.984	0.101	0.137	2
DL10-155	52	5.56	0.644	0.107	0.116	0.089	1
DL10-161	35	6.06	0.807	0.001	0.135	0.136	2
CL11-168	38	4.16	0.172	0.501	0.051	0.35	2
CL12-177	51	3.77	0.833	1.098	0.220	0.116	3
DL12-179	45	4.85	0.404	1.040	0.083	0.060	2
DL12-185	58	5.58	0.882	0.700	0.159	0.116	2
DL13-202	50	2.98	0.182	0.853	0.061	0.026	2
CM13-204	50	2.93	0.193	0.167	0.066	0.027	1
CL13-209	50	4.01	0.411	0.490	0.802	0.036	1
DL13-215	7	4.68	0.324	0.039	0.076	0.042	1
DL13-217	39	5.10	0.589	0.028	0.115	0.094	2
DL13-221	46	5.38	0.330	-0.981	0.063	0.0487	2
CM14-228	60	2.20	0.109	-0.867	0.055	0.014	1
CM14-230	47	2.81	0.201	0.652	0.042	0.031	1

Sample Number	No. of Observations	R_o (mean)	Standard Deviation	Skewness Coefficient	Variation Coefficient	Standard Deviation of Mean	No. of Modes
CL14-233	32	3.70	0.227	0.391	0.051	0.061	2
DL14-238	7	5.10	0.881	-0.418	0.173	0.333	1
TR15-253	50	1.76	0.084	0.036	0.048	0.012	1
TR15-257	14	1.71	0.039	0.051	0.021	0.030	1
DL15-259	50	2.51	0.337	-0.690	0.134	0.047	2
DL15-263	43	4.21	0.764	0.559	0.181	0.118	2
CR15-266	28	5.60	0.613	0.101	0.109	0.116	2
CM16-270	11	2.02	0.268	-0.290	0.132	0.080	2
DL16-274	50	2.80	0.140	-0.082	0.048	0.019	2
CR16-279	18	3.81	0.450	-0.387	0.118	0.106	3
CR16-287	63	5.05	0.634	-0.332	0.126	0.080	2
CM17-290	48	2.26	1.247	-1.060	0.551	0.181	3
CR17-295	51	3.48	0.337	-0.255	0.097	0.047	2
CR17-308	52	4.83	0.354	0.699	0.073	0.049	3
DL18-313	7	1.72	0.271	0.241	0.029	0.081	1
DL18-315	6	1.73	0.286	0.356	0.031	0.031	1
TR19-322	63	1.55	0.079	0.813	0.051	0.010	1
TR19-324	56	1.63	0.119	0.924	0.074	0.016	1
TR19-325	51	1.70	0.098	0.072	0.077	0.014	1
CR19-326	19	2.19	0.350	-0.294	0.158	0.079	2
CR19-328	39	2.84	0.122	-0.135	0.043	0.019	2
CR19-331	21	3.62	0.400	0.633	0.110	0.087	3
CR19-334	28	4.46	0.463	0.247	0.104	0.087	2

Sample Number	No. of Observations	R_0 (mean)	Standard Deviation	Skewness Coefficient	Variation Coefficient	Standard Deviation of Mean	No. of Modes
CR19-337	25	4.98	0.881	1.944	0.178	0.275	2
TR20-40	69	1.70	0.198	0.286	0.116	0.024	2
DL20-41	66	1.68	0.132	-0.115	0.078	0.016	2
DL20-42	51	1.72	0.174	0.029	0.101	0.024	2
CR20-44	6	2.26	0.381	0.210	0.302	0.029	1
CR20-47	43	2.10	0.189	1.230	0.093	0.039	1
CR20-50	25	4.98	0.881	1.944	0.178	0.275	2